Take it personal! Genetic differences in G protein-coupled receptors as studied with label-free technology

Hillger, J.M.

Take it personal!

Genetic differences in G protein-coupled receptors as studied with label-free technology

by Julia Maria Hillger

The research described in this thesis was performed at the Division of Medicinal Chemistry of the Leiden Academic Centre for Drug Research, Leiden University (Leiden, The Netherlands).

Printed by Optima Grafische Communicatie

Cover design: Julia M. Hillger

Thesis layout: Julia M. Hillger

ISBN: 978-94-6361-019-3

Take it personal!

Genetic differences in G protein-coupled receptors as studied with label-free technology

Proefschrift
ter verkrijging van
de graad van Doctor aan de Universiteit Leiden,
op gezag van Rector Magnificus prof. mr. C.J.J.M. Stolker,
volgens besluit van het College voor Promoties
te verdedigen op donderdag 7 december 2017
klokke 15:00
door

Julia Maria Hillger

geboren te Hamburg, Duitsland
in 1988

Promotor:	Prof. dr. A.P. IJzerman
Co-Promotor:	Dr. L.H. Heitman
Promotiecommissie:	Prof. dr. Hubertus Irth (Chair, Leiden University)
	Prof. dr. Joke Bouwstra (Secretary, Leiden University)
	Prof. dr. Evi Kostenis (University Bonn, Germany)
	Prof. dr. Martina Schmidt (University Groningen)
	Prof. dr. Bob van de Water (Leiden University)

About the title and cover pages

The title is a word play on the common statement “don’t take it personal”. While this saying may be good advice in many cases, there are distinct advantages to “take” medication personal. Genetic differences between individuals can affect both diseases and drug action. Therefore much research effort is focused on making medicine personalized, to tailor it better to the individual patient or situation, to increase beneficial effects and decrease side-effects.

The cover artwork was inspired by a quote from Jim Watson, the co-discoverer of DNA’s double helix structure, who told Time magazine in 1989: " We used to think our fate was in our stars. Now we know, in large measure, our fate is in our genes." (Quoted in *Time*, “The Gene Hunt”, by Leon Jaroff, March 20, 1989). The art on the cover was made from actual experimental xCELLigence data generated during this thesis while investigating the influence of genetic differences on G protein-coupled receptors. In the decorations on the edges, the xCELLigence data dissolves into a double helix as a further reference to the DNA that underlies the data itself. The distribution of the stars resembles the distribution of cell clusters, similar to how the lymphoblastoid cell lines, the cellular model system used throughout this thesis, look like under a microscope when grown on xCELLigence plates. The cover artwork also reminds of the season in which the defense of this thesis is held.

The artwork on the chapter title pages is an abstract representation of both DNA and the strings of golden electrodes embedded in xCELLigence plates.

Content

CHAPTER 1

General Introduction

About this thesis

This thesis describes the study of the influences of genetic variation on a specific class of drug targets, the G protein-coupled receptors (GPCRs), using a combination of personal cellular models and novel label-free assay technology. The results obtained herein will likely assist in the translation of early *in vitro* experiments to more clinically relevant studies in the course of the drug discovery pipeline. Eventually, the findings in this thesis hopefully contribute to the development of clinically more effective drugs and advance the current 'one-size-fits-all' paradigm into the realm of precision medicine. In this first chapter, I introduce the concepts of precision medicine, importance of GPCRs as drug targets and prevalent sources of genetic variation. Moreover, I discuss the advantages and opportunities that arise from combining a novel label-free assay technology with personal cell lines. In the last section of this chapter, I specifically outline the objectives of this thesis.

Precision medicine

Historically, conventional disease treatments have been based on diagnosing a patient with a general disease state and providing a corresponding generalized drug treatment. However, while successful to a degree, such one-size-fits-all treatments may be ineffective or harbor dangers for the individual patient. Inter-individual variability in drug effectiveness poses a significant challenge for the conventional strategies. Even today's best sold, 'blockbuster' drugs, poster children of the current treatment paradigm, work in only 35% - 75% of patients due to influences of genetics, lifestyle and environmental differences [1, 2]. Hence, modern medicine is undergoing a paradigm shift towards a more personalized, patient-customized treatment model, for which a large part is based on a deeper understanding at a molecular level [3, 4]. For this emerging concept known as personalized or precision medicine, it is paramount to better understand the effects of a drug not only in the overall population, but in the individual patient as well [5]. Customization using a sub-population or patient's individual characteristics, e.g. genetic information, could decrease risks of ineffective treatment, dosing or side-effects [2, 6, 7]. Genetic testing is already available for approximately 2000 clinical conditions today, most of which are in oncology. Two successful examples are genetic tests for HER2-positive breast cancer which serve as a predictor of response to the drug Herceptin, and CYP450 polymorphisms which affect the action and metabolism of drugs such as selective serotonin-reuptake inhibitors [6-9]. Despite the promise shown by these examples, most drug targets and disease mechanisms are still in

dire need of further research to determine whether, and how, genetic variation affects both pathology and drug responses.

GPCRs and genetic differences

The majority of drug targets today are GPCRs, a specific class of membrane proteins. In fact, 30-40% of all current drugs work by influencing GPCR function [10, 11]. This is no surprise as approximately 800 GPCRs are encoded by the human genome. Over 300 of these are considered druggable, i.e. they constitute current or future drug targets [12]. Due to their ubiquity, GPCRs are involved in almost all aspects of human physiology from vision to immune response [13]. In general terms, the role of a GPCR is to translate an extracellular signal, which can range from photons to odorants, hormones or neurotransmitters, into a cellular response. Depending on the nature of ligand and receptor, the cellular effect can vary from changes in morphology to proliferation, differentiation and survival (**Figure 1**).

Due to their physiological importance, it is highly interesting to decipher the influence of genetic variation in GPCR-mediated drug responses in the context of personalized medicine [5, 14]. Several studies have already linked GPCR polymorphisms to diseases and drug response variation [14-18], including for instance serotonin [15], dopamine [14, 16, 19-21], adenosine [22-24], purinergic [25, 26] and cannabinoid [17, 18] receptors, and many other commonly targeted GPCRs [14].

Single Nucleotide Polymorphisms

One prevalent source of genetic differences which can lead to an alteration in the drug target are Single Nucleotide Polymorphisms (SNPs). SNPs make up 84 to 95% of the total human genetic variation and are defined as single-base variations with a presence in at least one percent of the population. Consequently, SNPs are quite common, with on average around one SNP per 300 bases [27]. These variations can cause a multitude of differences in the end-product of genes, depending on their location and nucleotide difference. For example, a SNP can cause a new start- or stopcodon to appear, cause the transcript to be removed or even change the encoded amino acid with a different one, i.e. a so called missense SNP. SNPs that somehow change the amino acid sequence of the resulting protein are known as non-synonymous SNPs. It is believed that such changes are the most prevalent source of differences in GPCR response to drugs (**Figure 2**).

A common example is the association between SNPs on the chemokine 2 and 5

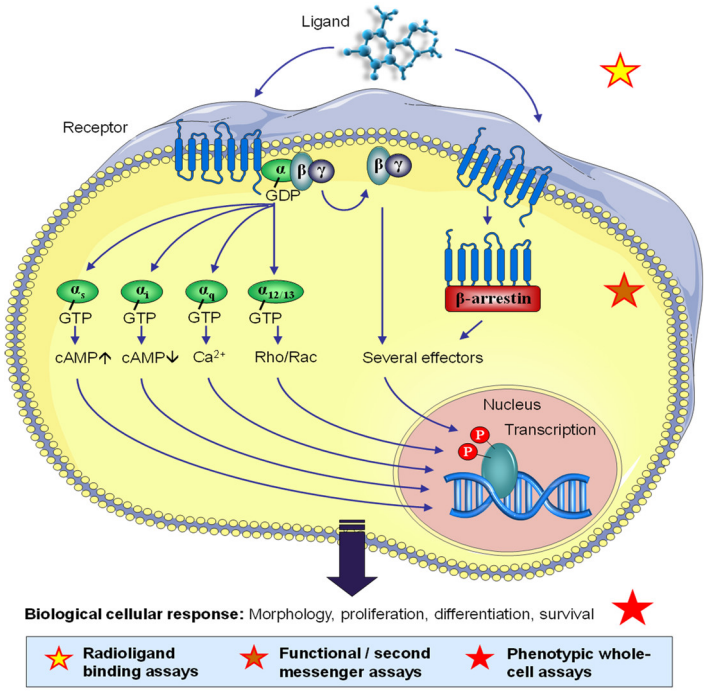

Figure 1: GPCR signaling and *in vitro* assays. When a ligand binds to and activates a GPCR, the receptor in turn activates the G protein. The trimeric G protein dissociates and can activate various secondary messenger pathways, leading via a cascade of reactions to an eventual cellular response. Traditional drug development programs are often target-focused, i.e. relying on *in vitro* assays which use reporter systems for the investigated target. Such reporter systems include for instance the use of radioactive labels or fluorescent dyes for ligand, target or effector labeling, or of more downstream reporter gene constructs. Such modifications, however, may influence target pharmacology. Label-free whole-cell assays are phenotypic assays that capture the biological cellular response in real-time, without focusing on merely one pathway and without requiring any such modifications, potentially providing a better physiological context. Image constructed using components from Servier Medical Art by Servier (*http://www.servier.com/Powerpoint-image-bank*).

receptors (CCR2 and CCR5) and the delayed or increased onset of AIDS after HIV infection [28]. In another instance, a SNP-caused tryptophan to arginine change in the β3-adrenergic receptor has been associated with obesity [29]. A set of four SNP locations on the dopamine D3 receptor have been associated with schizophrenia, where the susceptibility to the disease is most likely caused by the combined effect of these SNPs [30]. In the GRM1 glutamate receptor, the presence of SNPs in the splice region between two exons causes a new splice variant lacking one transmembrane domain, again associated with schizophrenia symptoms [31]. These examples emphasize that the possible influence of SNPs on GPCRs can be quite

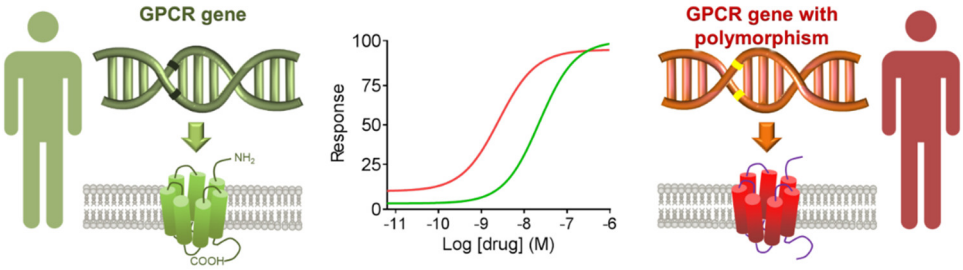

Figure 2: Effects on individuals of SNPs in GPCRs. GPCR polymorphisms can lead to differences in drug response between individuals, potentially changing drug effectiveness and risks of side-effects.

profound. However, the knowledge of polymorphism effects in GPCRs is still scant as of today. Hence we sought to find out more on the influence SNPs have on ligand-induced GPCR function in this thesis.

Lymphoblastoid Cell Lines

Most evidence supporting the influence of GPCR polymorphism effects are based on statistic association with occurrence of a disease, or by functional characterization in artificial, heterologous cell lines [14, 16, 17]. Both methods lack the final, well-defined physiological link that would allow us to understand more precisely how a polymorphism changes GPCR effects in an individual patient [32, 33]. Such understanding could be provided by directly measuring drug responses in patient material or cells as a model system.

An upcoming phenomenon in the past two decades are biobanks, which collect and store biological material to support modern medical research such as -omics approaches and personalized medicine. For this purpose, biobanks provide biomaterial resources including tissues, cells, blood, and serum from patients with specific diseases, specific populations or individuals with specific traits [34-36]. One type of cells used in many biobanks as a preferred choice for storing genetic material are lymphoblastoid cell lines (LCLs), which are derived from a person's B-Lymphocytes [37, 38]. Renowned consortia with LCL libraries include the Centre d'Étude du Polymorphisme Humain, the International HapMap and 1000 genomes projects [39-43]. In most cases, however, LCLs are merely used as a source of DNA or RNA for genotyping, expression or methylation studies [16, 37].

In this thesis, we set out to show that LCLs can be used as a model system to directly study polymorphism effects on GPCR function on a cellular level.

Label-free technologies

Traditional GPCR assays are often label-based, which have definite disadvantages when venturing to remain as close to the physiological situation as possible. These assays rely on (chemical) engineering by, for instance, radioligand tagging or overexpression of the receptor (**Figure 1**). All of such alterations to the cell may influence its physiology leading to for instance identification of false-positive or false-negative hits [44]. Furthermore, such assays are mostly pathway-biased as they typically focus on only one cellular event in a specific signaling pathway [45]. Another drawback is that they often lack the sensitivity required for receptors endogenously expressed in cell lines, as this is much lower level than in specifically engineered cell lines. In short, such assays are not well-suited for investigating subtle polymorphism changes on endogenous receptors in their native environment.

However, new assays are emerging that enable measurements in endogenous cell lines and hereby provide greater, more relevant biological insight. By eliminating any need for labels, label-free cellular biosensors have the capability of assessing endogenous receptor function in their native physiological settings [46]. They are more sensitive, less invasive and monitor drug effects on a whole cell in real-time [33, 47, 48]. Hence, label-free assays are also more translational towards a correlation between *in vitro* and *in vivo* findings [49, 50]. Moreover, the sensitivity of these label-free assays allows monitoring of standard effects such as GPCR activation or inhibition as well as detection of smaller changes such as biased signaling [33, 51], which may also be affected by polymorphisms [5]. In short, label-free technologies offer unique advantages for precision medicine as they offer the ability to monitor small changes in GPCR signaling or drug responses in the native cellular context.

Objective and overview of this thesis

Aim and set-up

The aim of the study was to provide detailed insight in the influence of genetic variation on ligand-induced GPCR function within the general human population. Our selection process of SNP containing GPCRs to be investigated with label-free technology and LCLs is visualized in **Figure 3**. In this thesis we focused on SNPs that are likely to have a profound effect on GPCR signaling responses by changing the amino acid sequence, in particular the so-called missense SNPs. The biobank employed in this research, the Netherlands Twin Registry (NTR; *http://www.tweelingenregister.org/en/*) [39], offered genotyped LCLs of individuals with a family structure consisting of parents and twin siblings. We first established an overview of such SNPs on each druggable, non-olfactory GPCR gene within these NTR individuals, after

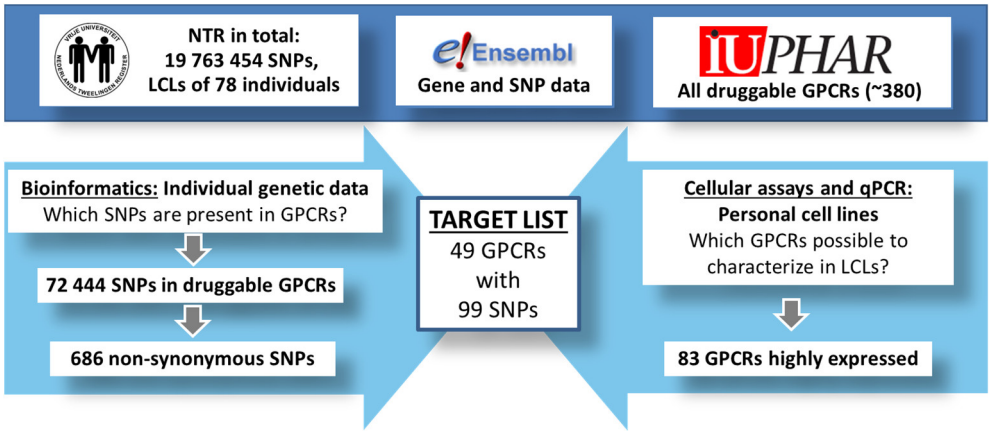

Figure 3: Flowchart of target selection. The selection was aimed at identifying all druggable GPCRs containing non-synonymous SNPs that were well enough expressed to allow functional characterization in LCLs from the NTR. For the bioinformatics, the selection was limited to non-synonymous SNPs in druggable GPCRs. The genotype data of the cell lines was provided by the NTR, as part of the Genomes of the Netherlands (GoNL) consortium [39]. A list of all druggable non-olfactory GPCRs was downloaded from the IUPHAR database. SNPs within each gene were extracted from the NTR data using PLINK, an open-source whole genome association analysis toolset, and annotated with their SNP-consequence types (gene data, SNP location and consequences were extracted from Ensembl). Cellular assays and qPCR were used to determine which GPCRs were expressed above a threshold that allowed functional responses to be measured using the label-free technology.

which we pursued several interesting cases in GPCRs commonly used in drug research.

Three separate cases of common polymorphisms that affect GPCR signaling and cellular effects were discovered, each revealing different properties including the sensitivity of partial versus full agonists, different chemical scaffolds and intron versus missense SNPs. These examples should provide the reader with insights that will hopefully lead to the development of clinically more effective drugs and drug treatment paradigms in the long term.

Outline of this thesis

The concept of using patient-derived cell lines as model systems is introduced and discussed in **Chapter 2**. This chapter furthermore highlights the advantages of label-free technology for assays on such cell lines.

Chapter 3 focuses on the optimization and application of an impedance-based label-free assay, the xCELLigence, to suspension cells such as LCLs to allow direct measurement of cellular effects of GPCR signaling.

Chapter 4 presents the case of the Adenosine A_{2A} receptor, in which an intron SNP is related to differential cellular effects of a partial agonist, but not full agonists or antagonists. **Chapter 5** summarizes the effects on a highly common non-synonymous polymorphism on the Cannabinoid Receptor 2, to which different chemical scaffolds show different sensitivity. **Chapter 6** presents the case of the Glucose-Dependent Insulinotropic Polypeptide (GIP) Receptor, in which a missense SNP that has often been associated with diseases changes the cellular effects of the endogenous ligand.

The research presented in these chapters highlights that coding and non-coding, common and less common genetic variations in GPCRs can affect endogenous signaling as well as drug effects.

An overall conclusion from the results described in this thesis and forthcoming opportunities for drug discovery and treatment are presented and discussed in **Chapter 7**.

References

1. Carey, J. *Making personalized medicine pay*. BusinessWeek 2010 [cited 2015 24.06.2015]; Available from: *http://www.bloomberg.com/bw/magazine/content/10_05/b4165058407403.htm*.
2. van't Veer, L.J. and R. Bernards, *Enabling personalized cancer medicine through analysis of gene-expression patterns.* Nature, 2008. **452**(7187): p. 564-70.
3. Kojima, R., D. Aubel, and M. Fussenegger, *Novel theranostic agents for next-generation personalized medicine: small molecules, nanoparticles, and engineered mammalian cells.* Curr Opin Chem Biol, 2015. **28**: p. 29-38.
4. Lu, Y.F., et al., *Personalized medicine and human genetic diversity.* Cold Spring Harb Perspect Med, 2014. **4**(9).
5. Venkatakrishnan, A.J., et al., *Molecular signatures of G-protein-coupled receptors.* Nature, 2013. **494**(7436): p. 185-94.
6. Mirnezami, R., J. Nicholson, and A. Darzi, *Preparing for precision medicine.* The New England journal of medicine, 2012. **366**(6): p. 489-91.
7. Katsanis, S.H., G. Javitt, and K. Hudson, *Public health. A case study of personalized medicine.* Science, 2008. **320**(5872): p. 53-4.
8. Weng, L., et al., *Pharmacogenetics and pharmacogenomics: a bridge to individualized cancer therapy.* Pharmacogenomics, 2013. **14**(3): p. 315-24.
9. Probst-Schendzielorz, K., R. Viviani, and J.C. Stingl, *Effect of Cytochrome P450 polymorphism on the action and metabolism of selective serotonin reuptake inhibitors.* Expert Opin Drug Metab Toxicol, 2015. **11**(8): p. 1219-32.
10. Overington, J.P., B. Al-Lazikani, and A.L. Hopkins, *How many drug targets are there?* Nat Rev Drug Discov, 2006. **5**(12): p. 993-6.
11. Rask-Andersen, M., M.S. Almen, and H.B. Schioth, *Trends in the exploitation of novel drug targets.* Nat Rev Drug Discov, 2011. **10**(8): p. 579-90.
12. Russ, A.P. and S. Lampel, *The druggable genome: an update.* Drug Discov Today, 2005. **10**(23-24): p. 1607-10.
13. Lagerstrom, M.C. and H.B. Schioth, *Structural diversity of G protein-coupled receptors and significance for drug discovery.* Nat Rev Drug Discov, 2008. **7**(4): p. 339-57.
14. Sadee, W., et al., *Genetic variations in human G protein-coupled receptors: implications for drug therapy.* AAPS pharmSci, 2001. **3**(3): p. 54-80.
15. Davies, M.A., et al., *Pharmacologic analysis of non-synonymous coding h5-HT2A SNPs reveals alterations in atypical antipsychotic and agonist efficacies.* Pharmacogenomics J, 2006. **6**(1): p. 42-51.
16. Docherty, S.J., et al., *A genetic association study of DNA methylation levels in the DRD4 gene region finds associations with nearby SNPs.* Behav Brain Funct, 2012. **8**: p. 31-44.
17. Ishiguro, H., et al., *Brain cannabinoid CB2 receptor in schizophrenia.* Biol Psychiatry, 2010. **67**(10): p. 974-82.
18. Tong, D., et al., *Association of single-nucleotide polymorphisms in the cannabinoid receptor 2 gene with schizophrenia in the Han Chinese population.* J Mol Neurosci, 2013. **51**(2): p. 454-60.

19. Al-Fulaij, M.A., et al., *Pharmacological analysis of human D1 AND D2 dopamine receptor missense variants.* Journal of molecular neuroscience : MN, 2008. **34**(3): p. 211-23.
20. Ishiguro, H., et al., *Mutation and association analysis of the 5' region of the dopamine D3 receptor gene in schizophrenia patients: identification of the Ala38Thr polymorphism and suggested association between DRD3 haplotypes and schizophrenia.* Molecular psychiatry, 2000. **5**(4): p. 433-8.
21. Lundstrom, K. and M.P. Turpin, *Proposed schizophrenia-related gene polymorphism: expression of the Ser9Gly mutant human dopamine D3 receptor with the Semliki Forest virus system.* Biochemical and biophysical research communications, 1996. **225**(3): p. 1068-72.
22. Bodenmann, S., et al., *Polymorphisms of ADORA2A modulate psychomotor vigilance and the effects of caffeine on neurobehavioural performance and sleep EEG after sleep deprivation.* British journal of pharmacology, 2012. **165**(6): p. 1904-13.
23. Childs, E., et al., *Association between ADORA2A and DRD2 polymorphisms and caffeine-induced anxiety.* Neuropsychopharmacology : official publication of the American College of Neuropsychopharmacology, 2008. **33**(12): p. 2791-800.
24. Freitag, C.M., et al., *Adenosine A(2A) receptor gene (ADORA2A) variants may increase autistic symptoms and anxiety in autism spectrum disorder.* European child & adolescent psychiatry, 2010. **19**(1): p. 67-74.
25. Buscher, R., et al., *P2Y2 receptor polymorphisms and haplotypes in cystic fibrosis and their impact on Ca2+ influx.* Pharmacogenetics and genomics, 2006. **16**(3): p. 199-205.
26. Wesselius, A., et al., *Association of P2Y(2) receptor SNPs with bone mineral density and osteoporosis risk in a cohort of Dutch fracture patients.* Purinergic signalling, 2013. **9**(1): p. 41-9.
27. Kruglyak, L. and D.A. Nickerson, *Variation is the spice of life.* Nature Genetics, 2001. **27**(3): p. 234-236.
28. Fellay, J., et al., *Common genetic variation and the control of HIV-1 in humans.* PLoS Genet, 2009. **5**(12): p. e1000791.
29. Mitchell, B.D., et al., *A paired sibling analysis of the beta-3 adrenergic receptor and obesity in Mexican Americans.* J Clin Invest, 1998. **101**(3): p. 584-7.
30. Sivagnanasundaram, S., et al., *A cluster of single nucleotide polymorphisms in the 5'-leader of the human dopamine D3 receptor gene (DRD3) and its relationship to schizophrenia.* Neurosci Lett, 2000. **279**(1): p. 13-6.
31. Frank, R.A., et al., *Clustered coding variants in the glutamate receptor complexes of individuals with schizophrenia and bipolar disorder.* PLoS One, 2011. **6**(4): p. e19011.
32. Eglen, R. and T. Reisine, *Primary cells and stem cells in drug discovery: emerging tools for high-throughput screening.* Assay Drug Dev Technol, 2011. **9**(2): p. 108-24.
33. Yu, N., et al., *Real-time monitoring of morphological changes in living cells by electronic cell sensor arrays: an approach to study G protein-coupled receptors.* Anal Chem, 2006. **78**(1): p. 35-43.
34. Artene, S.A., et al., *Biobanking in a constantly developing medical world.* ScientificWorldJournal, 2013. **2013**: p. 343275.

35. Ministers, C.o.E.a.C.o., *Recommendation Rec 4 of the Committee of Ministers to Member States on Research on Biological Materials of Human Origin*, S. European Commission, France, Editor 2006.
36. *https://ec.europa.eu/research/swafs/pdf/pub_archive/biobanks-for-europe_en.pdf*. 03.05.2016].
37. Sie, L., S. Loong, and E.K. Tan, *Utility of lymphoblastoid cell lines.* J Neurosci Res, 2009. **87**(9): p. 1953-9.
38. Sugimoto, M., et al., *Steps involved in immortalization and tumorigenesis in human B-lymphoblastoid cell lines transformed by Epstein-Barr virus.* Cancer research, 2004. **64**(10): p. 3361-4.
39. Willemsen, G., et al., *The Netherlands Twin Register biobank: a resource for genetic epidemiological studies.* Twin Res Hum Genet, 2010. **13**(3): p. 231-45.
40. Abecasis, G.R., et al., *A map of human genome variation from population-scale sequencing.* Nature, 2010. **467**(7319): p. 1061-73.
41. Welsh, M., et al., *Pharmacogenomic discovery using cell-based models.* Pharmacological reviews, 2009. **61**(4): p. 413-29.
42. Dausset, J., et al., *Centre d'etude du polymorphisme humain (CEPH): collaborative genetic mapping of the human genome.* Genomics, 1990. **6**(3): p. 575-7.
43. Wheeler, H.E. and M.E. Dolan, *Lymphoblastoid cell lines in pharmacogenomic discovery and clinical translation.* Pharmacogenomics, 2012. **13**(1): p. 55-70.
44. Lee, P.H., et al., *Evaluation of dynamic mass redistribution technology for pharmacological studies of recombinant and endogenously expressed g protein-coupled receptors.* Assay Drug Dev Technol, 2008. **6**(1): p. 83-94.
45. Tran, E. and F. Ye, *Duplexed label-free G protein--coupled receptor assays for high-throughput screening.* J Biomol Screen, 2008. **13**(10): p. 975-85.
46. Verdonk, E., et al., *Cellular dielectric spectroscopy: a label-free comprehensive platform for functional evaluation of endogenous receptors.* Assay Drug Dev Technol, 2006. **4**(5): p. 609-19.
47. Fang, Y., *Label-Free Receptor Assays.* Drug Discov Today Technol, 2011. **7**(1): p. e5-e11.
48. Rocheville, M., et al., *Mining the potential of label-free biosensors for seven-transmembrane receptor drug discovery.* Progress in molecular biology and translational science, 2013. **115**: p. 123-42.
49. Ferrie, A.M., H. Sun, and Y. Fang, *Label-free integrative pharmacology on-target of drugs at the beta(2)-adrenergic receptor.* Sci Rep, 2011. **1**: p. 33.
50. Morse, M., et al., *Ligand-directed functional selectivity at the mu opioid receptor revealed by label-free integrative pharmacology on-target.* PLoS One, 2011. **6**(10): p. e25643.
51. Stallaert, W., et al., *Impedance responses reveal beta(2)-adrenergic receptor signaling pluridimensionality and allow classification of ligands with distinct signaling profiles.* PLoS One, 2012. **7**(1): p. e29420.

CHAPTER 2

Label-free technology and patient cells: from early drug development to precision medicine

Julia M. Hillger

Wai-Ling Lieuw

Laura H. Heitman

Adriaan P. IJzerman

Drug discovery today, 2017. pii: S1359-6446(17)30153-8.

DOI: http://dx.doi.org/10.1016/j.drudis.2017.07.015

Abstract

Drug development requires physiologically more appropriate model systems and assays to increase understanding of drug action and pathological processes in the human individual. Specifically patient-derived cells offer great opportunities as representative cellular model systems. Moreover, with novel label-free cellular assays it is often possible to investigate complex biological processes in their native environment. Combining these two offers distinct opportunities for increasing physiological relevance.

Here, we review impedance-based label-free technologies in the context of patient samples, focusing on commonly used cell types including fibroblasts, blood components and stem cells. Applications extend as far as tissue-on-a-chip models. Thus, applying label-free technologies to patient samples can produce highly biorelevant data and with it unique opportunities for drug development and precision medicine.

Introduction

Two significant challenges in today's drug development are the inter-individual variability in drug effectiveness, and lack of translatability of preclinical results. Simultaneously, modern medicine is shifting towards personalized or precision medicine, which proposes to use individual characteristics of a specific patient or sub-population to tailor drug prescriptions, hereby decreasing risks of ineffective dosing or side-effects [1]. Challenges to achieve this are in a generally perceived lack of understanding of the molecular details of drug action and of pathological processes in the human individual. This, in turn, is to a large degree brought about by insufficient physiological representability of model systems and assays used in drug research. Traditional drug research has relied on a target-focused approach by screening compounds in *in vitro* assays. Such assays traditionally use reporter systems, for instance radiolabeled or fluorescent probes, dyes, and reporter gene constructs, all of which are modifications that may influence target pharmacology (**Box 1, Fig. 1**). In addition, cellular

BOX 1: Traditional label-based versus label-free assays.

Traditional label-based assays follow drug effects and cellular functions by chemical attachment of a "label" to the drug molecule, drug target or downstream effectors. These can consist of for instance radiolabeled or fluorescent probes or dyes. Reporter-based assays introduce specifically regulated gene promoters as biomarkers for specific events. Commonly used reporter genes involve visually identifiable characteristics such as fluorescent and luminescent proteins.

Label-free assays do not require any such modifications as they measure cellular changes by alternative detection means, without the need for introducing chemical or bioengineered modifications.

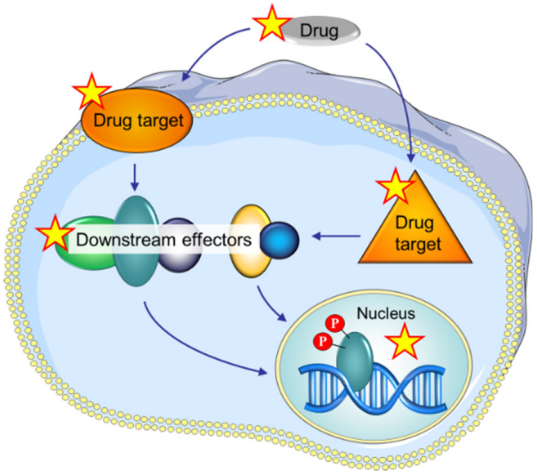

Figure 1. Traditional label-based assays. Stars highlight where effects are often measured by introducing labels or reporters. Image constructed using components from Servier Medical Art by Servier (*http://www.servier.com/Powerpoint-image-bank*).

models and cell systems are often selected based on habit and technical feasibility rather than disease relevance, resulting in physiologically less representative heterologous or recombinant cells lines. Such renewable in vitro cell sources have been essential in facilitating drug discovery and certainly have merits for studying target or drug action in more detail. However, both assay and model systems are factors that can contribute to an eventual lack of clinical effectiveness and thus the issues experienced in the drug development to date, such as high attrition rates [2]. To fully comprehend the mechanisms underlying pathologies, drug response and its variation in individuals, functional characterization on a physiologically relevant molecular and cellular level is essential. Hence, the focus is shifting onto more physiologically appropriate cellular models and readout systems. Specifically patient-derived cells offer great opportunities when used directly as a model system. Novel label-free cellular assays are a new type of phenotypic assay able to acquire the molecular-level understanding from complex biological processes in their native environment [1, 2]. Applying them to human primary cells can increase physiological relevance [3-5]. In this review, we highlight the realm of these possibilities, by focusing on the application of one type of such label-free cellular assays, based on impedance, on some of the most common types of human primary cells derived from patient samples.

Advantages of Label-free cellular assay technologies

The two currently most used forms of label-free cellular biosensors are impedance- or optics-based. Extensive reviews on the detection principles are provided elsewhere [6-8]. In short, the ECIS, xCELLigence, and CellKey systems use an electrode array biosensor to measure impedance changes in a cell monolayer (**Fig. 2**). Optical systems such as the EPIC and BIND use resonant waveguide grating to detect dynamic mass redistribution in cells. Both optical and impedance methods detect a wide spectrum of cellular changes, from cell adhesion to life cycle processes such as proliferation, growth and death, as well as pathogen infections and response, cell migration and signaling such as receptor signaling or cell-cell communication [6]. Hence, these label-free assays are also known as phenotypic assays.

In this review, we focus on impedance-based assays which are applicable to a broad range of samples, are highly versatile and can integrate many assays into one (see also **Fig. 3**). For instance, such assays record a variety of cellular parameters including proliferation, adhesion and cellular morphology in one combined read-out in real-time(**Fig. 3A**). This is a particular advantage over many traditional assays, which often interrogate one aspect only of a given pathway or a cellular response (e.g., second messenger accumulation).

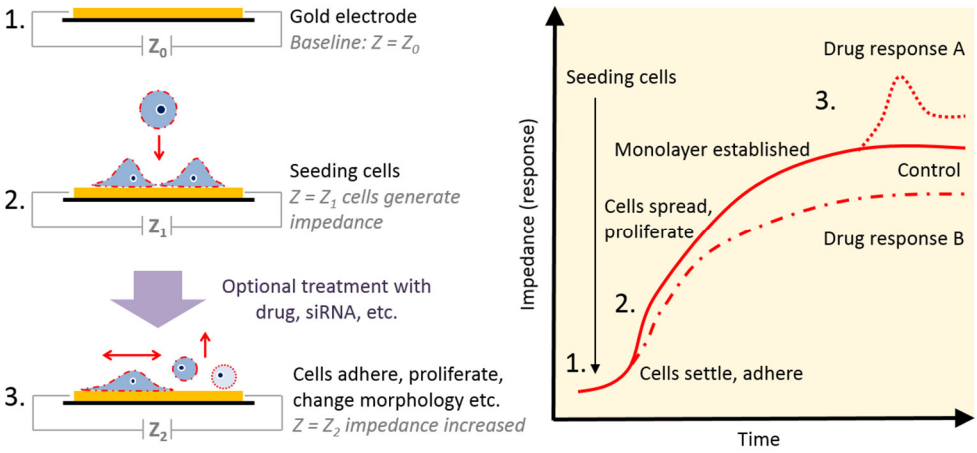

Figure 2. Principle of impedance-based label-free cellular assays. Cell attachment to gold electrodes generates impedance by changing the local ionic environment at the electrode-solution interface. Relative changes in impedance (Z) are recorded in real-time. **1.** Prior to the seeding of cells, baseline impedance is Z0. **2.** As cells adhere to the electrodes, impedance increases proportionally. **3.** Changes in cell number, adhesion, viability and morphology are directly reflected in the impedance profile. Impedance-based label-free cellular assays can detect a wide range of cellular events including cell proliferation, division, growth, death, migration and signaling. All these parameters can in turn be affected by drugs. For instance, depending on the moment of drug treatment, drugs can result in response A by initiating receptor signaling or drug response B by decreasing overall proliferation.

Impedance-based assays offer the distinct advantage of a direct read-out of drug action in real-time. While there are also traditional assays which record specific functions in real-time (e.g., Ca^{2+}-mobilization assays) impedance measurements offer the benefits of real-time measurements in both acute (eg. direct receptor signalling) and chronic settings (e.g., cellular proliferation). Besides recording the abovementioned cellular functions, impedance-based label-free assays also provide some specialist applications such as electrical stimulation for pore formation (**Fig. 3D**) and co-culture without contact (**Fig. 3H**), though these may require specialized recording or plate equipment (**Fig. 3B, 3E, 3H**). Overall, impedance-based assays have already successfully been applied to an extensive list of targets, including highly important drug target classes such as G protein-coupled receptors (GPCRs) [6, 9], nuclear receptors [10] and receptor tyrosine kinases [11]. Applications extend as far as toxicity screens on cardiac function [12] and migration of cancer cells in 3D cultures [13] (**Fig. 3B** and **3E**). Furthermore, almost any cell type can be studied. Examples include standard recombinant cell lines, primary and stem cells, both adherent as well as suspension cell types [6, 9, 14] (see also **Table 1**). This is because in comparison to many traditional assays, label-free technologies offer a sensitive, less invasive detection methodology that monitors drug

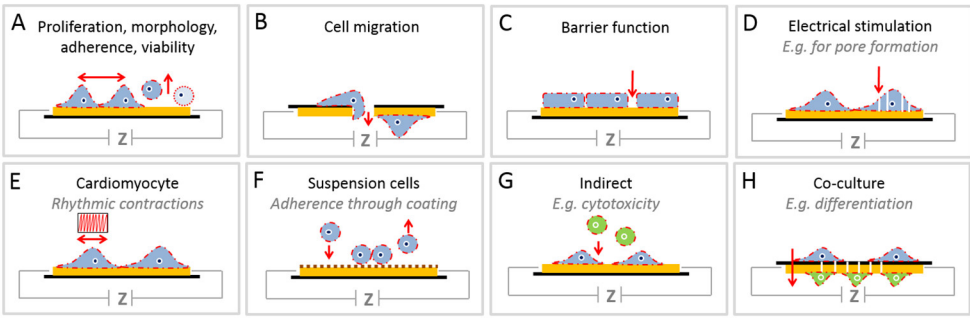

Figure 3: Typical applications of impedance-based label-free cellular assays. (**A**) General label-free cellular assay formats are capable of monitoring many cellular functions such as adherence, proliferation, viability and morphology. Additional specialized assay applications exist for instance to (**B**) monitor cell migration (e.g. through a porous membrane, xCELLigence), (**C**) measure barrier functionality for instance in a wound scratch assay, (**D**) apply electrical impulses e.g. to increase cellular permeability (ECIS) and (**E**) measure (cardio)-myocyte contractility (xCELLigence CARDIO system). (**F**) Besides adherent cells, label-free cellular assays are also applicable to suspension cells and capable of monitoring interactions between two cell types, for instance by (**G**) cytotoxicity of effector cells on another type of target cell, or (**H**) cell-cell communication without actual cellular contact (xCELLigence co-culture set-up).

effects on a whole cell. Furthermore, without the need for tagging, labeling or recombinant expression, cellular functions can be studied in a more physiological context, including a vast amount of endogenously expressed targets and pathways. Simultaneously, sensitivity is often high enough to distinguish subtle changes in mechanisms of action in e.g., GPCR signaling bias [6, 14]. Receptors are linked to various downstream signaling pathways, termed signaling pluridimensionality. Ligands can be biased towards one or some particular downstream pathways, potentially resulting in different pharmacological effects. For instance, closely related agonists for the β2- adrenergic receptor induced subtly yet distinctly different response signatures as a consequence of such bias [15, 16].

Hence, as a number of reviews have already summarized, label-free technologies can offer distinct advantages for drug development. They capture compound action in a dynamic time-resolved manner, allow for identification of leads independent of prior assumptions of signaling pathways and enable the use of more native systems at higher through-put. As a cell-phenotypic screen, they can be used for target identification, compound screening, lead selection, investigating mechanism of action and testing drug safety and toxicity [14, 17]. In this review we particularly focus on applications involving patient cells. This offers opportunities both for drug development and precision medicine research by sensitively detecting an extensive variety of pharmacological effects under minimally invasive conditions in a clinically relevant endogenous context of primary cells, and even patient samples.

Nowadays, such samples are increasingly available to support research, for instance by their systematic collection in biobanks.

Advantages of primary human cells

Over the past decades, numerous biobanks have emerged to support medical research by programmed storage of biological material and corresponding data. These biomaterials include tissues, (stem) cells, blood, and serum, all of which have played a critical role in medical research. These materials are actively used from translational and personalized medicine research to target and drug discovery [18, 19]. For human physiology, primary human cells are considered a much better model system than the more traditional cellular models such as rodent, recombinant, or immortalized non-tissue specific human cell lines, and even better than *in-vivo* rodent models [20-22]. While the mentioned cellular models certainly have merits, for instance ease-of-use or to attain initial understanding of pathways, their physiological relevance is questioned increasingly. In recombinant cell lines, target overexpression, differences in intracellular metabolic conditions and products from other genes could modify cellular responses [5]. Well-established cell lines derived from a patient with a particular disease can be more representative of that specific pathological condition. However, these are generally immortalized cell lines derived from one particular patient sample a long time ago. Prolonged cell culture frequently leads to problems such as contamination or genotypic and phenotypic instability. These issues unfortunately contribute to irreproducibility in preclinical research, which is an increasingly well-recognized problem [23].

In general, primary cells express signaling pathways and retain many cellular functions that are seen *in vivo*, thus providing a more relevant context. Tissue or cell samples from healthy or patient volunteers are even more representative for (patho)physiology and closer to the situation in the clinic.

Application to patient samples and primary human cells

Many patient-related biomaterials can and have already been studied using impedance-based label-free technologies, of which some prominent examples are discussed here. The sample types most commonly studied include fibroblasts and blood components, but applications also extend to endothelial, epithelial and stem cells (**Table 1**). In these examples, label-free impedance-based assays are employed to monitor a wide range of cellular effects, including specific functions such as migration, epithelial barrier function or

Table 1. Application examples of impedance-based label-free cellular technology to patient samples and stem-cell related types.

Type	Subtype	Technology	Material source	Reference
Blood components	Antibodies	xCELLigence	Type I diabetes patients, type II diabetes patients and healthy controls	[37]
	PBMCs	xCELLigence	From healthy volunteers but tested on patient material	[32, 33]
	Plasma and cells therein	ECIS	Healthy volunteers vs. trauma patients	[35]
		ECIS	Hantavirus Cardiopulmonary Syndrome patients	[36]
	Monocytes	ECIS	Patients with peripheral vascular disease and abdominal aortic aneurysm	[31]
	Neutrophils	ECIS	Critically ill septic patients	[34]
	Serum	ECIS	Scleroderma patients	[27]
Cancer cells and related cells	γδ T cells	xCELLigence	Healthy volunteers and B-lineage acute lymphoblastic leukemia patients	[60]
	Glioblastoma cells	xCELLigence	Paired tumoral and peritumoral tissue samples from glioblastoma patients	[54]
	Malignant melanoma cells	xCELLigence	Malignant melanoma of the ciliary body from a female patient	[55]
	Malignant pleural effusions	xCELLigence	Patients with solid tumors	[59]
	Mesenchymal chondrosarcoma cells	xCELLigence	Newly established cell line from patient	[56]
	Mononuclear cells	xCELLigence	Normal controls and breast cancer patients	[61]
	Myxofibrosarcoma cells	xCELLigence	Myxofibrosarcoma patient	[58]
	Non-small-cell lung carcinoma cells	xCELLigence	Non-small-cell lung carcinoma patient	[57]
	Normal and neoplastic mammary cells	xCELLigence	Patient-derived primary human breast cancer epithelial cells	[8]
	Ovarian cancer cells	xCELLigence	Serous ovarian cancer patient and endometrioid peritoneal cancer patient	[53]
Chondrocytes	Chondrocytes and cartilage tissue	xCELLigence	Osteoarthritic patients	[32]

Fibro-blasts	Benign prostatic hyperplasia	xCELLigence	Benign prostatic hyperplasia patients	[26]
	Dermal	ECIS	Scleroderma patients and normal controls	[27]
	Orbital	ECIS	Patients with or without Graves' disease	[24]
	Synovial	xCELLigence	Patients with rheumatoid arthritis or osteoarthritis	[28-30]
iPSCs and similar stem cell types	Adipose stromal/ stem cells	ECIS	Healthy human donors of varying age groups	[51]
		xCELLigence	Female patients undergoing liposuction, model for obesity	[52]
	iPSC cardiomyocytes	xCELLigence	Healthy human donors or commercial from Cellular Dynamics (CDI; *http://www.cellulardynamics.com/products/cardiomyocytes.html*)	[12, 43-45]
	iPSC Retinal pigment epithelium	ECIS	Age-related macular degeneration patient and unaffected sibling	[47]
	Mesenchymal stromal/stem cells	ECIS and xCELLigence	From bone marrow (three donors) and adipose tissue (two donors)	[48]
		xCELLigence	From endometrial lining of the human uterus of premenopausal women	[49]
		xCELLigence	Healthy human donors	[50]
		xCELLigence	Osteoarthritic patients	[33]
Myo-blasts	Skeletal muscle myoblasts and myotubes	xCELLigence	Chronic heart failure patients and age and gender-matched healthy donors	[62, 63]

cardiomyocyte beating (Fig. 3). Overall, the highlighted examples show that impedance-based label-free technology is highly versatile with an extensive range of applications.

Fibroblasts

The earliest applications of label-free assays to fibroblasts date back to over two decades. In one early example, prostaglandin E2 was shown to play a significant role in Graves' disease pathology by comparing morphological changes of orbital fibroblasts from patients with and without Graves' disease versus dermal fibroblasts (**Fig. 3A**). The authors chose ECIS over traditional light microscopy after testing both methodologies head to head, as it offered insight into the subtle, rapid cellular changes, especially into the underlying kinetics [24].

Since then, label-free cellular assays have been applied to other types of fibroblasts. Fibroblasts are in fact the most common cell type in human connective tissue and can often

retain memory of their previous tissue context, thus giving rise to numerous fibroblast types (Table 1). They are also among the most commonly employed clinical and biobanked samples in general [25]. For instance, Nolte *et al.* demonstrated a potential strategy against hyper-proliferating fibroblasts by treating fibroblasts from benign prostatic hyperplasia patients with small interfering RNA against the transcription factor serum response factor. Effects on cell proliferation and growth inhibition were detected with the xCELLigence (Fig. 3A) [26]. Another notable study involved dermal fibroblasts and sera from scleroderma patients, which is discussed later [27].

Finally, in a clinically relevant setting synovial fibroblasts from patients with rheumatoid arthritis (RA) or osteoarthritis (OA) obtained during knee surgery were investigated. In the most recent ones, Lowin *et al.* used the xCELLigence to show that the endocannabinoid system is involved in regulating inflammatory effects in RA [28]. This suggested a potential treatment for RA with synthetic cannabinoids, demonstrated in a later study [29]. Similar studies showed further contributors to the pathogenesis of RA that modify cellular functions and adhesion of synovial fibroblasts, the most recent of which are included in Table 1 [30]. The relevance and implications of these findings for potential treatment options are of translational value as the cells were obtained from patients with the disease.

Blood cells

Blood is an easily obtained patient material and is thus often biobanked [25]. Hence, various types of blood components or cells are used in medical research and have been investigated using impedance-based label-free cellular assays.

Several studies involving monocytes have been published. Interestingly, monocytes are often measured indirectly by quantifying their effect on another cell type. A layer of adherent target cells is grown on the electrodes, after which they are exposed to the effector cells, here monocytes, which induce for instance cytotoxicity in the target cells (Fig. 3G). Lee *et al.* used ECIS to reveal differences between patients of peripheral vascular disease and abdominal aortic aneurysm to find better methods for targeted therapy. Monocytes of peripheral vascular disease patients induced higher endothelial barrier dysfunction [31].

Another particularly useful type of blood cells are peripheral blood-derived mononuclear cells (PBMCs). Hopper *et al.* showed PBMCs enhanced osteoarthritic human chondrocyte migration, which could be the basis for a treatment strategy for OA. The PBMCs were derived from healthy volunteers, while chondrocytes and cartilage tissue explants were from patients undergoing total knee replacement. Here, migration and chemokinetic potential of the cells

were measured using a specialized migration assay format of the xCELLigence (**Fig. 3B**) [32]. Later it was shown that PBMCs also enhanced migration and chondrogenic differentiation of multipotent mesenchymal stromal cells (MSCs) from knees of OA patients [33].

Other types of blood components have been assayed using label-free technology as well, although most of them again rely on an indirect measurement through effects on another cell type. For instance, neutrophils from critically ill septic patients were found to reduce endothelial barrier integrity to a greater extent than untreated normal neutrophils in an ECIS assay [34]. Human serum was also employed in some studies. In an early example by Huang *et al.*, ECIS was used to demonstrate differences in micromotions of dermal fibroblasts from patients with scleroderma and normal controls, as well as the effect of sera from patients on fibroblast behavior [27]. Rahbar *et al.* measured the effects of plasma samples from healthy volunteers and severely injured trauma patients on human endothelial cells using ECIS. Material of patients with low plasma colloid osmotic pressure caused an increase in cell permeability [35]. In a similar manner, plasma samples of patients with Hantavirus Cardiopulmonary Syndrome were shown to induce loss of cell-cell adhesion in epithelial and endothelial cells in ECIS [36]. Finally, Jackson *et al*. employed xCELLigence to demonstrate that anti-calcium channel autoantibodies from patients with type I diabetes inhibit the adherence of Rat insulinoma cells, while antibodies from type II diabetes patients and healthy controls did not [37].

The reason that all these blood components are measured indirectly is twofold. On one hand, studying their effect on the function of other cell types provides more physiological context. On the other hand, many of the cell types involved are suspension cells. Label-free technology was long deemed incompatible with suspension cells, as the detection mechanism positioned at the bottom of the well requires cells to adhere [7]. However, a number of studies demonstrated that suspension cells are amenable to label-free technologies as well, with both optical and impedance-based biosensors. Interestingly, impedance-based assays appear less susceptible to decreased cellular adherence than optical biosensors [7], and hence potentially applicable to an even broader range of cell types. Examples include various types of blood cells, one notably involving personal cell lines. For instance, CellKey was used to directly measure GPCR signaling in monocytes, neutrophils and PBMCs, though these were not in fact patient material [38, 39]. The xCELLigence was applied to lymphoblastoid cell lines (LCLs) from participants of the Netherlands Twin Register to show effects of single nucleotide polymorphisms on GPCR signaling [9, 40]. On these

occasions, increased cell densities and usage of adherence-mediating agents were sufficient to allow measurements (Fig. 3F). LCLs are in fact used as a preferred choice for storing genetic material, including in biobanks of renowned consortia such as the International HapMap project [25, 41].

iPSC and common stem-cell types

Stem cells carry great promise for rendering physiologically more relevant cell models, in particular induced pluripotent stem cells (iPSCs). By reprogramming of e.g. fibroblasts into a pluripotent state, iPSCs can be derived that maintain the disease genotype and phenotype indefinitely. These iPSCs then provide a source of models for an expansive range of adult differentiated cells, possibly even for each individual patient, which has the potential to personalize drug discovery [42]. Many of the cell types derived from such iPSCs can be investigated using label-free technology. For one of these, a specific type of application has been developed for the xCELLigence, namely a cardiomyocyte-based biosensor. Safety pharmacology studies that evaluate potential cardiac (side) effects of drug candidates are an essential part of drug development. The xCELLigence RTCA Cardio System detects the beating rhythm of cardiomyocytes (Fig. 3E). It has been applied to human iPSC derived cardiomyocytes (hiPS-CMs) on several occasions to investigate risks of drug-induced arrhythmia and general cardiotoxicity, of which the most recent publications are listed in Table 1 [12, 43-45]. Rhythmic beating is essential for cardiomyocyte function, but has traditionally been hard to investigate in simple *in vitro* assays. Phenotypic measurements of native cellular systems are more suited for this [46]. The xCELLigence Cardio System capturing cardiac beating was in fact the most sensitive of various tests for detecting compounds with known clinical cardiac risk [43], and can be used to evaluate potential clinical drug candidates [12].

Another stem cell-based study involved iPSC-derived retinal pigment epithelium (RPE) as a disease-model-on-a-chip of age-related macular degeneration (AMD). In general, epithelial and endothelial cells are often studied using label-free technology, and some specific assay formats related to formation and disruption of monolayers have been developed for these (e.g. barrier function, Fig. 3C). Here, RPE cells from a patient with inherited AMD and an unaffected sibling were examined using an ECIS electrical wound healing assay. Real-time monitoring over a 25-day period demonstrated the establishment and maturation of RPE layers on the microelectrode arrays, in which a spatially controlled damage to the cell layer was introduced to mimic AMD. Apparently, label-free technology can be used to measure long-term effects, and is apparently suited for tissue-on-a-chip technology. This offers

translational value by enabling real-time, quantitative and reproducible patient-specific studies [47].

Another stem cell type of interest are MSCs, which are attractive candidates for tissue engineering due to their wide mesodermal differentiation potential. Angstmann *et al.* compared ECIS and xCELLigence in search for standardized quality control assays to monitor differentiation and high-throughput screening that is both non-invasive and time-resolved. They studied MSCs isolated from two different tissues of various donors, namely bone marrow and adipose tissue. Impedance measurements were used to discriminate osteogenic from adipogenic differentiation, which showed modulating effects of extracellular matrix components [48]. Label-free assays were also used to establish culture conditions for expansion of endometrial MSC (eMSC) isolated from endometrial lining of the human uterus of premenopausal women [49] or to test MSC labelling by a new type of nanoparticle [50].

In another instance, ECIS was used to monitor proliferation and osteogenic differentiation of human adipose stem cells (hASC) from donor populations of different ages. This assay could be used to predict the osteogenic potential for patient-specific bone tissue engineering [51]. Finally, Berger *et al.* studied molecular mechanisms in human obesity in hASCs from liposuctions of female patients. Studying lipid uptake and adipocyte differentiation with the xCELLigence, the authors identified several dysregulated adipocyte-specific genes involved in fatty acid storage or cell adhesion [52].

Other cell types

Label-free assays are suited for virtually any cell type and have in fact been applied to numerous others besides the most commonly biobanked samples highlighted above.

A further category of particular interest are cancer and related cell types. Here, impedance-based cellular assays are most often used to measure migratory and invasive properties (e.g. **Fig. 3B**), which are key characteristics for any (metastatic) cancer type. For instance, the xCELLigence was used to monitor the motility of primary human normal mammary cells versus patient-derived breast cancer epithelial cells [8], migration in various ovarian cancer patient samples [53] and proliferation and response to kinase inhibitors in patients' glioblastoma samples [54]. Others have evaluated (potential) treatment options on a patient's malignant melanoma cells [55] and on a newly established mesenchymal chondrosarcoma cell line from a patient [56]. Two other publications used the xCELLigence for characterization of newly established cell lines from patient samples, offsetting them versus parental tumor tissue or traditionally used carcinoma cell lines [57, 58]. Finally, Ruiz *et al.* applied the xCELLigence to patients' own cancer cells for *in vitro* selection of the most

promising treatment, in this case for human carcinoma cells from malignant pleural effusions [59]. This is an illustrative example of possible applications in precision medicine.

Impedance-based technologies are also suited to test potential cell-based therapies (Fig. 3G). Seidel *et al.* demonstrated the therapeutic potential of γδ T cells for antibody-based immunotherapy in pediatric patients with B-lineage acute lymphoblastic leukemia (ALL). γδ T cells were derived from healthy blood donors as well as from a patient with common-ALL. The xCELLigence was used to measure γδ T cell lysis in a breast adenocarcinoma cell line in real-time, and outperformed the traditional endpoint assay [60]. In a similar manner, others studied the ability of mononuclear cells from normal and breast cancer patients to kill different breast cancer cell lines in the presence or absence of trastuzumab [61].

Myoblasts from muscle biopsy samples are another cell type of interest. In a recent example, Sente *et al.* studied pathological mechanisms of heart failure. Using the xCELLigence, they observed myoblast adiponectin signaling, differentiation, proliferation and viability in primary myoblasts and myotubes from chronic heart failure patients and age- and gender-matched healthy donors [62, 63].

From drug discovery to precision medicine

Due to their versatility, label-free assays and patient cells, when combined, can be utilized at various stages of medicines research. As a cell-phenotypic screen, label-free assays are well suited for target identification, compound screening andlead selection. Likewise they allow the investigation of mechanisms of action and the testing of drug efficacy and safety [14, 17]. In this review we provided typical examples involving patient cells, which offer increased physiological context. As such patient samples are often in limited supply, this set-up is not so much used for e.g., screening drug candidates but rather for understanding disease mechanisms and testing potential treatments. This was done by Lowin *et al*. in the context of rheumatoid arthritis to identify drug targets, to subsequently test compounds and to define possible treatments [28, 41]. In a more integrated approach the combination of patient cells and label-free assays resulted in tissue-on-a-chip technology, as demonstrated by Gamal *et al.*[47]. It is to be expected that the advent of stem cell technology will radically change the availability of patient-derived materials [42, 64], which would allow a further integration of label-free assays. This would be an ideal starting point for the advancement of precision medicine, if patient-derived material can be made available readily, on demand, and in larger quantities. In this light the question arises whether label-free technologies can be developed that take the three-dimensionality of advanced cellular models and organoids

into account [65-67]. In drug safety and toxicity research, iPSC-derived cardiomyocytes can be used in a label-free setting to evaluate potential cardiac (side) effects of drug candidates [12, 43]. Finally, the combination of patient cells and label-free technology can be used for clinical compound selection, for instance by measuring patient cell responses *in vitro* as means of selecting the most promising treatment. This has been demonstrated by profiling drug treatment responses of patient derived malignant pleural effusions in a study by Ruiz *et al.* [59], with the aim to provide drug treatment of cancer in a personalized manner.

Conclusion

Physiologically more appropriate cellular models and readout systems are needed to increase representability and translational value. Patient-derived cells can provide pathological and physiological context, and biobanking has increased the availability of human primary samples for research. Label-free impedance-based assays can and have been applied to a wide range of such samples. These assays indeed increase physiological representability by omitting reporter-based modifications and measuring physiological cell function in real-time. Thus, combining label-free assays with human primary samples offers a uniquely biorelevant set-up for the purposes of drug development and precision medicine.

References

1. Kojima, R., D. Aubel, and M. Fussenegger, *Novel theranostic agents for next-generation personalized medicine: small molecules, nanoparticles, and engineered mammalian cells.* Curr Opin Chem Biol, 2015. **28**: p. 29-38.
2. Moller, C. and M. Slack, *Impact of new technologies for cellular screening along the drug value chain.* Drug Discov Today, 2010. **15**(9-10): p. 384-90.
3. Verdonk, E., et al., *Cellular dielectric spectroscopy: a label-free comprehensive platform for functional evaluation of endogenous receptors.* Assay Drug Dev Technol, 2006. **4**(5): p. 609-19.
4. McGuinness, R., *Impedance-based cellular assay technologies: recent advances, future promise.* Curr Opin Pharmacol, 2007. **7**(5): p. 535-40.
5. Eglen, R. and T. Reisine, *Primary cells and stem cells in drug discovery: emerging tools for high-throughput screening.* Assay Drug Dev Technol, 2011. **9**(2): p. 108-24.
6. Fang, Y., *Combining label-free cell phenotypic profiling with computational approaches for novel drug discovery.* Expert opinion on drug discovery, 2015. **10**(4): p. 331-43.
7. Lieb, S., et al., *Label-free analysis of GPCR-stimulation: The critical impact of cell adhesion.* Pharmacological research : the official journal of the Italian Pharmacological Society, 2016. **108**: p. 65-74.
8. Mandel, K., et al., *Characterization of spontaneous and TGF-beta-induced cell motility of primary human normal and neoplastic mammary cells in vitro using novel real-time technology.* PLoS One, 2013. **8**(2): p. e56591.
9. Hillger, J.M., et al., *Getting personal: Endogenous adenosine receptor signaling in Lymphoblastoid Cell Lines.* Biochem Pharmacol, 2016.
10. Czajka, A.A., et al., *Family of microRNA-146 Regulates RARbeta in Papillary Thyroid Carcinoma.* PLoS One, 2016. **11**(3).
11. Chanakira, A., et al., *Hypoxia Differentially Regulates Arterial and Venous Smooth Muscle Cell Migration.* PLoS One, 2015. **10**(9): p. e0138587.
12. Zhang, X., et al., *Multi-parametric assessment of cardiomyocyte excitation-contraction coupling using impedance and field potential recording: A tool for cardiac safety assessment.* J Pharmacol Toxicol Methods, 2016. **81**: p. 201-16.
13. Febles, N.K., A.M. Ferrie, and Y. Fang, *Label-free single cell kinetics of the invasion of spheroidal colon cancer cells through 3D Matrigel.* Analytical chemistry, 2014. **86**(17): p. 8842-9.
14. Rocheville, M., et al., *Mining the potential of label-free biosensors for seven-transmembrane receptor drug discovery.* Progress in molecular biology and translational science, 2013. **115**: p. 123-42.
15. Fang, Y. and A.M. Ferrie, *Label-free optical biosensor for ligand-directed functional selectivity acting on beta(2) adrenoceptor in living cells.* FEBS Lett, 2008. **582**(5): p. 558-64.
16. Stallaert, W., et al., *Impedance responses reveal beta(2)-adrenergic receptor signaling pluridimensionality and allow classification of ligands with distinct signaling profiles.* PLoS One, 2012. **7**(1): p. e29420.
17. Fang, Y., *Label-free drug discovery.* Frontiers in pharmacology, 2014. **5**(52).

18. Artene, S.A., et al., *Biobanking in a constantly developing medical world.* ScientificWorldJournal, 2013. **2013**: p. 343275.
19. Astrin, J.J. and F. Betsou, *Trends in Biobanking: A Bibliometric Overview.* Biopreserv Biobank, 2016. **14**(1): p. 65-74.
20. Al-Ahmad, A., et al., *Nature-inspired antimicrobial polymers--assessment of their potential for biomedical applications.* PLoS One, 2013. **8**(9): p. e73812.
21. Seok, J., et al., *Genomic responses in mouse models poorly mimic human inflammatory diseases.* Proceedings of the National Academy of Sciences of the United States of America, 2013. **110**(9): p. 3507-12.
22. Schulz, S., et al., *Interactive fibroblast-keratinocyte co-cultures: an in vivo-like test platform for dental implant-based soft tissue integration.* Tissue engineering. Part C, Methods, 2012. **18**(10): p. 785-96.
23. Freedman, L.P., et al., *Reproducibility: changing the policies and culture of cell line authentication.* Nature methods, 2015. **12**(6): p. 493-7.
24. Reddy, L., et al., *Assessment of rapid morphological changes associated with elevated cAMP levels in human orbital fibroblasts.* Exp Cell Res, 1998. **245**(2): p. 360-7.
25. Nicola Daniele, M.C., Claudio Pellegrini, Entela Shkëmbi and F. Zinno, *Biobanks and Clinical Research: An "Interesting" Connection.* Peertechz Journal of Cytology and Pathology, 2016. **1**(1): p. 034-043.
26. Nolte, A., et al., *Small interfering RNA transfection against serum response factor mediates growth inhibition of benign prostatic hyperplasia fibroblasts.* Nucleic Acid Ther, 2013. **23**(1): p. 62-70.
27. Huang, C.N., et al., *Sera from patients with scleroderma inhibit fibroblast micromotions monitored electrically.* J Rheumatol, 1999. **26**(6): p. 1312-7.
28. Lowin, T., et al., *Anti-inflammatory effects of N-acylethanolamines in rheumatoid arthritis synovial cells are mediated by TRPV1 and TRPA1 in a COX-2 dependent manner.* Arthritis Res Ther, 2015. **17**(321): p. 015-0845.
29. Lowin, T., G. Pongratz, and R.H. Straub, *The synthetic cannabinoid WIN55,212-2 mesylate decreases the production of inflammatory mediators in rheumatoid arthritis synovial fibroblasts by activating CB2, TRPV1, TRPA1 and yet unidentified receptor targets.* J Inflamm, 2016. **13**(15): p. 016-0114.
30. Bohm, M., et al., *alpha-MSH modulates cell adhesion and inflammatory responses of synovial fibroblasts from osteoarthritis patients.* Biochem Pharmacol, 2016. **116**: p. 89-99.
31. Lee, E.S., et al., *Monocytic adhesion molecule expression and monocyte-endothelial cell dysfunction are increased in patients with peripheral vascular disease versus patients with abdominal aortic aneurysms.* J Surg Res, 2012. **177**(2): p. 373-81.
32. Hopper, N., et al., *Peripheral blood derived mononuclear cells enhance osteoarthritic human chondrocyte migration.* Arthritis Res Ther, 2015. **17**: p. 199.
33. Hopper, N., et al., *Peripheral blood derived mononuclear cells enhance the migration and chondrogenic differentiation of multipotent mesenchymal stromal cells.* Stem Cells Int, 2015. **2015**: p. 323454.
34. Fox, E.D., et al., *Neutrophils from critically ill septic patients mediate profound loss of endothelial barrier integrity.* Crit Care, 2013. **17**(5): p. R226.

35. Rahbar, E., et al., *Endothelial glycocalyx shedding and vascular permeability in severely injured trauma patients.* J Transl Med, 2015. **13**: p. 117.
36. Bondu, V., et al., *Elevated cytokines, thrombin and PAI-1 in severe HCPS patients due to Sin Nombre virus.* Viruses, 2015. **7**(2): p. 559-89.
37. Jackson, M.W. and T.P. Gordon, *A novel impedance-based cellular assay for the detection of anti-calcium channel autoantibodies in type 1 diabetes.* J Immunol Methods, 2010. **361**(1-2): p. 31-6.
38. Leung, G., et al., *Cellular Dielectric Spectroscopy: A Label-Free Technology for Drug Discovery.* Journal of the Association for Laboratory Automation, 2005. **10**(4): p. 258-269.
39. Molecular Devices Inc., *Analyzing Endogenous Receptors in Non-Adherent Cell Lines and Primary Cells with the CellKey Small Sample 96W Microplate.* CellKey System Application Highlight 5, 2008.
40. Hillger, J.M., et al., *Phenotypic screening of cannabinoid receptor 2 ligands shows different sensitivity to genotype.* Biochemical pharmacology, 2017.
41. Welsh, M., et al., *Pharmacogenomic discovery using cell-based models.* Pharmacological reviews, 2009. **61**(4): p. 413-29.
42. Hosoya, M. and K. Czysz, *Translational Prospects and Challenges in Human Induced Pluripotent Stem Cell Research in Drug Discovery.* Cells, 2016. **5**(4).
43. Doherty, K.R., et al., *Structural and functional screening in human induced-pluripotent stem cell-derived cardiomyocytes accurately identifies cardiotoxicity of multiple drug types.* Toxicol Appl Pharmacol, 2015. **285**(1): p. 51-60.
44. Chaudhari, U., et al., *Identification of genomic biomarkers for anthracycline-induced cardiotoxicity in human iPSC-derived cardiomyocytes: an in vitro repeated exposure toxicity approach for safety assessment.* Arch Toxicol, 2016. **90**(11): p. 2763-2777.
45. Hu, N., et al., *High-performance beating pattern function of human induced pluripotent stem cell-derived cardiomyocyte-based biosensors for hERG inhibition recognition.* Biosens Bioelectron, 2015. **67**: p. 146-53.
46. Li, X., et al., *Cardiotoxicity screening: a review of rapid-throughput in vitro approaches.* Arch Toxicol, 2016. **90**(8): p. 1803-16.
47. Gamal, W., et al., *Real-time quantitative monitoring of hiPSC-based model of macular degeneration on Electric Cell-substrate Impedance Sensing microelectrodes.* Biosensors and Bioelectronics, 2015. **71**: p. 445-455.
48. Angstmann, M., et al., *Monitoring human mesenchymal stromal cell differentiation by electrochemical impedance sensing.* Cytotherapy, 2011. **13**(9): p. 1074-89.
49. Rajaraman, G., et al., *Optimization and scale-up culture of human endometrial multipotent mesenchymal stromal cells: potential for clinical application.* Tissue engineering. Part C, Methods, 2013. **19**(1): p. 80-92.
50. Skopalik, J., et al., *Mesenchymal stromal cell labeling by new uncoated superparamagnetic maghemite nanoparticles in comparison with commercial Resovist--an initial in vitro study.* Int J Nanomedicine, 2014. **9**: p. 5355-72.
51. Nordberg, R.C., et al., *Electrical Cell-Substrate Impedance Spectroscopy Can Monitor Age-Grouped Human Adipose Stem Cell Variability During Osteogenic Differentiation.* Stem Cells Transl Med, 2016. **7**: p. 2015-0404.

52. Berger, E., et al., *Pathways commonly dysregulated in mouse and human obese adipose tissue: FAT/CD36 modulates differentiation and lipogenesis.* Adipocyte, 2015. **4**(3): p. 161-80.
53. Jacob, F., et al., *The glycosphingolipid P(1) is an ovarian cancer-associated carbohydrate antigen involved in migration.* British journal of cancer, 2014. **111**(8): p. 1634-45.
54. Cruceru, M.L., et al., *Signal transduction molecule patterns indicating potential glioblastoma therapy approaches.* OncoTargets and therapy, 2013. **6**: p. 1737-49.
55. Li, J., et al., *The proliferation of malignant melanoma cells could be inhibited by ranibizumab via antagonizing VEGF through VEGFR1.* Mol Vis, 2014. **20**: p. 649-60.
56. de Jong, Y., et al., *Inhibition of Bcl-2 family members sensitizes mesenchymal chondrosarcoma to conventional chemotherapy: report on a novel mesenchymal chondrosarcoma cell line.* Lab Invest, 2016. **96**(10): p. 1128-37.
57. Bartscht, T., et al., *The Src family kinase inhibitors PP2 and PP1 effectively block TGF-beta1-induced cell migration and invasion in both established and primary carcinoma cells.* Cancer Chemother Pharmacol, 2012. **70**(2): p. 221-30.
58. Lohberger, B., et al., *The novel myxofibrosarcoma cell line MUG-Myx1 expresses a tumourigenic stem-like cell population with high aldehyde dehydrogenase 1 activity.* BMC Cancer, 2013. **13**: p. 563.
59. Ruiz, C., et al., *Culture and Drug Profiling of Patient Derived Malignant Pleural Effusions for Personalized Cancer Medicine.* PLoS One, 2016. **11**(8).
60. Seidel, U.J., et al., *γδ T Cell-Mediated Antibody-Dependent Cellular Cytotoxicity with CD19 Antibodies Assessed by an Impedance-Based Label-Free Real-Time Cytotoxicity Assay.* Frontiers in immunology, 2014. **5**: p. 618.
61. Kute, T., et al., *Understanding key assay parameters that affect measurements of trastuzumab-mediated ADCC against Her2 positive breast cancer cells.* Oncoimmunology, 2012. **1**(6): p. 810-821.
62. Sente, T., et al., *Primary skeletal muscle myoblasts from chronic heart failure patients exhibit loss of anti-inflammatory and proliferative activity.* BMC cardiovascular disorders, 2016. **16**: p. 107.
63. Sente, T., et al., *Tumor necrosis factor-alpha impairs adiponectin signalling, mitochondrial biogenesis, and myogenesis in primary human myotubes cultures.* Am J Physiol Heart Circ Physiol, 2016. **310**(9): p. 26.
64. Rony, I.K., et al., *Inducing pluripotency in vitro: recent advances and highlights in induced pluripotent stem cells generation and pluripotency reprogramming.* Cell proliferation, 2015. **48**(2): p. 140-56.
65. Lee, J., et al., *Nonmediated, Label-Free Based Detection of Cardiovascular Biomarker in a Biological Sample.* Adv Healthc Mater, 2017. **21**(10): p. 201700231.
66. Smout, M.J., et al., *A novel high throughput assay for anthelmintic drug screening and resistance diagnosis by real-time monitoring of parasite motility.* PLoS neglected tropical diseases, 2010. **4**(11): p. e885.
67. Shin, S.R., et al., *Label-Free and Regenerative Electrochemical Microfluidic Biosensors for Continual Monitoring of Cell Secretomes.* Adv Sci, 2017. **4**(5).

CHAPTER 3

Whole-cell biosensor for label-free detection of GPCR-mediated drug responses in personal cell lines

Julia M. Hillger

Jeffison Schoop

Dorret I. Boomsma

P. Eline Slagboom

Adriaan P. IJzerman

Laura H. Heitman

Biosens Bioelectron, 2015. **74**: p. 233-242
DOI: https://doi.org/10.1016/j.bios.2015.06.031

Abstract

Deciphering how genetic variation in drug targets such as G protein-coupled receptors (GPCRs) affects drug response is essential for precision medicine. GPCR signaling is traditionally investigated in artificial cell lines which do not provide sufficient physiological context. Patient-derived cell lines such as lymphoblastoid cell lines (LCLs) could represent the ideal cellular model system. Here we describe a novel label-free, whole-cell biosensor method for characterizing GPCR-mediated drug responses in LCLs. Generally, such biosensor technology is deemed only compatible with adherent cell lines. We optimized and applied the methodology to study cellular adhesion properties as well as GPCR drug responses in LCLs, which are suspension cells. Coating the detector surface with the extracellular matrix protein fibronectin resulted in cell adherence and allowed detection of cellular responses. A prototypical GPCR present on these cells, i.e. the cannabinoid receptor 2 (CB_2R), was selected for pharmacological characterization. Receptor activation with the agonist JWH133, blockade by antagonist AM630 as well as downstream signaling inhibition by PTX could be monitored sensitively and receptor-specifically. Potencies and effects were comparable between LCLs of two genetically unrelated individuals, providing the proof-of-principle that this biosensor technology can be applied to LCLs, despite their suspension cell nature, in order to serve as an in vitro model system for the evaluation of individual genetic influences on GPCR-mediated drug responses.

Introduction

Inter-individual variability in drug action and clinical effectiveness forms a challenge in today's drug treatment and development. In fact, variation in drug response that arises from genetic, lifestyle and environmental differences causes even blockbuster drugs to work in only 75% to merely 35% of all [1, 2]. Personalized medicine, or, more broadly defined, precision medicine proposes to personalize drug prescriptions using a sub-population or patient's individual characteristics, e.g. genetic information, and thereby decrease risks of ineffective treatment, dosing or side-effects [2-4]. In order to achieve this, it is paramount to determine whether, and how, genetic variation affects drug responses. Today, genetic testing is available for around 2000 clinical conditions, particularly in oncology [3, 5]. Two poster children of personalized medicine are HER2-positive breast cancer tests as a predictor of response to the drug herceptin and screens for CYP450 polymorphisms that are known to affect treatment with e.g. selective serotonin-reuptake inhibitors [3, 4].

The majority of therapeutic targets to date are formed by a class of membrane proteins, the G protein-coupled receptors (GPCRs) [6]. More than 30% of all currently marketed drugs exert their therapeutic effect by directly binding to and influencing GPCR function. Due to their ubiquity GPCRs are involved in a plethora of physiological processes. It is therefore highly interesting to decipher the influence of genetic variation in GPCR-mediated drug responses [7, 8]. While several examples have linked GPCR polymorphisms to disease and drug response variation, research has mostly focused on the statistics of genotype influences followed by functional characterization in heterologous cell lines [8-10]. Heterologous cell lines are, however, systems with artificial receptor expression and represent a non-physiological, cellular context [11, 12]. To fully understand the underlying mechanism of polymorphism influence, functional characterization on a physiologically relevant molecular and cellular level is vital. An ideal setup would be to use patient-derived cell lines as a model system to assess polymorphism influences on drug response.

A well-established example of such personal cell lines are lymphoblastoid cell lines (LCLs), which to date are a preferred choice for storing a person's genetic material [13, 14]. Numerous consortia have built and actively utilize LCL libraries, including the Centre d'Étude du Polymorphisme Humain (CEPH), the International HapMap and 1000 genomes projects [15-19]. However, LCLs are mainly used as a source of DNA or RNA for genotyping, expression or methylation studies [9, 13]. Functional cellular assays on LCLs have seldom been performed [13, 20, 21] with virtually none for GPCRs. Only Morag and Gurwitz et al. studied the influence of a few GPCR antagonists on LCL growth [20]. In fact, many traditional cellular

assays, especially for GPCRs, are incompatible with LCLs as they require labeling and cell or target engineering. Another drawback is that they generally lack the sensitivity required for such endogenous cell lines which often have low target expression levels. Recently developed label-free technologies offer a more sensitive, less invasive solution and can monitor drug effects on a whole cell in real-time [12, 22, 23]. The sensitivities of these label-free assays is high enough for standard applications such as GPCR activation or inhibition down to detection of small changes such as biased signaling [12, 24]. It may very well be that receptor polymorphisms induce subtle yet important changes in drug-target binding, signaling bias and receptor subtype selectivity [7]. Label-free technologies are therefore ideal for precision medicine purposes, as they harbor the ability to pick up small changes in GPCR signaling or drug responses in the physiologically relevant context of endogenous cells. One disadvantage, however, is that the detection method of label-free assays generally requires cells to adhere to the detector surface at the bottom of the well [12, 23] and unfortunately, LCLs are by nature non-adherent suspension cells [25]. However, several reports have been published recently on the application of label-free technology to suspension cells, including various types of blood cells [26, 27]. To solve the above listed challenges we developed a methodology for a label-free, impedance-based whole-cell assay that allows characterization of GPCR signaling in LCLs despite their suspension cell nature. This enables the use of LCLs as an in vitro cellular model system to evaluate individual differences in GPCR-mediated drug responses.

Material and methods

Chemicals and reagents

The LCLs were kindly provided within the framework of this collaboration [15]. Fibronectin from bovine plasma, poly-D-lysine (PDL) and unsupplemented RPMI 1640 cell culture medium were purchased from Sigma Aldrich (Steinheim, Germany). Collagen I from rat tail was purchased from Fisher Scientific (Illkirch, France). The GPCR agonist JWH133 was purchased from TOCRIS (Bristol, UK), ATP from Sigma Aldrich and AM630 from Cayman Chemicals Company (Ann Arbor, Michigan, USA). RGD peptide (GRGDTP) and RGE peptide (GRGESP) were purchased from AnaSpec/Tebu-bio (Heerhugowaard, the Netherlands). $G\alpha_i$ blocking pertussis toxin (PTX) was purchased from Sigma Aldrich. All other chemicals were of analytical grade and obtained from standard commercial sources.

Lymphoblastoid cell line generation

The LCLs had previously been generated at the Rutgers Institute (Department of Genetics, Piscataway, NJ, USA) using a standard transformation protocol [15]. In short, peripheral B-lymphocytes were exposed to Epstein–Barr Virus (EBV) by treatment with filtered medium from a Marmoset cell line in the presence of phytohemaglutinin (PHA) during the first week of culture [13, 14, 28]. Cultures were maintained for 8–12 weeks to adapt and expand the EBV transformed lymphocytes and subsequently cryopreserved.

Cell culture

Two LCLs from two genetically unrelated individuals were used for the experiments presented in this manuscript. Cryopreserved cells were thawed, resuscitated and multiple aliquots frozen for future use. Of note, LCLs were disposed of after culturing them for maximally 120 days. LCLs were grown as suspension cells in culture medium consisting of RPMI 1640 (25 mM HEPES and $NaHCO_3$) supplemented with 15% Fetal Calf Serum (FCS), 50 mg/mL streptomycin and 50 IU/mL penicillin at 37 °C and 5% CO_2. Cells were subcultured twice a week at a ratio of 1:5 on 10 cm ø plates.

Label-free whole-cell biosensor analysis (xCELLigence RTCA system)

Detection principle

Whole-cell assays were performed using the xCELLigence RTCA system [12], a real-time cell analyzer (RTCA) based on the electrical impedance generated by cells attaching to gold electrodes embedded on the bottom of the microelectronic E-plates. Cell attachment changes the local ionic environment at the electrode-solution interface, thereby generating impedance. Such relative changes in impedance (*Z*) are summarized as a dimensionless parameter, the so-called Cell Index (CI), and displayed in a real-time plot. In detail, a very weak electrical signal is applied to the sensor electrodes, where the AC excitation voltage level is in the lower mV range and the resulting current is in the µA range (output test signal is 22 mV rms ± 20% with max. 5 mV DC offset at 10, 25 and 50 kHz). The RTCA analyzer determines cell indeces at these three predetermined optimal midrange frequencies and the average speed of measurement is approximately 150–250 ms for each individual well. In order to increase usability and ease for the user, the RTCA system provided by the manufacturer has pre-set conditions for amplitude, applied potential, frequency range and used frequency for extrapolation of results [29, 30], which were used in all experiments

presented in this manuscript. The CI value at a given time point is defined by the formula in **Eq. (1)**:

Equation (1) $CI = (Z_i - Z_0)\ \Omega / 15\ \Omega$

where Z_i is the impedance at each individual time point and Z_0 represents the baseline impedance in the absence of cells, which is measured prior to the start of the experiment. The CI in the absence of cells is therefore defined as 0. As cells adhere to the electrodes, impedance and the corresponding CI increase proportionally. Impedance changes thereby reflect variations in cell number and degree of adhesion, as well as cellular viability and morphology [12, 22]. Such cellular parameters are also affected upon activation of GPCR signaling, thereby resulting in impedance changes and real-time monitoring of cellular signaling events [12]. Typically, GPCR-mediated activation would result in an increase in cell adhesion and overall increase in CI, while a lower CI would indicate loss of adhesion [31].

General protocol

The wells of 16 or 96 well E-plates were coated with 50 µl of fibronectin (10 µg/ml), unless stated otherwise. After 30 min incubation at room temperature, the coating liquid was removed and all plates were air dried for at least 1 h prior to use. LCLs were harvested by re-suspending in cell culture medium after brief treatment with EDTA and centrifuged twice at 200*g* for 5 min. Background impedance (Z_0) was measured after adding 45 µL, or in case of antagonist experiments 40 µL, of culture media to 16 or 96 well E-plates, respectively. In all cases, final well volumes after cell and ligand addition were 100 µL. Cells were seeded by adding 50 µL of cell suspension containing 50,000 cells per well, unless stated otherwise. To ensure accurate seeding densities, cells were counted using Trypan blue staining and a BioRad TC10 automated cell counter. After resting at room temperature for 30–60 min, the E-plate was placed into the recording station situated in a 37 °C and 5% CO_2 incubator. Impedance was measured every 15 min overnight. Cells were stimulated by a GPCR ligand or vehicle control in 5 µl after 18–20 h, unless specified otherwise. To record GPCR activation, CI was recorded for at least 30 min with a recording schedule of 15 s intervals for 20 min, followed by intervals of 1 min, 5 min and finally 15 min.

For assay optimization purposes, cells were stimulated with the purinergic P2Y receptor agonist ATP at a saturating concentration of 100 µM. As compound solubility of JWH133 and AM630 required addition of dimethylsulfoxide (DMSO), the final DMSO concentration upon ligand or vehicle addition was kept at 0.25% DMSO for all wells and assays. For agonist assays,

cells were stimulated with increasing concentrations of JWH133. For antagonist assays, cells were pre-incubated for 30 min with 5 µl of the antagonist AM630 at increasing concentrations or vehicle control. Subsequently, cells were challenged with a submaximal agonist concentration equal to the agonist's EC_{80} value (100 nM for JWH133) or vehicle control.

For coating trials, wells were coated with 50 µl of varying coatings such as poly-D-lysine (0.1 mg/ml), collagen I (50 µg/ml), pure Fetal Calf Serum or fibronectin (0.1–50 µg/ml). Non-coated wells were used as control condition. After removing coating liquid, only poly-D-lysine plates were washed with 3×100 µl PBS before use.

To assess the specificity of LCL adherence to fibronectin, assay medium was supplemented with increasing concentrations of the integrin blocking RGD peptide GRGDTP [1 µM–1 mM] or the inactive control RGE peptide GRGESP [1 mM]. Normal assay medium was used as control and non-coated wells were used for reference.

For studies on $G\alpha_i$ coupling, cells were seeded in assay medium containing 100 ng/ml Pertussis Toxin (PTX).

Data analysis

Experimental data were obtained with RTCA Software 1.2 (Roche Applied Science) and subsequently exported and analyzed using GraphPad Prism 5.0 (GraphPad Software Inc., San Diego, CA, USA). For data analysis, ligand responses were normalized to Δ cell index (Δ CI) after subtracting baseline (vehicle control) to correct for any agonist-independent effects. Overall, a threshold of 0.01 Δ CI was kept for considering responses different from baseline. Peak responses were defined as highest Δ CI observed within 30 min after compound addition. Peak values and experimental Δ CI traces were exported to Prism for further analysis; construction of bar graphs or dose-response curves by nonlinear regression and calculation of IC_{50}, EC_{50} and EC_{80} values. All values obtained are means of at least three independent experiments performed in duplicate. Statistical significance was determined using Student's *t*-test for two values or two column comparison, e.g. comparing pEC_{50} values between individuals. Comparison of the means of multiple data sets, e.g. the peak Δ CI of ATP responses of various coating conditions, was performed by one-way ANOVA, followed by a Tukey's post test for comparison of all columns or a Dunnett's post test when comparing to vehicle or non-coated control. To get an indication of statistical assay reproducibility under optimized assay conditions, correlation analysis was performed for the dose–response curves for both the CB_2R agonist as well as antagonist for each cell line.

Results

Coating allows detection of GPCR responses

At first various common coatings known to mediate cellular adherence were tested for their ability to allow detection of GPCR signaling in LCLs, for which ATP was chosen as a typical GPCR ligand. The result of a representative coating experiment is shown in **Fig. 1**. Following LCL seeding, an initial increase in impedance related to cell adhesion, growth and division was observed (**Fig. 1A**). The overall levels of impedance after 1 h and 18 h, i.e. shortly prior to ligand addition, are summarized in **Fig. 1B** and **C**. Impedance levels after 1 h are likely to reflect initial cellular adhesion, while impedance after 18 h is also influenced by cellular proliferation or more prolonged changes in cellular morphology. Subsequent addition of the agonist ATP induced changes in LCL morphology that were recorded in real-time (**Fig. 1A** and **D**). Typically, ATP addition resulted in an immediate dose-dependent increase of impedance to a peak level. Subsequently, the CI trace gradually decreased towards a plateau within a period of 30 min.

Lack of coating resulted in no adherence or detection of GPCR response. Even though poly-D-lysine initially caused a high amount of cellular adherence equal to fibronectin (**Fig. 1B**) this declined drastically over the course of 18 h (**Fig. 1C**) and allowed little to no detection of GPCR response (**Fig. 1D** and **E**). Even though both poly-D-lysine and collagen coating resulted in significant impedance levels in comparison to non-coated wells just before ATP addition (18 h, **Fig. 1C**), both of them failed to allow detection of an ATP-induced response (**Fig. 1D** and **E**) as growth curves had dropped to or below baseline levels (CI<0). Fibronectin coating, on the other hand, did mediate cellular adherence over a longer time course resulting in a stable growth curve and sufficient window for detection of GPCR signaling (**Fig. 1D** and **E**).

Of note, coating experiments performed on LCLs from a second individual, individual 2, gave virtually identical results (*data not shown*).

Subsequently, the amount of fibronectin required for stable impedance levels and GPCR signal detection was further optimized. While initially all amounts of fibronectin resulted in impedance above non-coated levels (**Fig. 2A** and **B**), only fibronectin levels from 5 µg/ml or higher maintained impedance above non-coated up to 18 h (**Fig. 2A** and **C**). Significant ATP signaling was detected from 10 to 50 µg/ml fibronectin coating (**Fig. 2D** and **E**). In fact, 25 and 50 µg/ml were indistinguishable in impedance level and ATP response window. 10 µg/ml resulted in slightly lower effects, but still gave stable impedance levels and response window,

which were both not statistically significantly different from 25 or 50 µg/ml. Fibronectin concentration effects were comparable for another cell line from individual 2 (*data not shown*). Therefore, a fibronectin concentration of 10 µg/ml was chosen for all further experiments.

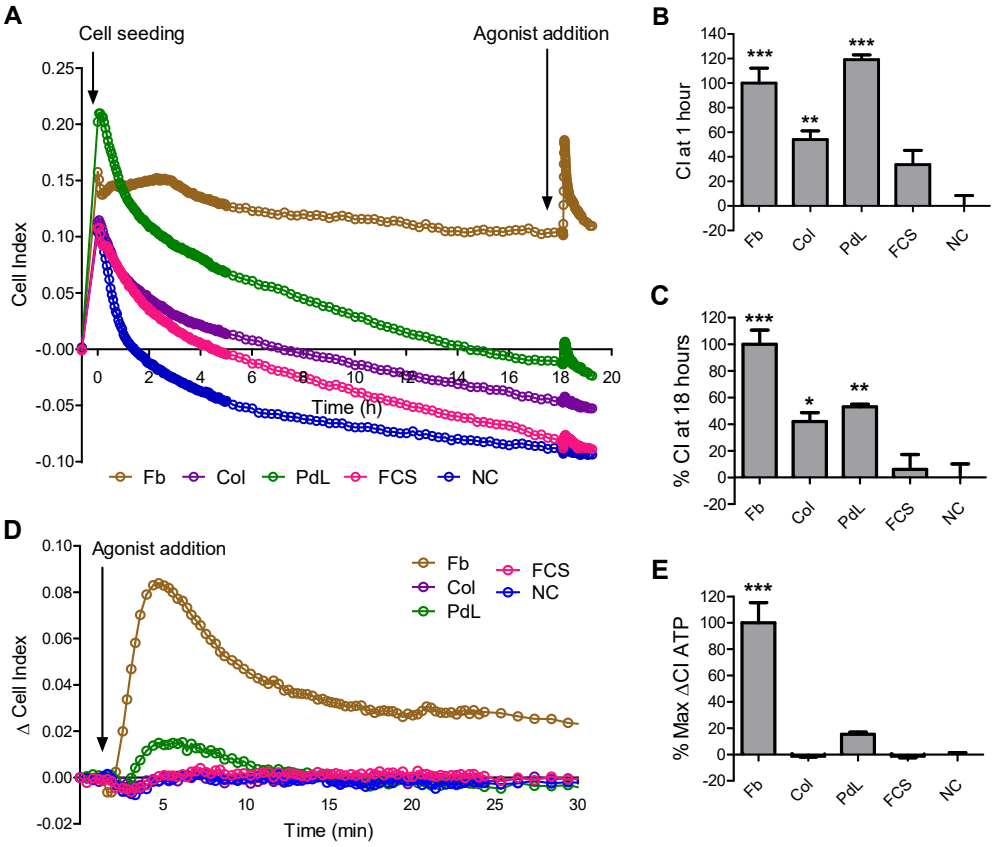

Figure 1. Fibronectin coating mediates LCL adhesion to allow detection of GPCR response. Electrodes were coated with various standard coatings, i.e. fibronectin (Fb; [50 µg/ml]), collagen I (Col; [50 µg/ml]) poly-D-lysine (PdL; [0.1 mg/ml]) and Fetal Calf Serum (FCS). Non-coated (NC) wells were used as a control. Cells were stimulated with the agonist (ATP [100 µM]) after 18 h of growth. Representative xCELLigence traces of a full experiment (**A**) and a baseline-corrected ATP response (**D**) are given. Time point 0 represents the time of cell seeding (**A**) and agonist addition (**D**), respectively. Bar graphs summarize the differences in cell index (CI) shortly after seeding (**B**, 1 h) and prior to agonist addition (**C**, 18 h), both normalized to fibronectin (100%) and non-coated (0%) wells. (**E**) Bar graph of baseline-corrected Δ cell index (Δ CI) of peak ATP response per coating condition, normalized to fibronectin (100%) and non-coated (0%) wells. Data are mean ± SEM from three separate experiments performed in quadruplicate (**B, C**) and duplicate (**E**) using one cell line (individual 1, 50,000 cells/well). Significance compared to control was tested using one-way ANOVA with Dunnett's post-hoc test. *=p<0.05, **=p<0.01, ***=p<0.001.

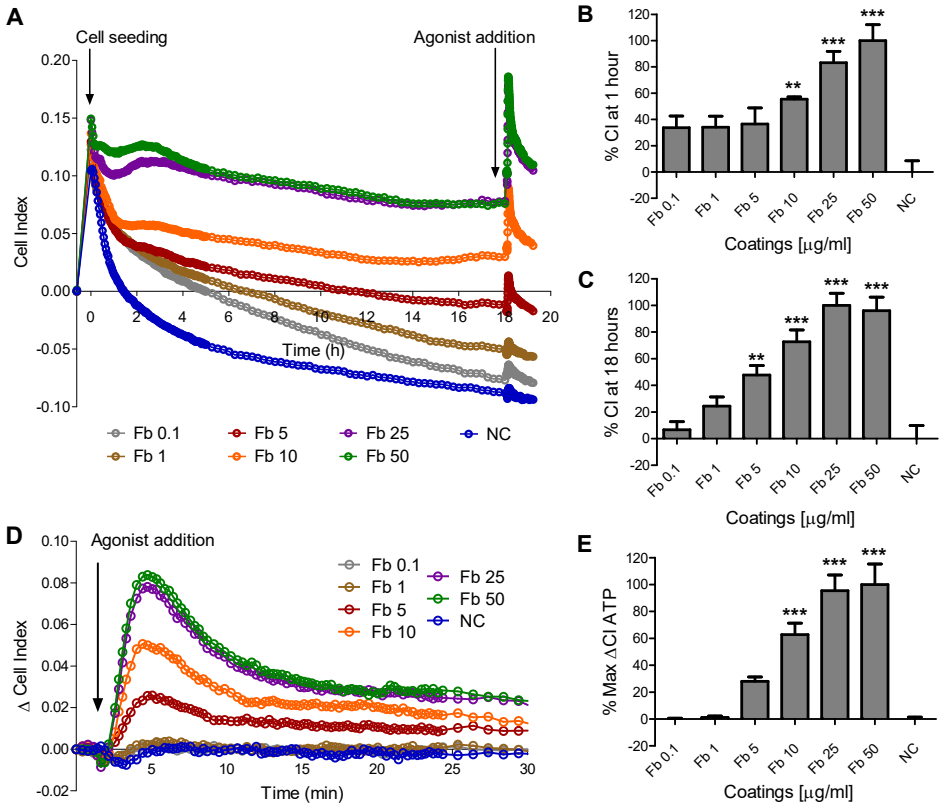

Figure 2. Titration of fibronectin coating concentration. Electrodes were coated with different amounts of fibronectin from 0.1–50 µg/ml. Non-coated (NC) wells were used as a control. Cells were stimulated with agonist (ATP [100 µM]) 18 h after seeding. Representative xCELLigence traces of a full experiment (**A**) and a baseline-corrected GPCR agonist response (**D**) are given. Time point 0 represents time of cell seeding (**A**) or agonist addition (**D**). Bar graphs indicate the cell index (CI) shortly after seeding (B, 1 h) and prior to agonist addition (C, 18 h), both normalized to fibronectin (100%) and non-coated (0%) wells. (**E**) Bar graphs represent the baseline-corrected Δ cell index (Δ CI) at peak ATP response, normalized to fibronectin (100%) and non-coated (0%) wells. Data are mean ± SEM from three separate experiments performed in quadruplicate (**B, C**) and duplicate (**E**) using one cell line (individual 1, 50,000 cells/well). Significance compared to control was tested using one-way ANOVA with Dunnett's post-hoc test. *=p<0.05, **=p<0.01, ***=p<0.001.

LCLs specifically adhere to fibronectin

In order to confirm the specificity of LCLs' interaction with fibronectin, inhibition of fibronectin adherence by small, integrin-targeting peptides containing the RGD motif was characterized. Addition of RGD peptide to the assay medium decreased the LCLs' attachment to fibronectin, as reflected by a decreased cell index (**Fig. 3A** and **B**), though not to levels as low as the non-coated control. This inhibition was concentration-dependent (**Fig. 3B**). However the effect decreased over time and was not noticeable after 18 h or, therefore, on

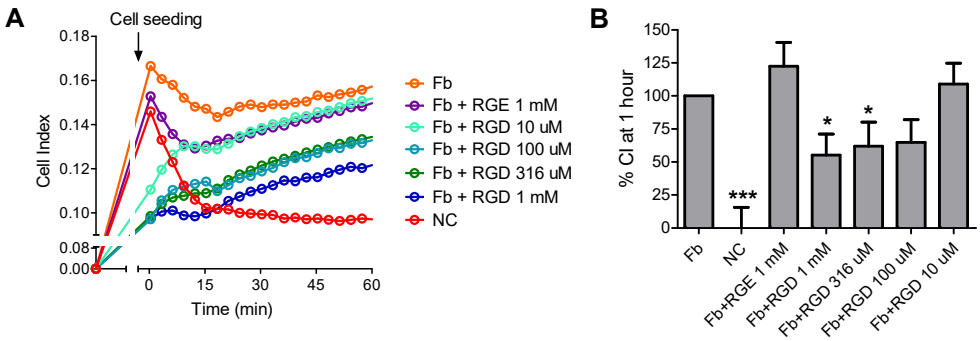

Figure 3. Influence of peptides blocking the fibronectin interaction. Cells were seeded on fibronectin coated plates (Fb; [10 µg/ml]) in assay medium containing varying concentrations of RGD peptide [1 mM–1 µM], inactive reference peptide RGE [1 mM] or normal medium. Non-coated (NC) wells were used as reference. Cells were stimulated by agonist addition (ATP [100 µM]) after 18 h growth. (**A**) Representative full xCELLigence traces, where time point 0 represents the time of cell seeding. (**B**) Bar graphs indicate cell index (CI) 1 h after seeding, normalized to fibronectin (100%) and non-coated (0%) wells. Data derived from six separate experiments performed in quadruplicate using LCLs of one individual (individual 1, 50,000 cells/well). Statistical significance versus control RGE peptide was determined using one-way ANOVA with Dunnett's post-hoc test. *=p<0.05, **=p<0.01, ***=p<0.001.

ATP response *(data not shown)*. Treatment with the inactive RGE peptide at a high concentration (1 mM) did not affect any part of the impedance readout, thereby confirming that LCL adherence was affected by specific inhibition of integrin–fibronectin interactions. Similar experiments performed on LCLs from a second individual, individual 2, gave comparable results (*data not shown*).

Seeding density and stimulation time affect GPCR response

Next to optimization of coating, assay conditions were further optimized by evaluating various LCL densities. The experimental results are summarized in **Fig. 4**. Both the height of the growth curves (**Fig. 4A** and **B**) and the GPCR signal (**Fig. 4C** and **D**) increased accordingly with the cell density.

The cell index after 18 h (**Fig. 4B**) was significantly different between all seeding densities, except between 50,000 and 25,000 cells/well. While 25,000 and 50,000 cells/well showed no statistically significant difference in growth curve, they did show significant differences in detection of an ATP signal (**Fig. 4D**). 25,000 cells/well gave an insufficient window for full pharmacological characterization and was not statistically different from the control. 50,000 Cells/well, however, was sufficient to allow a reliable detection of a GPCR signal. Interestingly, the ATP response was not statistically different from the condition with

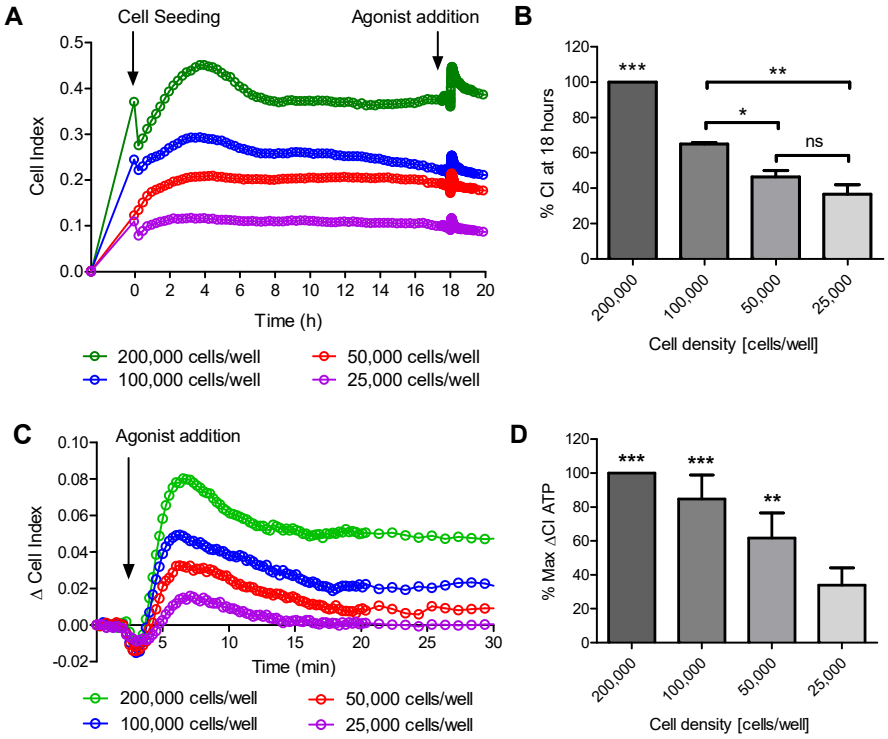

Figure 4. Seeding density influences growth curve and window of GPCR response. Cells were seeded in four different densities (25,000–200,000 cells/well). Cells were stimulated with the agonist (ATP [100 µM]) after 18 h of growth. Representative xCELLigence trace of a full experiment (**A**) and a baseline-corrected ATP response (**C**). Time point 0 represents the time of cell seeding (**A**) or agonist addition (**C**). Bar graphs indicate the cell index (CI) shortly prior to agonist addition normalized to CI=0 (**B**, 18 h) and baseline-corrected Δ cell index (Δ CI) at peak ATP response, normalized to vehicle control (**D**). Data are mean ± SEM from three separate experiments performed in quadruplicate (**B**) and duplicate (**D**) using one cell line (individual 1). Statistical significance was determined using one-way ANOVA with Tukey post-hoc test to compare all columns to each other (**B**) and Dunnett's post-hoc test to compare values to vehicle control (**D**). ns=not significant (p>0.05), *=p<0.05, **=p<0.01, ***=p<0.001.

100,000 cells/well. Irrespective of specific statistical significances, both the basal level of impedance as reflected in the growth curve and the ATP response increase in height along with the seeding density. As 50,000 cells/well was the lowest cell density that allowed reliable measurements of GPCR activation, this cell density was chosen for all further experiments. Similar experiments performed on LCLs from a second individual, individual 2, gave comparable results (*data not shown*).

Additionally, as the LCL's growth curve appeared to reach a stable plateau much earlier than 18–20 h (**Fig. 5A**), stimulation after 5 h was also investigated. GPCR stimulation after

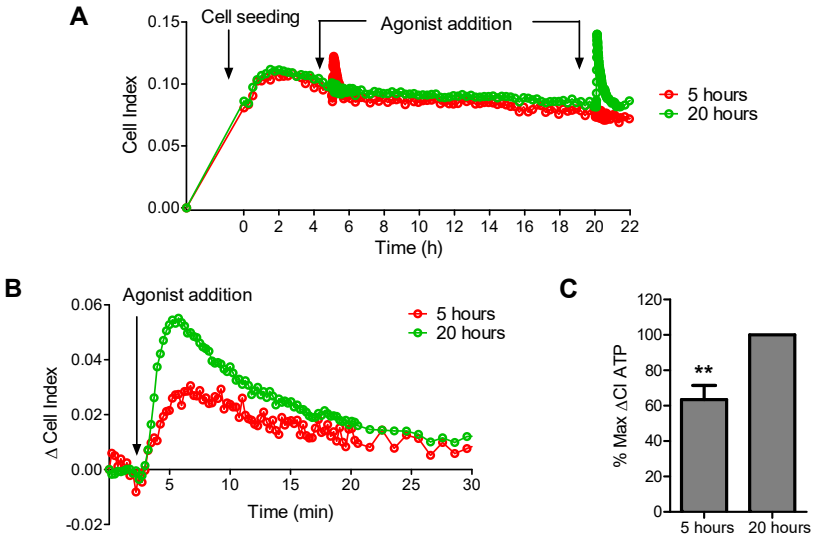

Figure 5. Influence of growth phase duration. Two cell lines were stimulated with the GPCR agonist ATP [100 µM] immediately after reaching growth plateau at 5 h or after a longer duration of growth at 20 h. Representative xCELLigence traces of a full experiment (**A**) and a baseline-corrected ATP response (**B**). Time point 0 represents the time of cell seeding (**A**) or agonist addition (**B**). (**C**) Bar graphs indicate the baseline-corrected Δ cell index (Δ CI) at peak ATP response, normalized to vehicle control. Data represents means of four separate experiments performed in duplicate using the LCLs of one individual (individual 1, 50,000 cells/well). Statistical significance was determined using Student's *t*-test. *=p<0.05, **=p<0.01, ***=p<0.001.

20 h gave a significantly higher response than stimulation after 5 h, despite the fact that the growth curve plateau had been reached after 5 h (**Fig. 5B** and **C**). Comparable effects were observed on LCLs from a second individual (*individual 2, data not shown*).

Detailed pharmacological characterization of GPCR signaling in LCLs is possible

After completing assay optimization, the resulting protocol was applied for full pharmacological characterization of an example GPCR. For this purpose, a GPCR with well characterized pharmacology and known to be expressed in LCLs was chosen, i.e. the cannabinoid receptor 2 (CB_2R; Ensembl gene: ENSG00000188822). A result of a representative experiment along with concentration-effect curves is provided in **Fig. 6**. Responses from two cell lines from two unrelated individuals were recorded and compared.

Addition of a CB_2R selective agonist JWH133 resulted in an immediate and concentration- dependent increase of impedance (**Fig. 6A** and **B**), which was similar in shape to the recorded ATP responses (**Fig. 1**, **Fig. 2** and **Fig. 3**). The impedance increase was concentration-dependently reduced by pretreatment with the CB_2R selective antagonist

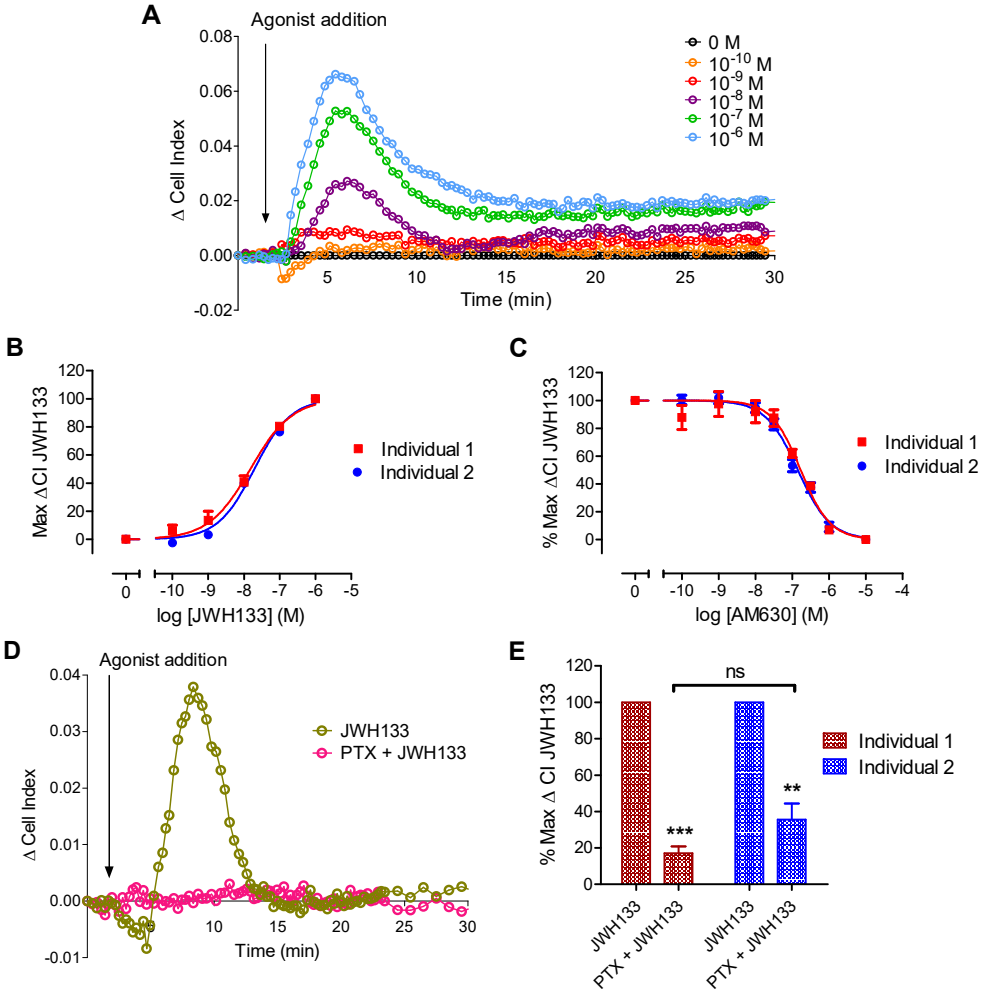

Figure 6. Characterization of Cannabinoid receptor 2 responses in two genetically unrelated LCLs. Cell lines were stimulated with a CB_2R selective agonist JWH133 18 h after seeding (50,000 cells/well). (**A**) Representative example of a baseline-corrected JWH133 response [1 µM–100 pM]. (**B**) Dose-response curves of JWH133 derived from peak Δ cell index (Δ CI) within 30 min after agonist addition. pEC_{50} values of JWH133 were 7.82±0.07 (individual 1) and 7.71±0.04 (individual 2). (**C**) Cell lines were pre-incubated for 30 min with increasing concentrations of AM630 [10 µM–100 pM] before stimulation with JWH133 [EC_{80}: 100 nM]. Dose-response curves of AM630 were derived from peak Δ CI within 30 min after agonist addition. pIC_{50}values for AM630 were 6.77±0.06 (individual 1) and 6.85±0.04 (individual 2). To test coupling to $G\alpha_i$proteins, cells were seeded and grown in assay medium with or without PTX [100 ng/ml] and stimulated with JWH133 [EC_{80}: 100 nM]. (**D**) Representative example of baseline-corrected JWH133 response in the absence and presence of PTX. (**E**) Bar graphs show the PTX effect on peak Δ cell index (Δ CI) of JWH133 response, normalized to vehicle control. Data represents the means of four separate experiments performed in duplicate. Statistical significance was calculated by Student's *t*-test. ns=not significant ($p>0.05$), *=$p<0.05$, **=$p<0.01$, ***=$p<0.001$. pEC_{50} and pIC_{50} values did not differ significantly between the two individuals.

AM630 (**Fig. 6C**). Concentration-effect curves were obtained by peak analysis of corresponding agonist-induced CI changes. Potencies of JWH133, given as pEC_{50} values, were 7.82±0.07 (15 nM) and 7.71±0.04 (20 nM) on individual 1 and individual 2, respectively. Antagonist IC_{50} values for AM630 were obtained by stimulating cells with a submaximal (EC_{80}) concentration of JWH133 following antagonist pre-incubation. The pIC_{50} values for AM630 were 6.77±0.06 (169 nM) and 6.85±0.04 (141 nM) on individual 1 and individual 2, respectively. Both agonist pEC_{50} and antagonist pIC_{50} values did not differ significantly between the two individuals. In order to get an indication of overall assay reproducibility under these optimized conditions, correlation analysis was performed for the dose–response curves for both the CB_2R agonist as well as antagonist. Experiments were reproducible with a coefficient of correlation (Pearson's r) of minimum 0.95 (p<0.05) for both individuals and at all concentrations of the agonist and 0.85 for the antagonist (p<0.01).

The influence of blocking the $G\alpha_i$-coupled pathway upon CB_2R activation was examined for both cell lines, as shown in **Fig. 6D** and **E**. Addition of PTX to the assay medium effectively diminished the CB_2R response to agonist JWH133 (**Fig. 6D**) in a similar manner for both cell lines (**Fig. 6E**). This confirmed that the LCLs' response to the selective CB_2R agonist was dependent on the $G\alpha_i$ pathway.

Discussion

Personal cell lines, such as LCLs that are commonly used for storing an individual's genetic material [13], can offer a model system to investigate individual differences in drug response in a physiologically relevant, cellular context. The introduction of highly sensitive, label-free technologies that allow cellular assays with minimal modifications makes harvesting this potential possible. In the present study, we have setup and optimized a label-free methodology for investigating GPCR-mediated drug responses in LCLs and characterized a prototypical GPCR for proof-of-principle.

As P2Y receptors (Ensembl family: ENSFM00760001715026) are abundantly present on virtually all cell types, including LCLs [32, 33], ATP was chosen as initial ligand for the methodological setup. In fact, P2Y receptors represent one of the few examples with functional characterization in LCLs. Lee et al. investigated ATP-induced P2Y receptor responses in LCLs using a single-cell fluorescent microscopy technique. While this traditional, label-based technique measured little response at an ATP concentration of 100 µM, the label-free assay used in our study was able to measure a clear response at the same concentration (**Fig. 1**, **Fig. 2**,**Fig. 3**, **Fig. 4** and **Fig. 5**). This emphasizes the advantage and

opportunity of using label-free techniques to measure GPCR signaling in LCLs over traditional, label-based methodologies, as they offer highly increased sensitivity and lower detection limits.

The initial experimental setup was based on previously published protocols for adherent cell lines [24, 31, 34]. While label-free assays are often deemed incompatible with suspension cells, some application examples exist for various label-free assays based on optical or impedance detection. These include various types of blood cells. For instance, GPCR signaling was measured in primary human neutrophils and THP-1 cells, a human monocyte cell line, using an optics-based assay [27, 35]. The impedance-based CellKey technology was used to measure GPCR signaling in monocyte cell lines (THP-1 and U937), neutrophils and primary normal peripheral blood monocytes (PBMCs) [36, 37]. Both these technologies have the disadvantage of being performed in buffer and at room temperature, while xCELLigence assays use more physiologically relevant conditions like normal cell culture medium and a temperature of 37 ˚C. Application of xCELLigence technology to suspension cells has been reported, however not for investigating GPCR signaling. Obr *et al*. [38] applied the technology to measure the effect of histone deacetylase inhibitors on hematopoietic cells. Martinez-Serra *et al.* [26] investigated the cytotoxic effect of antineoplastic agents on cells from hematological malignancies, which included the leukemia lymphoblast cell line K562. It is well known that the cell density and distribution on the electrodes can significantly influence impedance and experimental readout [12, 22, 23]. In previous cases, fibronectin was often used to achieve cell adherence combined with increased cell densities with an optimal range of 60,000 to 45,000 cells/well [26, 27, 35, 38]. Accordingly, we first tested various standard coating conditions and optimized cell density for impedance recordings in LCLs and found similar conditions to be optimal for LCLs. In our hands, LCL densities of 50,000 cells/well were sufficient for detection of a robust GPCR response (**Fig. 4**), a number that is merely 2.5-fold higher than common for adherent cells [24, 31, 34] and very comparable to existing suspension cell protocols described above.

Following LCL seeding onto fibronectin-coated plates, an initial increase in impedance related to cell adhesion, growth and division was observed, as is similar for any adherent cell line [31, 34]. Fibronectin was capable of mediating LCL adherence sufficiently for the measurement of a GPCR response after 18 h (**Fig. 1**) in a concentration-dependent manner (**Fig. 2**). It has been shown that LCLs can attach to fibronectin [39] and that LCLs express the α4β1 and αvβ3 type integrins [40], which are known to interact with fibronectin [41, 42]. Most fibronectin-binding integrins interact with a RGD tripeptide active site of fibronectin [41-43]. Small soluble RGD peptides have been shown to compete for integrin binding [43,

44] and one of those partially blocked the LCL's cellular interaction with the fibronectin coating (**Fig. 3**). The inactivity of the RGE control peptide confirmed that adherence was due to a specific interaction of LCL's integrins with fibronectin. Interestingly, around 50% of LCL adherence remained even in the presence of a high concentration of the RGD peptide. This remaining adhesion is most likely mediated through another motif in fibronectin, the LDV motif, which is known to be the predominant binding site for the α4β1 integrin [42]. Poly-D-lysine is known to mediate cellular adhesion by changing surface charges [45, 46], but failed to maintain LCL adherence at sufficiently high levels for detection of an ATP response despite an initially equally high adherence as fibronectin (**Fig. 1**). LCLs have been shown to attach to poly-L-lysine at the same concentration, however, for a shorter timeframe than the 18 h in our experiments, i.e. 4 h [33]. Moreover, collagen, which also mediates cellular adhesion through specific integrins [41], failed to promote adhesion of LCLs. Collagen-interacting integrins are thus likely not present in LCLs, while fibronectin-specific integrins are. Furthermore, the findings agree with Martinez-Serra *et al*. who showed that cells from hematological malignancies, including the leukemia lymphoblast cell line K562, attached more efficiently to fibronectin than to collagen, laminin or gelatin [26].

Following the methodological optimization, we showed that in-depth pharmacological characterization of GPCRs is possible in LCLs using the CB_2 receptor as a prototypical example (**Fig. 6**). This receptor is well expressed in LCLs [47] and has been investigated in a heterologous cell line on the xCELLigence [31], but has not yet been functionally characterized in LCLs until now. With recombinant cell lines, it is straightforward to confirm that an impedance signal is receptor-specific by using the untransfected parental cell line as negative control [31, 34]. However, this is not possible for endogenously expressed receptors, as is the case for LCLs used in this study. Therefore, proof of a receptor-specific response was provided by the concentration-dependent receptor activation with a CB_2 receptor selective agonist, JWH133, and inhibition of that response by a CB_2 receptor selective antagonist, AM630 [31, 48, 49]. Both JWH133 and AM630 effects were comparable between LCLs from two different individuals (**Fig. 6**), as was expected as both cell lines carried the same genotype for all non-synonymous variants (*data not shown*). Furthermore, both JWH133 and AM630 effects on LCLs were comparable to literature values obtained in heterologous cell lines. Scandroglio et al. determined the potency of JWH133 and AM630 in traditional and label-free assays using a for GPCR investigations typical heterologous cell system, a recombinant CHO cell line. Agonist JWH133 had a comparable potency in both impedance and traditional cAMP assays of 29.9±20.5 nM and 30±7.3 nM, respectively, showing that label-free assays yield values equal to traditional techniques. Similarly,

JWH133's potency determined in the present study on LCLs (pEC_{50}: 7.82±0.07 (15 nM) for individual 1, 7.71±0.04 (20 nM) for individual 2) were very comparable to Scandroglio et al.'s values on the CHO-cells. Furthermore, these authors showed that AM630 was able to antagonize JWH133's effects, however they did not report an IC_{50} value for this inhibition. Literature values for AM630 include an IC_{50} of 128.6±40.6 nM in a traditional cAMP assay on a recombinant CHO cell line [48]. On LCLs, AM630 readily antagonized JWH133 effects with a very comparable potency (pIC_{50}: 6.77±0.06 (169 nM) for individual 1, 6.85±0.04 (141 nM) for individual 2).

Besides for measuring cellular effects on GPCR signaling by agonists or antagonists, the label-free xCELLigence system is also well suited to monitor inhibition of downstream pathways [31, 50]. The CB_2 receptor is known to predominantly couple to the $G\alpha_i$-pathway and it was previously shown that JWH133 signaling on CHO cells could be inhibited by $G\alpha_i$-blocker PTX [31, 51]. Similarly, PTX effectively diminished the CB_2R response to JWH133 in LCLs of both individuals (**Fig. 6**), which thereby confirmed that the LCLs' response to the agonist was indeed dependent on the Gαi-pathway. Taken together, the effects of JWH133 in LCLs are mediated by the CB_2 receptor. While the effects and potencies of the CB_2R ligands were comparable between the endogenous LCLs and the recombinant CHO cells, LCLs represent a more relevant physiological context as they are cell lines with specific individual genetic material.

LCLs already form a large resource for personalized medicine research, as they are commonly used to investigate association of genetic variation to disease or drug response [9, 13, 21]. Moreover, large libraries of LCLs have already been built and are actively utilized in numerous consortia [15-19]. Investigation of GPCR drug responses in LCLs may further help the advancement of precision medicine. Examples linking GPCR polymorphisms to drug response to date are sparse and focus on statistic associations followed by validating polymorphism influences by generating these variants in heterologous cell lines [10]. Heterologous cell lines, however, are labor intensive to make and represent a different, non-physiological cellular context than cells of an individual [11, 12]. Receptor overexpression, differences in intracellular metabolic conditions as well as products from other genes could modify cellular responses. Therefore, screening receptor responses in LCLs from persons with potentially interesting polymorphisms may offer a more direct way of validation. Expression studies indicate that LCLs express a wide range of druggable GPCRs that are of interest for drug research, besides the CB_2 and P2Y receptors investigated in this study [47]. Next to investigation of GPCRs, label-free technology offers a wide range of other

applications and has similarly been applied to other important classes of drug targets, such as receptor tyrosine kinases [52, 53].

Conclusion

In conclusion, the current paper shows that direct characterization of GPCR activity in LCLs is possible with a highly sensitive label-free technology, the xCELLigence. Despite that such biosensor technology is deemed only compatible with adherent cell lines, we were able to optimize the assay for the suspension cell LCLs. Using the CB_2R as a prototypical GPCR, we were able to show that receptor activation by an agonist, blockade by an antagonist, as well as inhibition of downstream signaling could be monitored sensitively and receptor-specifically. The resemblance of cellular responses between LCLs from two unrelated individuals confirms that the methodology is robust and applicable to LCLs in general. This offers the ability to use LCLs not just as a mere source of DNA for genetic studies, but also as a functional, physiologically more relevant cellular model system for detailed investigation of GPCR pharmacology in vitro. Ultimately, a mechanistic link may be made between polymorphisms and drug response variation in individuals. Thus combining the resolution power of a whole-cell label-free method with LCLs opens vast possibilities for research on precision medicine.

Acknowledgments

This research was supported by the Center for Collaborative Genomic Studies on Mental Disorders at the National Institute of Mental Health (NIMH) [NIMH U24 MH068457-06]. The LCLs used in this study were kindly provided within the framework of this collaboration [15] and are part of the Netherlands Twin Registry (NTR; *http://www.tweelingenregister.org/en/*), part of the Center for Collaborative Genomic Studies on Mental Disorders [NIMH U24 MH068457-06]. Data and biomaterials (such as cell lines) are available to qualified investigators and may be accessed by following a set of instructions stipulated on the NIMH website (*https://www.nimhgenetics.org/access_data_biomaterial.php*).

We thank Dr. A. Brooks (Department of Genetics, Rutgers University, Piscataway, NJ, USA) for preparation of the lymphoblastoid cell lines and Prof. E.A.J.M. Goulmy (Transplantation biology, Leiden University and Leiden University Medical Center, Leiden, the Netherlands) for her advice on the research and manuscript.

References

1. Carey, J. *Making personalized medicine pay*. BusinessWeek 2010 [cited 2015 24.06.2015]; Available from: *http://www.bloomberg.com/bw/magazine/content/10_05/b4165058407403.htm*.
2. van't Veer, L.J. and R. Bernards, *Enabling personalized cancer medicine through analysis of gene-expression patterns.* Nature, 2008. **452**(7187): p. 564-70.
3. Mirnezami, R., J. Nicholson, and A. Darzi, *Preparing for precision medicine.* The New England journal of medicine, 2012. **366**(6): p. 489-91.
4. Katsanis, S.H., G. Javitt, and K. Hudson, *Public health. A case study of personalized medicine.* Science, 2008. **320**(5872): p. 53-4.
5. Weng, L., et al., *Pharmacogenetics and pharmacogenomics: a bridge to individualized cancer therapy.* Pharmacogenomics, 2013. **14**(3): p. 315-24.
6. Overington, J.P., B. Al-Lazikani, and A.L. Hopkins, *How many drug targets are there?* Nat Rev Drug Discov, 2006. **5**(12): p. 993-6.
7. Venkatakrishnan, A.J., et al., *Molecular signatures of G-protein-coupled receptors.* Nature, 2013. **494**(7436): p. 185-94.
8. Sadee, W., et al., *Genetic variations in human G protein-coupled receptors: implications for drug therapy.* AAPS pharmSci, 2001. **3**(3): p. 54-80.
9. Docherty, S.J., et al., *A genetic association study of DNA methylation levels in the DRD4 gene region finds associations with nearby SNPs.* Behav Brain Funct, 2012. **8**: p. 31-44.
10. Ishiguro, H., et al., *Brain cannabinoid CB2 receptor in schizophrenia.* Biol Psychiatry, 2010. **67**(10): p. 974-82.
11. Eglen, R. and T. Reisine, *Primary cells and stem cells in drug discovery: emerging tools for high-throughput screening.* Assay Drug Dev Technol, 2011. **9**(2): p. 108-24.
12. Yu, N., et al., *Real-time monitoring of morphological changes in living cells by electronic cell sensor arrays: an approach to study G protein-coupled receptors.* Anal Chem, 2006. **78**(1): p. 35-43.
13. Sie, L., S. Loong, and E.K. Tan, *Utility of lymphoblastoid cell lines.* J Neurosci Res, 2009. **87**(9): p. 1953-9.
14. Sugimoto, M., et al., *Steps involved in immortalization and tumorigenesis in human B-lymphoblastoid cell lines transformed by Epstein-Barr virus.* Cancer research, 2004. **64**(10): p. 3361-4.
15. Willemsen, G., et al., *The Netherlands Twin Register biobank: a resource for genetic epidemiological studies.* Twin Res Hum Genet, 2010. **13**(3): p. 231-45.
16. Abecasis, G.R., et al., *A map of human genome variation from population-scale sequencing.* Nature, 2010. **467**(7319): p. 1061-73.
17. Welsh, M., et al., *Pharmacogenomic discovery using cell-based models.* Pharmacological reviews, 2009. **61**(4): p. 413-29.
18. Dausset, J., et al., *Centre d'etude du polymorphisme humain (CEPH): collaborative genetic mapping of the human genome.* Genomics, 1990. **6**(3): p. 575-7.
19. Wheeler, H.E. and M.E. Dolan, *Lymphoblastoid cell lines in pharmacogenomic discovery and clinical translation.* Pharmacogenomics, 2012. **13**(1): p. 55-70.

20. Morag, A., et al., *Human lymphoblastoid cell line panels: novel tools for assessing shared drug pathways.* Pharmacogenomics, 2010. **11**(3): p. 327-40.
21. Li, L., et al., *Discovery of genetic biomarkers contributing to variation in drug response of cytidine analogues using human lymphoblastoid cell lines.* BMC genomics, 2014. **15**: p. 93-115.
22. Fang, Y., *Label-Free Receptor Assays.* Drug Discov Today Technol, 2011. **7**(1): p. e5-e11.
23. Rocheville, M., et al., *Mining the potential of label-free biosensors for seven-transmembrane receptor drug discovery.* Progress in molecular biology and translational science, 2013. **115**: p. 123-42.
24. Stallaert, W., et al., *Impedance responses reveal beta(2)-adrenergic receptor signaling pluridimensionality and allow classification of ligands with distinct signaling profiles.* PLoS One, 2012. **7**(1): p. e29420.
25. Avila-Carino, J., et al., *Search for the critical characteristics of phenotypically different B cell lines, Burkitt lymphoma cells and lymphoblastoid cell lines, which determine differences in their functional interaction with allogeneic lymphocytes.* Cancer Immunol Immunother, 1991. **34**(2): p. 128-32.
26. Martinez-Serra, J., et al., *xCELLigence system for real-time label-free monitoring of growth and viability of cell lines from hematological malignancies.* OncoTargets and therapy, 2014. **7**: p. 985-94.
27. Schroder, R., et al., *Applying label-free dynamic mass redistribution technology to frame signaling of G protein-coupled receptors noninvasively in living cells.* Nat Protoc, 2011. **6**(11): p. 1748-60.
28. Miller, G. and M. Lipman, *Release of infectious Epstein-Barr virus by transformed marmoset leukocytes.* Proceedings of the National Academy of Sciences of the United States of America, 1973. **70**(1): p. 190-4.
29. *RTCA DP Instrument Operator's Manual, version 2013.* ACEA Biosciences Inc.
30. *RTCA SP Instrument Operator's Manual, version 2013.* ACEA Biosciences Inc.
31. Scandroglio, P., et al., *Evaluation of cannabinoid receptor 2 and metabotropic glutamate receptor 1 functional responses using a cell impedance-based technology.* Journal of biomolecular screening, 2010. **15**(10): p. 1238-47.
32. Jacob, F., et al., *Purinergic signaling in inflammatory cells: P2 receptor expression, functional effects, and modulation of inflammatory responses.* Purinergic signalling, 2013. **9**(3): p. 285-306.
33. Lee, D.H., et al., *Expression of P2 receptors in human B cells and Epstein-Barr virus-transformed lymphoblastoid cell lines.* BMC immunology, 2006. **7**: p. 22-33.
34. Guo, D., et al., *Functional efficacy of adenosine A(2)A receptor agonists is positively correlated to their receptor residence time.* British journal of pharmacology, 2012. **166**(6): p. 1846-59.
35. Gedge, L., *Corning® Epic® Label-Free Cell-Based Assay: Development of a Suspension Cell Assay Using a Human Monocyte Cell Line (THP-1 Cells).* Corning Life Sciences Application note, 2010.
36. Leung, G., et al., *Cellular Dielectric Spectroscopy: A Label-Free Technology for Drug Discovery.* Journal of the Association for Laboratory Automation, 2005. **10**(4): p. 258-269.

37. Molecular Devices Inc., *Analyzing Endogenous Receptors in Non-Adherent Cell Lines and Primary Cells with the CellKey Small Sample 96W Microplate.* CellKey System Application Highlight 5, 2008.
38. Obr, A., et al., *Real-time monitoring of hematopoietic cell interaction with fibronectin fragment: the effect of histone deacetylase inhibitors.* Cell adhesion & migration, 2013. **7**(3): p. 275-82.
39. Stupack, D.G., et al., *Matrix valency regulates integrin-mediated lymphoid adhesion via Syk kinase.* The Journal of cell biology, 1999. **144**(4): p. 777-88.
40. Rincon, J., J. Prieto, and M. Patarroyo, *Expression of integrins and other adhesion molecules in Epstein-Barr virus-transformed B lymphoblastoid cells and Burkitt's lymphoma cells.* International journal of cancer. Journal international du cancer, 1992. **51**(3): p. 452-8.
41. Humphries, J.D., A. Byron, and M.J. Humphries, *Integrin ligands at a glance.* Journal of cell science, 2006. **119**(Pt 19): p. 3901-3.
42. Johansson, S., et al., *Fibronectin-integrin interactions.* Frontiers in bioscience : a journal and virtual library, 1997. **2**: p. d126-46.
43. Gilchrist, C.L., et al., *Functional integrin subunits regulating cell-matrix interactions in the intervertebral disc.* Journal of orthopaedic research : official publication of the Orthopaedic Research Society, 2007. **25**(6): p. 829-40.
44. Atienza, J.M., et al., *Dynamic monitoring of cell adhesion and spreading on microelectronic sensor arrays.* Journal of biomolecular screening, 2005. **10**(8): p. 795-805.
45. Jacobson, B.S. and D. Branton, *Plasma membrane: rapid isolation and exposure of the cytoplasmic surface by use of positively charged beads.* Science, 1977. **195**(4275): p. 302-4.
46. Yavin, E. and Z. Yavin, *Attachment and culture of dissociated cells from rat embryo cerebral hemispheres on polylysine-coated surface.* The Journal of cell biology, 1974. **62**(2): p. 540-6.
47. Vincent, M., et al., *Genome-wide transcriptomic variations of human lymphoblastoid cell lines: insights from pairwise gene-expression correlations.* Pharmacogenomics, 2012. **13**(16): p. 1893-904.
48. Ross, R.A., et al., *Agonist-inverse agonist characterization at CB1 and CB2 cannabinoid receptors of L759633, L759656, and AM630.* British journal of pharmacology, 1999. **126**(3): p. 665-72.
49. Howlett, A.C., et al., *International Union of Pharmacology. XXVII. Classification of cannabinoid receptors.* Pharmacological reviews, 2002. **54**(2): p. 161-202.
50. Schroder, R., et al., *Deconvolution of complex G protein-coupled receptor signaling in live cells using dynamic mass redistribution measurements.* Nature biotechnology, 2010. **28**(9): p. 943-9.
51. Gkoumassi, E., et al., *Virodhamine and CP55,940 modulate cAMP production and IL-8 release in human bronchial epithelial cells.* British journal of pharmacology, 2007. **151**(7): p. 1041-8.
52. Atienza, J.M., et al., *Label-free and real-time cell-based kinase assay for screening selective and potent receptor tyrosine kinase inhibitors using microelectronic sensor array.* Journal of biomolecular screening, 2006. **11**(6): p. 634-43.
53. Zhuang, G., et al., *Phosphoproteomic analysis implicates the mTORC2-FoxO1 axis in VEGF signaling and feedback activation of receptor tyrosine kinases.* Science signaling, 2013. **6**(271): p. ra25.

CHAPTER 4

Getting personal: Endogenous adenosine receptor signaling in Lymphoblastoid Cell Lines

Julia M. Hillger

Carina Diehl

Eric van Spronsen

Dorret I. Boomsma

P. Eline Slagboom

Laura H. Heitman

Adriaan P. IJzerman

Biochem Pharmacol, 2016. **115**: p. 114-22
DOI: https://doi.org/10.1016/j.bcp.2016.06.006

Abstract

Genetic differences between individuals that affect drug action form a challenge in drug therapy. Many drugs target G protein-coupled receptors (GPCRs), and a number of receptor variants have been noted to impact drug efficacy. This, however, has never been addressed in a systematic way, and, hence, we studied real-life genetic variation of receptor function in personalized cell lines. As a showcase we studied adenosine A_{2A} receptor ($A_{2A}R$) signaling in lymphoblastoid cell lines (LCLs) derived from a family of four from the Netherlands Twin Register (NTR), using a non-invasive label-free cellular assay. The potency of a partial agonist differed significantly for one individual. Genotype comparison revealed differences in two intron SNPs including rs2236624, which has been associated with caffeine-induced sleep disorders. While further validation is needed to confirm genotype-specific effects, this set-up clearly demonstrated that LCLs are a suitable model system to study genetic influences on $A_{2A}R$ response in particular and GPCR responses in general.

Introduction

The majority of therapeutic drug targets to date are within the G protein-coupled receptor (GPCR) superfamily, a class of membrane-bound proteins [1, 2]. As such, GPCRs have been widely and intensively studied for the development of new therapeutics. Among the most well-studied members of this group are the adenosine receptors, a family comprising of 4 different subtypes: A_1, A_{2A}, A_{2B} and A_3 [3]. The various subtypes have been implied in a broad range of diseases and (patho)-physiological conditions, such as a variety of respiratory and inflammatory conditions for the A_{2A} or cardiovascular disorders for the A_1 [4]. Likewise, a wide variety of compounds selectively activating, inhibiting or modulating these receptors are available to date [3, 4]. Some of these have even been or are currently in clinical trials [3, 4]. Adenosine itself has been long approved for treatment of supraventricular tachycardia [3] and one A_{2A}R antagonist, istradefylline, has made it to the market as adjuvant drug therapy for Parkinson's disease in Japan [5].

In the emerging era of personalized medicine, it is paramount for drug development to better understand the effects of a drug not only in the overall population, but in the individual patient as well [6]. Genetic differences between individuals can affect drug action. Accordingly, several examples linking GPCR polymorphisms to diseases and drug response variation already exist [7-11], which include many commonly targeted GPCRs [11] such as purinergic [12, 13], cannabinoid [9, 10] and adenosine [14-16] receptors. Specifically for the adenosine A2A receptor, Single Nucleotide Polymorphisms (SNPs) have been associated with for instance anxiety [17, 18], caffeine intake [17], or vigilance and sleep [14]. Despite these examples of statistical association of genotype and condition, as well as extensive mutational characterization of the adenosine receptors, little is known about the direct functional effect of receptor polymorphisms or SNPs. Therefore, an ideal set-up would be to use patient-derived material as a model system to study the influence of polymorphisms on receptor response.

Lymphoblastoid cell lines (LCLs) are one of the most common choices for storing a person's genetic material [19, 20] and can be used to study GPCR function as has been shown in **Chapter 3**. For example, Morag, Kirchheiner [21] studied the influence of a few GPCR antagonists on LCL growth. We recently published an even more direct way of measuring receptor function, including agonist and antagonist concentration-effect curves (**Chapter 3**). Using a newly developed, highly sensitive label-free cellular assay technology [22, 23], we have shown in **Chapter 3** that it is possible to measure an individual's GPCR response in LCLs using the cannabinoid receptor 2 as example . In such label-free assays one can monitor drug

effects on an intact cell in real-time, rather than being limited to a static, one-molecule-detection of ligand binding or second messenger accumulation, as is usually employed in GPCR and adenosine receptor research [3, 22-24].

In the current study we have applied this label-free methodology to assess personal adenosine A_{2A} receptor function in LCLs. We characterized A_{2A}R signaling with various types of ligands including endogenous and synthetic agonists, partial agonist and antagonists, among which istradefylline. To allow conclusions about genotype in relation to receptor response, we compared responses between the individuals of a family of four from the Netherlands Twin Register [25]. This family consisted of two genetically unrelated individuals, the parents, as well as their children, which were monozygotic twins. Confirming the comparability of monozygotic twins' responses is one of the standard ways to control for genotype-unrelated effects, and thereby assess a system's suitability for genetic studies [25, 26].

Material and methods

Chemicals and reagents

Fibronectin from bovine plasma, Roswell Park Memorial Institute (RPMI) 1640 cell culture medium (25 mM HEPES and NaHCO3), NECA, adenosine and ATP were purchased from Sigma Aldrich (Zwijndrecht, The Netherlands). CGS21680, ZM241385 and CCPA were purchased from Abcam Biochemicals (Cambridge, United Kingdom), Cl-IB-MECA from Tocris Bioscience (Bristol, United Kingdom) and istradefylline from Axon Medchem (Groningen, The Netherlands). BAY60-6583 was synthesized in-house. LUF compounds were synthesized as described by van Tilburg, von Frijtag Drabbe Kunzel [27] for LUF5448 and LUF5631, van Tilburg, Gremmen [28] for LUF5549 and LUF5550 and Beukers, Chang [29] for LUF5834. All other chemicals and reagents were of analytical grade and obtained from commercial sources, unless stated otherwise.

Lymphoblastoid cell line generation

The lymphoblastoid cell lines (LCLs) were generated from participants of the Netherlands Twin Register (NTR, VU, Amsterdam, The Netherlands) [25]. The LCLs were generated by the Rutgers Institute (Department of Genetics, Piscataway, NJ, USA) using a standard transformation protocol [25], as previously mentioned in **Chapter 3**. Peripheral B-lymphocytes were transformed with Epstein–Barr Virus (EBV) by treatment with filtered medium from a Marmoset cell line in the presence of phytohemaglutinin (PHA) during the

first week of culture [19, 20, 30]. Cultures were maintained for 8–12 weeks to expand the EBV transformed lymphocytes and subsequently cryopreserved.

Cell culture

LCLs from a family of four individuals, two parents (genetically unrelated; called Parent 1 and Parent 2) and their monozygotic twin (genetically equal; called Twin 1 and Twin 2), were used for the experiments presented in this manuscript. According to culture conditions described in **Chapter 3**, cryopreserved cells were thawed and resuscitated. LCLs were grown as suspension cells in RPMI 1640 (25 mM HEPES and NaHCO3) supplemented with 15% FCS, 50 mg/ml streptomycin, 50 IU/ml penicillin, at 37 °C and 5% CO2 and were subcultured twice a week at a ratio of 1:5 on 10 cm ø plates. LCLs were disposed of after maximally 120 days in culture.

qPCR

RNA from LCLs was isolated using RNeasy Mini kit (QIAGEN, Venlo, The Netherlands). The RNA was treated with optional on column DNase digestion using DNase I (QIAGEN) and converted to cDNA using Superscript III (Invitrogen, Bleiswijk, The Netherlands). cDNA was run on custom designed 384 well qPCR plates from Lonza (Copenhagen, DK), in accordance with a previous publication [31]. These plates contained primers for 379 GPCRs as well as 3 RAMPs, together with primers for Rn18s and genomic DNA (Primers are listed in Engelstoft et al. [31]). Genomic DNA sample was used as calibrator and the relative copy number was calculated as stipulated previously [31].

Label-free whole-cell analysis (xCELLigence RTCA system)

Instrumentation principle

Cellular assays were performed using the xCELLigence RTCA system [22] in accordance with previously published protocols (**Chapter 3**, [32]). Briefly, the real-time cell analyzer (RTCA) measures the whole-cell responses using a detection system based on electrical impedance. Impedance is generated through cell attachment to gold electrodes embedded on the bottom of the microelectronic E-plates, which changes the local ionic environment at the electrode-solution interface. Relative changes in impedance (Z) are recorded in real-time and summarized in the so-called Cell Index (CI), a dimensionless parameter. The CI at any given time point is defined as $(Z_i - Z_0)$ Ω/15 Ω, where Z_i is the impedance at each individual time point. Z_0 represents the baseline impedance in the absence of cells, which is measured prior to the start of the experiment and defined as 0. As cells adhere to the electrodes, impedance

and the corresponding CI increase proportionally. Changes in cell number and degree of adhesion, as well as cellular viability and morphology are directly reflected in the impedance profile [22, 23]. Such cellular parameters are also affected upon activation of GPCR signaling, thereby allowing real-time monitoring of cellular signaling events [22].

General protocol

xCELLigence assays on LCLs were performed in accordance with a protocol previously described in Chapter 3 with minor modifications. Briefly, cells were seeded onto fibronectin-coated E-plates (10 µg/ml) at 80,000 cells/well. All cell counts were performed using Trypan blue staining and a BioRad TC10 automated cell counter. E-plates were placed into the recording station situated in a 37 °C and 5% CO2 incubator and impedance was measured overnight. After 18 h, cells were stimulated by a GPCR ligand or vehicle control in 5 µl, unless specified otherwise. As compound solubility required addition of dimethylsulfoxide (DMSO), the final DMSO concentration upon ligand or vehicle addition was kept at 0.25% DMSO for all wells and assays.

For agonist screening purposes, cells were stimulated with agonist concentrations corresponding to 100 × K_i value for their respective receptors [4]. For the partial agonist screen, all partial agonists as well as reference agonist CGS21680 were tested at a concentration of 1 µM.

Agonist concentration–response curves were generated by stimulating cells with increasing concentrations of the respective agonist. For antagonist assays, cells were pre-incubated for 30 min with 5 µl of vehicle control or the respective antagonist at increasing concentrations. Subsequently, cells were challenged with a submaximal agonist concentration of CGS21680 that was equal to the agonist's EC_{80} value (100 nM) or vehicle control. Generally, compound dilutions for concentration–response curves were generated using the digital TECAN dispenser (Tecan Group, Männedorf, Switzerland).

Data analysis

Data were analyzed as stipulated in the previous protocol in Chapter 3. Briefly, experimental data were obtained with RTCA Software 1.2 (Roche Applied Science). Ligand responses were normalized to Δ cell index (Δ CI) and exported to GraphPad Prism 6.0 (GraphPad Software Inc., San Diego, CA, USA) for further analysis. Vehicle control was subtracted as baseline to correct for any agonist-independent effects. Peak responses were defined as highest Δ CI (Max ΔCI) observed within 60 min after compound addition. When stipulated, area under the curve (AUC ΔCI) within those 60 min was used as an additional parameter to analyze

response height. Peak values and experimental Δ CI traces were used for construction of bar graphs or concentration–effect curves by nonlinear regression and calculation of IC_{50}, EC_{50} and EC_{80} values. K_i values for antagonists were calculated using the Cheng–Prusoff equation [33] using the concentration of the agonist (CGS21680, 100 nM) and EC_{50} value corresponding to each cell line.

All values obtained are means of at least three independent experiments performed in duplicate, unless stated otherwise. Statistical significance was determined by comparison of the means of multiple data sets by a one-way ANOVA, followed by Tukey's post hoc test for comparison of all columns or a Dunnett's post hoc test when comparing to control or reference compound.

Processing of SNPs and genetic data

SNP data for the four individuals were obtained from the Genomes of the Netherlands consortium (*http://www.nlgenome.nl/*) of which the Netherlands Twin Register is part of and analyzed in-house using PLINK, an open-source whole genome association analysis toolset [34, 35].

Results

Label-free assays enable detection of adenosine A_{2A} receptor signaling in LCLs

The standard applications of label-free technologies such as the xCELLigence for GPCRs generally require adherent cell systems [22, 23, 32]. LCLs are suspension cells for which we have developed a protocol in which fibronectin coating of the plate wells allowed the LCLs to adhere (**Chapter 3**). With this approach we confirmed the presence or absence of adenosine receptor subtypes by testing selective agonists using LCLs of one individual as example (parent 2). These agonists included selective ligands such as CCPA for $hA_{1A}R$, CGS21680 for $hA_{2A}AR$, BAY60-6583 for $hA_{2B}AR$, Cl-IB-MECA for $hA_{3A}R$ and the unselective agonist NECA. To ensure full receptor occupancy, we tested the compounds at concentrations corresponding to 100 × K_i value for their respective receptor [4]. An example of resulting xCELLigence traces is provided in **Fig. 1**. Addition of the compounds induced changes in cellular morphology that were recorded in real-time. Typically, agonist addition resulted in an immediate increase of impedance to a peak level which gradually decreased toward a plateau within 30 min. Responses were normalized to the subtype unselective agonist NECA for reference. Overall, $hA_{2A}AR$ selective agonist CGS21680 gave the highest response which was close to the response to NECA itself, as would be expected from the expression data which showed that

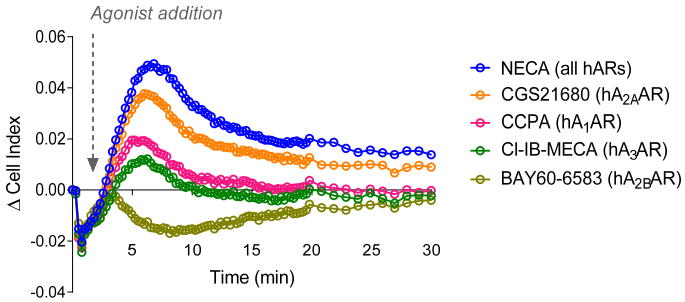

Figure 1. Adenosine receptor agonist screen. Cells were seeded onto fibronectin-coated wells (10 µg/ml) at 80,000 cells/well. After 18 h of growth, cells were stimulated with AR ligands at concentrations corresponding to 100 × K_i value for their respective receptor [4]. CCPA (83 nM) for hA_1AR at, CGS21680 (2.7 µM) for $hA_{2A}AR$, BAY60-6583 (36 µM) for $hA_{2B}AR$ and Cl-IB-MECA (140 nM) for hA_3AR were compared to the unselective hAR agonist NECA. Unselective NECA was tested a concentration of 14 µM which is at least 100 × K_i or more for all ARs. Representative xCELLigence traces of a baseline-corrected ligand response are given of one individual (parent 2), where time point 0 represents the time of ligand addition. Data are from at least three separate experiments performed in duplicate. Statistical differences of compound responses to NECA were analyzed using a one-way ANOVA with Dunnett's post hoc-test. $^{*}p < 0.05$, $^{**}p < 0.01$, $^{***}p < 0.001$, $^{****}p < 0.0001$. Response heights normalized to NECA (100 ± 1%) were for CCPA: 35 ± 5% , CGS21680: 67 ± 11%, BAY60-6583: 40 ± 14% and Cl-IB-MECA: 39 ± 10% .

$hA_{2A}AR$ is the highest expressed in LCLs while the other three subtypes were expressed to a much lower extent (receptor expression family mean ± SEM was $hA_{2A}AR$ 21.87 ± 5.41, $hA_{1A}R$ 1.35 ± 0.85, $hA_{2B}AR$ 0.88 ± 0.35 and hA_3AR 0.40 ± 0.37, calculated using a normalization factor derived from all genes expressed above genomic DNA levels, in accordance with a previous publication by Engelstoft et al. [31]). In fact, CGS21680 was the only compound whose response did not differ significantly from NECA. CCPA, the $hA_{1A}R$ agonist, and hA_3AR agonist CL-IB-MECA gave small responses (**Fig. 1**), most likely caused by a modest activation of $A_{2A}R$ at the concentrations used. While all other agonists displayed a positive impedance response, BAY60-6583 gave a small positive peak followed by a decline to a negative impedance plateau. Responses to all agonists from LCLs of a second individual, parent 1, gave comparable results in terms of conclusion of receptor subtype presence (*data not shown*).

$A_{2A}R$ agonist and antagonist responses compare well between monozygotic twins and their parents

Subsequently, the label-free methodology was applied to compare adenosine A_{2A}receptor related responses between LCLs derived from the four different individuals. We characterized $A_{2A}R$ signaling with various types of ligands, including the endogenous agonist adenosine as well as the synthetic non-selective agonist NECA and $A_{2A}R$ selective agonist

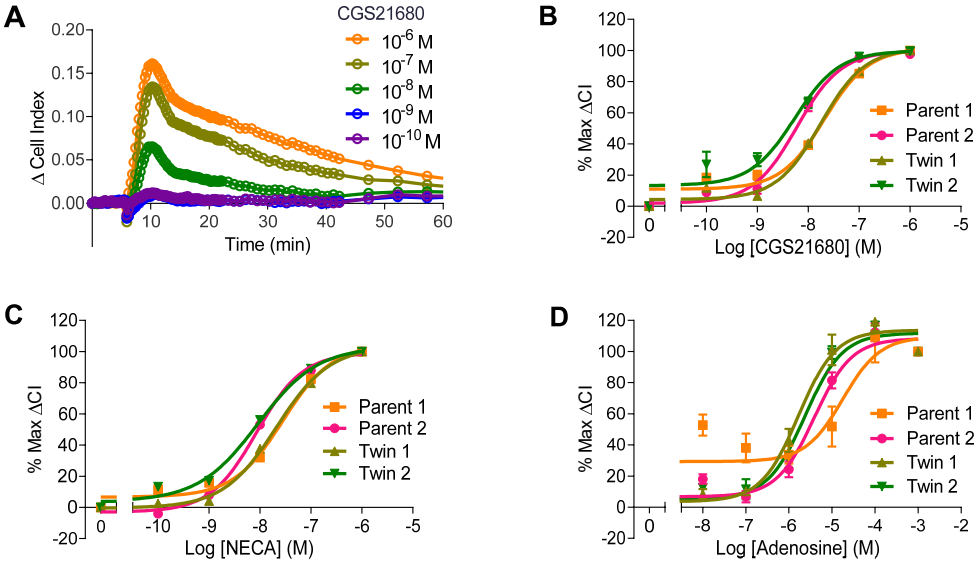

Figure 2. Characterization of full agonist responses in LCLs from a family of four from the NTR. The family consists of two genetically unrelated individuals, parent 1 and 2, and their children which are a monozygotic twin (twin 1 and twin 2). Cell lines were stimulated with endogenous agonist adenosine [1 nM–100 µM], synthetic agonists NECA or CGS21680 [100 pM–1 µM] 18 h after seeding (80,000 cells/well). Representative example of a baseline-corrected concentration-dependent CGS21680 response (**A**). Concentration–response curves for CGS21680 (**B**), NECA (**C**) and adenosine (**D**) were derived from peak Δ cell index (Δ CI) within 60 min after agonist addition (see Methods). Data in **B–D** represent the means ± SEM of at least three separate experiments performed in duplicate.

CGS21680. All three agonists displayed a similar shape of and height in response, both within each cell line and between individuals. An example of such a response is depicted in **Fig. 2A**. The corresponding concentration–response curves are shown in **Fig. 2B-D**. In a similar manner, concentration-inhibition curves for $A_{2A}R$ antagonists ZM241385 and istradefylline were obtained. An example trace of such an agonist/antagonist experiment is in **Fig. 3A** while the concentration-inhibition curves are represented in **Fig. 3B** and **C**. AllpEC_{50} and pIC_{50} values for the LCLs of the four individuals are summarized in **Table 1**. From the pIC_{50} values we derived affinity (pK_i) values for both antagonists using the Cheng–Prusoff equation. For ZM241385 these values were 8.29 ± 0.11, 9.00 ± 0.09, 8.88 ± 0.05 and 9.08 ± 0.08 for parent 1, parent 2, twins 1 and 2. pK_i values for istradefylline were 6.84 ± 0.17, 7.67 ± 0.07, 7.47 ± 0.05 and 7.88 ± 0.07, respectively.

$A_{2A}R$ partial agonist responses are measurable in LCLs

Finally, we tested a number of partial agonists synthesized in house, all at a concentration of

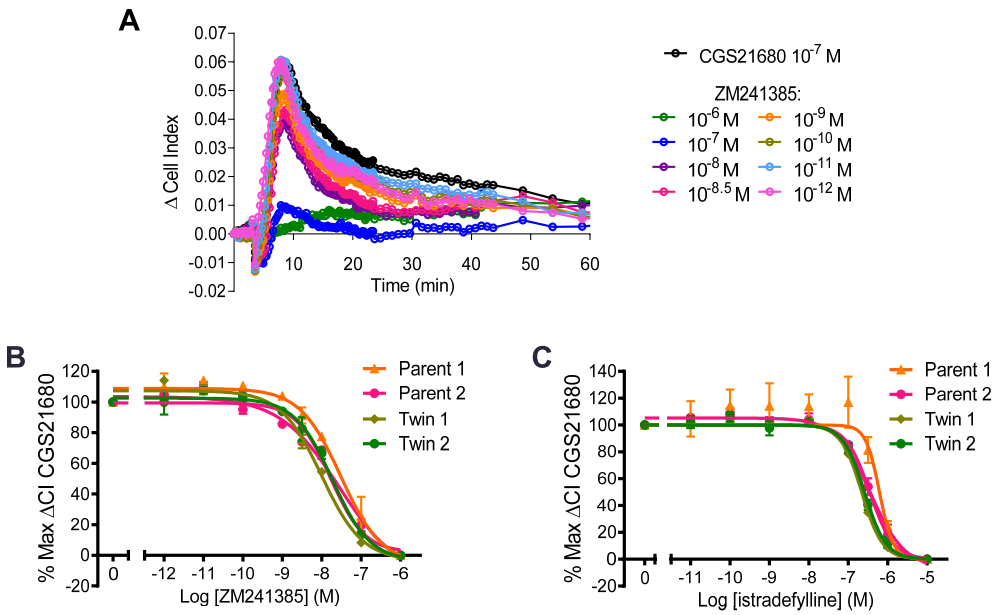

Figure 3. Characterization of A_{2A}R antagonist responses in LCLs from a family of four from the NTR. The family consists of two genetically unrelated individuals, parent 1 and 2, and their children which are a monozygotic twin (twin 1 and twin 2). For antagonist curves, cell lines were pre-incubated for 30 min with increasing concentrations of ZM241385 [10 pM–10 μM] before stimulation with CGS21680 [EC_{80}: 100 nM] 18 h after seeding (80,000 cells/well). Representative example of a baseline-corrected concentration-dependent response to ZM241385 (**A**). Concentration–response curves for ZM241385 (**B**) and istradefylline (**C**) were derived from peak Δ cell index (Δ CI) values within 60 min after agonist addition. Data in **B** and **C** represent the means ± SEM of at least three separate experiments performed in duplicate.

1 μM. An example trace of partial agonist and CGS21680 responses for LCLs of one individual is in **Fig. 4A**. Some partial agonists (LUF5549 and LUF5631) displayed high efficacy in this cell system, as their maximum response almost equaled that of the full agonist CGS21680 with 112 ± 9% and 95 ± 11%, respectively. LUF5448 and LUF5550 however showed robust partial agonistic behavior of 64 ± 5% and 40 ± 5% of maximal efficacy (**Fig. 4A**). Partial agonist LUF5834 gave a different shape of response, which was marked by a negative peak followed by a negative impedance plateau, which differed significantly from any other partial agonist or reference full agonist CGS21680 (**Fig. 4A**). Its maximum response was therefore at 17 ± 8%.

A_{2A} partial agonist response differs between individuals

In order to further demonstrate the sensitivity of the label-free technology combined with LCLs, one partial agonist was chosen to obtain concentration–response curves. LUF5448 was

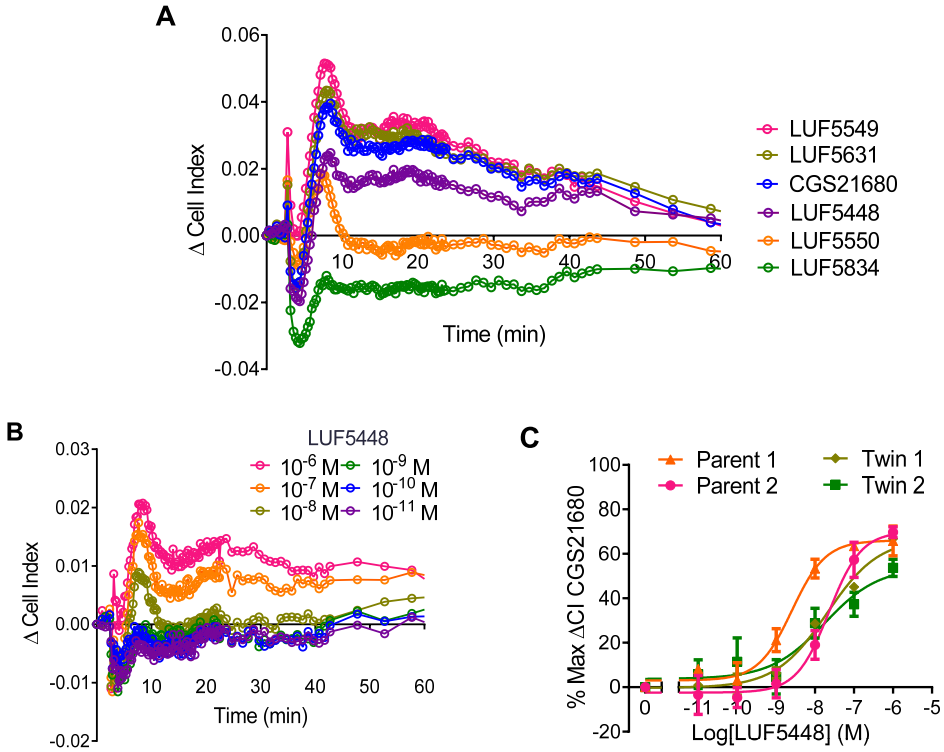

Figure 4. $A_{2A}R$ partial agonist responses in LCLs. Cells were stimulated 18 h after seeding (80,000 cells/well) with $A_{2A}R$ partial agonists as well as full agonist CGS21680 [all at 1 µM] for reference. (**A**) Representative example of a baseline-corrected response is given from one individual (parent 2). Maximal responses of partial agonists compared to CGS21680 were 112 ± 9% for LUF5549, 95 ± 11% for LUF5631, 64 ± 5% for LUF5448, 40 ± 5% for LUF5550 and 17 ± 8% for LUF5834. Statistical differences from CGS21680 were assessed with a one-way ANOVA with Dunnett's post hoc test. $^{*}p < 0.05$, $^{**}p < 0.01$, $^{***}p < 0.001$, $^{****}p < 0.0001$. (**B**) Representative example of a baseline-corrected response of $A_{2A}R$ partial agonist LUF5448 [10 pM–1 µM] for one individual (parent 2). (**C**) Concentration–response curves for all four individuals were derived from peak Δ cell index (Δ CI) within 60 min after agonist addition, normalized to CGS21680 as reference. Data are representative examples or means ± SEM of at least three separate experiments performed in duplicate.

chosen as a suitable candidate as it displayed robust partial agonistic behavior with a maximum effect of approx. 50% of the reference full agonist CGS21680. An example xCELLigence trace is provided in **Fig. 4B** while the corresponding concentration–response curves for the four individuals are summarized in **Fig. 4C**. Interestingly, while three of the individuals gave very comparable curves and pEC_{50} values, one of the parents differed significantly from all (**Table 1**), with an approx. tenfold higher potency (pEC_{50} value). LUF5448 behaved as a typical partial agonist on all cell lines with a % Max ΔCI of CGS21680 of 66 ± 7% for parent 1, 70 ± 2% for parent 2 and 67 ± 2% and 54 ± 4% for twins 1 and 2, respectively.

Table 1. Overview of the pEC_{50} and pIC_{50} values of Adenosine, NECA, CGS21680, ZM241385, istradefylline and LUF5448 for the tested individuals' LCLs. Data represents the means of at least three separate experiments performed in duplicate. Statistical analysis was performed with one-way ANOVA with Tukey post-hoc test. Asterisks highlight statistical differences to the other individuals (P1 = parent 1; P2 = parent 2; T1 = Twin 1; T2 = twin 2). * p<0.05, ** p<0.01,*** p<0.001.

Ligand	pEC_{50} / pIC_{50} (M)				
	Literature	Parent 1	Parent 2	Twin 1	Twin 2
Adenosine *Endogenous agonist*	*6.51 [36]*	6.34 ± 0.32	5.59 ± 0.13	5.94 ± 0.12	5.82 ± 0.16
NECA *Full non-selective agonist*	*8.60 ± 0.02 [32]* *7.59 ± 0.33 [37]*	7.54 ± 0.07 **T2; ***P2	8.06 ± 0.04 **T1; ***P1	7.68 ± 0.04 *T2; **P2	7.92 ± 0.07 *T1; **P1
CGS21680 *Full selective agonist*	*8.42 ± 0.05 [32]* *8.18 ± 0.36 [38]*	7.61 ± 0.14	8.20 ± 0.09	7.76 ± 0.08	8.30 ± 0.42
ZM241385 *Antagonist/ inverse agonist*	*8.80 [a] [4]*	7.52 ± 0.15	7.55 ± 0.17	8.01 ± 0.07	7.73 ± 0.10
Istradefylline *Antagonist/ inverse agonist*	*7.92 [a] [39]*	6.21 ± 0.09 *P2; **T1; ***T2	6.45 ± 0.04 *P1	6.66 ± 0.02 **P1	6.59 ± 0.03 ***P1
LUF5448 *Partial agonist*	*8.62 ± 0.19 [32]*	8.69 ± 0.11 **all	7.60 ± 0.11 **P1	7.69 ± 0.08 **P1	7.76 ± 0.26 **P1

a. K_I

Table 2. SNP genotype differences within the ADORA2A gene between the four individuals included in this study. The heterozygous differences of parent 1 to the other individuals are underlined. Data obtained from the NTR and analyzed in-house.

SNP	Genotype		
	Parent 1	Parent 2	Twins
rs34999116	T C	C C	C C
rs5751869	A G	A G	G G
rs5760410	A G	A G	G G
rs5751870	T G	T G	G G
rs5751871	T G	T G	G G
rs9624470	A G	A G	G G
rs11704959	A C	C C	A C
rs2298383	T C	T C	C C
rs3761420	A G	A G	G G
rs3761422	C T	C T	T T
rs2267076	C T	C T	T T
rs11704811	T C	C C	T C
rs17650801	G G	A G	G G
rs4822489	G T	G T	T T
rs2236624	C C	T C	T C
rs5751876	C T	C T	T T

Genotype differences between the four individuals

SNP data for the four individuals were obtained from the Genomes of the Netherlands consortium and analyzed in-house using PLINK, an open-source whole genome association analysis toolset [34, 35]. SNPs within the boundaries of the ADORA2A gene as defined by human genome overview GRCh37 were selected. Based on GRCh37 and dbSNP information (*http://www.ncbi.nlm.nih.gov/SNP/*), SNPs were further annotated according to position (e.g., intron, exon) and SNP type (e.g., missense, synonymous). The genotype differences of the individuals used in this study are summarized in **Table 2**.

Discussion

It is well established that label-free technologies can be applied to investigate GPCR signaling in heterologous as well primary adherent cell systems [22, 23, 32]. For instance, the xCELLigence system has successfully been applied to study ligand effects on the cannabinoid receptor 2 (CB2) and the metabotropic glutamate receptor 1 (mGluR1) using recombinant Chinese hamster ovary (CHO) cells [40]. Similarly, $A_{2A}R$ signaling has been studied in HEK293hA_{2A}AR cells using selective agonists as well as partial agonists [32]. While only such recombinant cell lines have been used to study $A_{2A}R$ signaling using label-free technology, $A_{2A}R$ function has been studied in some endogenous cell types using other, more traditional assays [38, 41, 42]. However, studying a person's $A_{2A}R$ response using a personal cell line such as the LCLs has not been possible up until now, and is therefore a translational step further toward precision medicine.

Applicability of this label-free technology to LCLs is, however, not entirely straightforward due to their suspension cell nature. Nonetheless, adherence levels after coating of the wells with fibronectin were sufficient to allow monitoring of receptor responses, as was demonstrated by testing adenosine receptor ligands (**Fig. 1**). Activation of $A_{2A}R$ receptors led to a typical increase in impedance often seen for GPCR ligands in LCLs. For instance, P2Y receptors (Ensembl family: ENSFM00760001715026) are abundantly present on many cell types, including LCLs [43, 44], which has made ATP a reference agonist for testing of functional LCL responses (**Chapter 3**). Interestingly, both adenosine receptor agonists and ATP display the same shape of response, which was also comparable to the response to cannabinoid receptor 2 (CB2) agonists as seen in earlier in **Chapter 3**. Herein we showed that LCL densities of 50,000 cells/well were sufficient for detection of a robust CB_2 as well as P2Y receptor response. In the present chapter seeding densities were increased to 80,000 cells/well to obtain a window sufficient for $A_{2A}R$ partial agonist characterization.

It is well known that $A_{2A}R$ are expressed in immune cells, including lymphocytes and LCLs [41, 45], which was confirmed in this study by both receptor expression levels in the qPCR experiments and the responses to selective adenosine receptor agonists in the label-free assay (**Fig. 1**). The results from these tests indicated that $A_{2A}R$ are the only adenosine receptors highly expressed in LCLs. This was further confirmed by the comparability of the responses of all three full agonists tested in this paper. The endogenous ligand adenosine as well as subtype unselective NECA and $A_{2A}R$ selective CGS21680 had comparable responses (**Fig. 2**) suggesting these were all mediated through the $A_{2A}R$. Similarly, antagonist responses were also measurable for all four different individuals (**Fig. 3**), strengthening the conclusion that responses are mediated through $A_{2A}R$ only.

While it is straightforward to confirm that an impedance response is a specific receptor-mediated effect with recombinant cell lines, namely by simply using the untransfected parental cell line as negative control [32, 40], this is not possible in cell lines with endogenous receptor expression. Therefore, for LCLs the most reliable way is to confirm overall receptor pharmacology with receptor subtype-selective agonists and antagonists. By showing that the $A_{2A}R$ selective antagonists ZM241385 and istradefylline competed with and blocked the signal of the $A_{2A}R$ selective agonist CGS21680 (Fig. 3), we confirmed that the impedance effects indeed originate from an $A_{2A}R$ response.

Overall, agonist pEC_{50} values for agonists were within a log unit from previously reported literature values obtained with standard functional assays on heterologous cell lines (**Table 1**). For instance, adenosine itself is within that range as it has been reported with an EC_{50} value of 310 nM in a cAMP assay on $hA_{2A}AR$ [36]. For the antagonists, the calculated pK_i values of ZM241385 and istradefylline were also within the range of previously published values. This calculation corrects for the fact that the same concentration of agonist was used during the assay, corresponding to the EC_{80} of CGS21680, while the efficacy of this agonist differed slightly between cell lines.

Following this characterization of full agonists and antagonists to verify the presence and functional relevance of $A_{2A}R$, a number of partial agonists were tested to demonstrate the sensitivity of the system. The set-up was well able to measure partial agonist effects on LCLs, quite comparable to our previous study on HEK293$hA_{2A}AR$ cells [32]. Interestingly, while most agonists induced an increase in impedance with a single peak in LCLs, there were two agonists which gave rise to a different shape of response. Both BAY60-6583 and the partial agonist LUF5834 responses were marked by a small peak followed by a negative impedance plateau, rather than one positive peak (**Fig. 1** and **Fig. 4**). Interestingly, both BAY60-6583 and LUF5834 belong to a structurally distinct class of non-ribose agonists, as opposed to all other

agonists tested in this paper. Hence, it seems that non-ribose agonists, while equally able to activate the $hA_{2A}AR$, give rise to a different cellular response than the more common ribose-containing agonists. This was not observed in the heterologous HEK293$hA_{2A}AR$ cell line where partial agonist LUF5834 had been tested previously [32], which highlights the differences of using an unmodified human cell line when characterizing compound effects. In fact, efficacies and signaling of ligands can differ under artificial or heterologous conditions due to a number of factors [22, 46]. Receptor overexpression, differences in intracellular metabolic conditions as well as products from other genes could modify cellular responses. Unfortunately, most studies of receptor function involve artificially expressed receptors in heterologous cell systems, such as CHO or HEK cells [3, 32]. While useful for high-throughput screening and fundamental research, such systems are far from the real-life situation in an individual. To move further toward the physiological situation, it is essential to study receptor function in a more endogenous setting such as LCLs. This is especially true when attempting to understand how polymorphisms may functionally affect the receptor and therefore the drug response of an individual.

Employing the LCLs, we investigated genotype effects on receptor response by comparing the effects of various types of $A_{2A}R$ ligands between the individuals of a family of four from the Netherlands Twin Register, which consisted of two genetically unrelated individuals, the parents, and their children, which were monozygotic twins. Overall, the results were comparable between all individuals. Analyzing and confirming the comparability of results obtained in monozygotic twins is one of the standard ways in genetic studies to control for genotype-unrelated effects, and assess a system's suitability for genetic studies [25, 26]. As expected, the twins did not differ significantly from each other, with exception of their pEC_{50} values for NECA ($p < 0.05$; **Table 1**). Interestingly, NECA was also the only ligand for which all individuals differed significantly in their pEC_{50} values. As monozygotic twins are genetically identical, these differences could not be related to genetic effects and therefore precluded any further conclusion about differences between the parents. However, parent 1 showed significant differences on two occasions, when all other three individuals, including the monozygotic twins, were comparable. This was the case with istradefylline as well as with the partial agonist LUF5448. While with istradefylline the difference was rather marginal within half a log unit, the potency shift (approx. tenfold higher) for LUF5448 was much more pronounced for parent 1. Partial agonists are deemed more sensitive to system-related differences in receptor function, for instance in receptor expression or downstream coupling, than full agonists or antagonists [28]. Therefore, the difference in potency possibly reflects subtle changes introduced by the genetic differences between individuals. While none of the

four individuals had non-synonymous SNPs in the ADORA2A gene (**Table 2**), there were some heterozygous differences present in non-coding SNPs. Two SNP differences were in line with the pEC_{50} and pIC_{50} changes, namely in which only parent 1 differed while parent 2 and the twins showed the same genotype and response. These were rs34999116 where parent 1 is heterozygote for the minor allele and rs2236624 where parent 1 is homozygote for the minor allele. Interestingly, the C-allele of rs2236624, which is located in intron 4 of the ADORA2A gene, has been associated with vigilance and sleep, while the CC genotype has been associated with anxiety in autism patients [14-16]. The TT genotype has been associated with pharmacotherapy-related toxicities in acute lymphoblastic leukemia [47]. Several studies have proposed a subtle effect on receptor expression as possible mechanism, as this intron SNP has intermediate regulatory potential [16, 47]. As we did not observe significant differences in receptor mRNA levels in our qPCR experiments, this regulation may affect the subsequent translation. Changes in receptor expression may affect G protein coupling efficiency, for which a partial agonist is more sensitive than a full agonist.

Although this genetic variation does not provide causal evidence that response differences as observed in the LCLs from these individuals are directly related to these SNPs, the experimental results show that the chosen methodology and set-up are capable of picking up individual differences in receptor signaling for the $A_{2A}R$. Although $A_{2A}R$ function has been studied in endogenous cell types [38, 41, 42], we made a further step toward both physiologically relevant conditions and personalized medicine by enabling the study of a person's $A_{2A}R$ response using a combination of LCLs from a family of four from the NTR and a non-invasive label-free cellular assay.

It is increasingly recognized that genetic differences between individuals form a large challenge in drug therapy indeed. In our study of real-life genetic variation of $A_{2A}R$ signaling, we found that partial agonist potency differed significantly for one individual with genotype differences in two intron SNPs, one of which has previously been associated with caffeine-induced sleep disorders. While further validation is needed to confirm genotype-specific effects, this set-up clearly demonstrated that LCLs are a suitable model system to study genetic influences on $A_{2A}R$ and GPCR responses in general. LCLs express a wide range of other 'drugable' GPCRs, besides the $A_{2A}R$, CB_2 and P2Y receptors investigated in this and earlier studies (**Chapter 3**, [45]). Therefore, screening receptor responses in LCLs may help to provide the mechanistic link between polymorphisms of various GPCRs and the individual variation in drug response.

Data access

The LCLs used in this study were kindly provided within the framework of this collaboration [25] and are part of the Netherlands Twin Register (NTR; *http://www.tweelingenregister.org/en/*), and part of the Center for Collaborative Genomic Studies on Mental Disorders (NIMH U24 MH068457-06). Data and biomaterials (such as cell lines) are available to qualified investigators, and may be accessed by following a set of instructions stipulated on the National Institute of Mental Health (NIMH) website (*https://www.nimhgenetics.org/access_data_biomaterial.php*).

Acknowledgements

This research was supported by the Center for Collaborative Genomic Studies on Mental Disorders (NIMH U24 MH068457-06). We thank Dr. A. Brooks (Department of Genetics, Rutgers University, Piscataway, NJ, USA) for preparation of the lymphoblastoid cell lines. We also thank Kristoffer L. Egerod from the Laboratory for Molecular Pharmacology, Department of Neuroscience and Pharmacology, Faculty of Health and Medical Sciences, University of Copenhagen, Denmark, for performing the qPCR analysis.

References

1. Overington, J.P., B. Al-Lazikani, and A.L. Hopkins, *How many drug targets are there?* Nat Rev Drug Discov, 2006. **5**(12): p. 993-6.
2. Russ, A.P. and S. Lampel, *The druggable genome: an update.* Drug Discov Today, 2005. **10**(23-24): p. 1607-10.
3. Fredholm, B.B., et al., *International Union of Basic and Clinical Pharmacology. LXXXI. Nomenclature and classification of adenosine receptors--an update.* Pharmacol Rev, 2011. **63**(1): p. 1-34.
4. Jacobson, K.A. and Z.G. Gao, *Adenosine receptors as therapeutic targets.* Nat Rev Drug Discov, 2006. **5**(3): p. 247-64.
5. Muller, T., *The safety of istradefylline for the treatment of Parkinson's disease.* Expert Opin Drug Saf, 2015: p. 1-7.
6. Venkatakrishnan, A.J., et al., *Molecular signatures of G-protein-coupled receptors.* Nature, 2013. **494**(7436): p. 185-94.
7. Davies, M.A., et al., *Pharmacologic analysis of non-synonymous coding h5-HT2A SNPs reveals alterations in atypical antipsychotic and agonist efficacies.* Pharmacogenomics J, 2006. **6**(1): p. 42-51.
8. Docherty, S.J., et al., *A genetic association study of DNA methylation levels in the DRD4 gene region finds associations with nearby SNPs.* Behav Brain Funct, 2012. **8**: p. 31-44.
9. Ishiguro, H., et al., *Brain cannabinoid CB2 receptor in schizophrenia.* Biol Psychiatry, 2010. **67**(10): p. 974-82.
10. Tong, D., et al., *Association of single-nucleotide polymorphisms in the cannabinoid receptor 2 gene with schizophrenia in the Han Chinese population.* J Mol Neurosci, 2013. **51**(2): p. 454-60.
11. Sadee, W., et al., *Genetic variations in human G protein-coupled receptors: implications for drug therapy.* AAPS pharmSci, 2001. **3**(3): p. 54-80.
12. Buscher, R., et al., *P2Y2 receptor polymorphisms and haplotypes in cystic fibrosis and their impact on Ca2+ influx.* Pharmacogenetics and genomics, 2006. **16**(3): p. 199-205.
13. Wesselius, A., et al., *Association of P2Y(2) receptor SNPs with bone mineral density and osteoporosis risk in a cohort of Dutch fracture patients.* Purinergic signalling, 2013. **9**(1): p. 41-9.
14. Bodenmann, S., et al., *Polymorphisms of ADORA2A modulate psychomotor vigilance and the effects of caffeine on neurobehavioural performance and sleep EEG after sleep deprivation.* British journal of pharmacology, 2012. **165**(6): p. 1904-13.
15. Childs, E., et al., *Association between ADORA2A and DRD2 polymorphisms and caffeine-induced anxiety.* Neuropsychopharmacology : official publication of the American College of Neuropsychopharmacology, 2008. **33**(12): p. 2791-800.
16. Freitag, C.M., et al., *Adenosine A(2A) receptor gene (ADORA2A) variants may increase autistic symptoms and anxiety in autism spectrum disorder.* European child & adolescent psychiatry, 2010. **19**(1): p. 67-74.
17. Rogers, P.J., et al., *Association of the anxiogenic and alerting effects of caffeine with ADORA2A and ADORA1 polymorphisms and habitual level of caffeine consumption.* Neuropsychopharmacology, 2010. **35**(9): p. 1973-83.

18. Hohoff, C., et al., *Adenosine A(2A) receptor gene: evidence for association of risk variants with panic disorder and anxious personality.* J Psychiatr Res, 2010. **44**(14): p. 930-7.
19. Sie, L., S. Loong, and E.K. Tan, *Utility of lymphoblastoid cell lines.* J Neurosci Res, 2009. **87**(9): p. 1953-9.
20. Sugimoto, M., et al., *Steps involved in immortalization and tumorigenesis in human B-lymphoblastoid cell lines transformed by Epstein-Barr virus.* Cancer research, 2004. **64**(10): p. 3361-4.
21. Morag, A., et al., *Human lymphoblastoid cell line panels: novel tools for assessing shared drug pathways.* Pharmacogenomics, 2010. **11**(3): p. 327-40.
22. Yu, N., et al., *Real-time monitoring of morphological changes in living cells by electronic cell sensor arrays: an approach to study G protein-coupled receptors.* Anal Chem, 2006. **78**(1): p. 35-43.
23. Fang, Y., *Label-Free Receptor Assays.* Drug Discov Today Technol, 2011. **7**(1): p. e5-e11.
24. Rocheville, M., et al., *Mining the potential of label-free biosensors for seven-transmembrane receptor drug discovery.* Progress in molecular biology and translational science, 2013. **115**: p. 123-42.
25. Willemsen, G., et al., *The Netherlands Twin Register biobank: a resource for genetic epidemiological studies.* Twin Res Hum Genet, 2010. **13**(3): p. 231-45.
26. Silventoinen, K., et al., *The CODATwins Project: The Cohort Description of Collaborative Project of Development of Anthropometrical Measures in Twins to Study Macro-Environmental Variation in Genetic and Environmental Effects on Anthropometric Traits.* Twin Res Hum Genet, 2015. **18**(4): p. 348-60.
27. van Tilburg, E.W., et al., *2,5'-Disubstituted adenosine derivatives: evaluation of selectivity and efficacy for the adenosine A(1), A(2A), and A(3) receptor.* Journal of medicinal chemistry, 2002. **45**(2): p. 420-9.
28. van Tilburg, E.W., et al., *2,8-Disubstituted adenosine derivatives as partial agonists for the adenosine A2A receptor.* Bioorganic & medicinal chemistry, 2003. **11**(10): p. 2183-92.
29. Beukers, M.W., et al., *New, non-adenosine, high-potency agonists for the human adenosine A2B receptor with an improved selectivity profile compared to the reference agonist N-ethylcarboxamidoadenosine.* Journal of medicinal chemistry, 2004. **47**(15): p. 3707-9.
30. Miller, G. and M. Lipman, *Release of infectious Epstein-Barr virus by transformed marmoset leukocytes.* Proceedings of the National Academy of Sciences of the United States of America, 1973. **70**(1): p. 190-4.
31. Engelstoft, M.S., et al., *Seven transmembrane G protein-coupled receptor repertoire of gastric ghrelin cells.* Mol Metab, 2013. **2**(4): p. 376-92.
32. Guo, D., et al., *Functional efficacy of adenosine A(2)A receptor agonists is positively correlated to their receptor residence time.* British journal of pharmacology, 2012. **166**(6): p. 1846-59.
33. Cheng, Y. and W.H. Prusoff, *Relationship between the inhibition constant (K1) and the concentration of inhibitor which causes 50 per cent inhibition (I50) of an enzymatic reaction.* Biochem Pharmacol, 1973. **22**(23): p. 3099-108.
34. Purcell, S., et al., *PLINK: a tool set for whole-genome association and population-based linkage analyses.* Am J Hum Genet, 2007. **81**(3): p. 559-75.
35. Purcell, S., *PLINK v1.07, http://pngu.mgh.harvard.edu/purcell/plink/*.

36. Yan, L., et al., *Adenosine receptor agonists: from basic medicinal chemistry to clinical development.* Expert Opin Emerg Drugs, 2003. **8**(2): p. 537-76.
37. Schulte, G. and B.B. Fredholm, *Human adenosine A(1), A(2A), A(2B), and A(3) receptors expressed in Chinese hamster ovary cells all mediate the phosphorylation of extracellular-regulated kinase 1/2.* Molecular pharmacology, 2000. **58**(3): p. 477-82.
38. Desai, A., et al., *Adenosine A2A receptor stimulation increases angiogenesis by down-regulating production of the antiangiogenic matrix protein thrombospondin 1.* Molecular pharmacology, 2005. **67**(5): p. 1406-13.
39. Kase, H., *Industry forum: Progress in pursuit of therapeutic A2A antagonists: The adenosine A2A receptor selective antagonist KW6002: Research and development toward a novel nondopaminergic therapy for Parkinson's disease.* Neurology, 2003. **61**(11 suppl 6): p. S97-S100.
40. Scandroglio, P., et al., *Evaluation of cannabinoid receptor 2 and metabotropic glutamate receptor 1 functional responses using a cell impedance-based technology.* Journal of biomolecular screening, 2010. **15**(10): p. 1238-47.
41. Sitkovsky, M.V., et al., *Physiological control of immune response and inflammatory tissue damage by hypoxia-inducible factors and adenosine A2A receptors.* Annu Rev Immunol, 2004. **22**: p. 657-82.
42. Escudero, C., et al., *Impaired A2A adenosine receptor/nitric oxide/VEGF signaling pathway in fetal endothelium during late- and early-onset preeclampsia.* Purinergic Signal, 2013. **9**(2): p. 215-26.
43. Jacob, F., et al., *Purinergic signaling in inflammatory cells: P2 receptor expression, functional effects, and modulation of inflammatory responses.* Purinergic signalling, 2013. **9**(3): p. 285-306.
44. Lee, D.H., et al., *Expression of P2 receptors in human B cells and Epstein-Barr virus-transformed lymphoblastoid cell lines.* BMC immunology, 2006. **7**: p. 22-33.
45. Vincent, M., et al., *Genome-wide transcriptomic variations of human lymphoblastoid cell lines: insights from pairwise gene-expression correlations.* Pharmacogenomics, 2012. **13**(16): p. 1893-904.
46. Eglen, R. and T. Reisine, *Primary cells and stem cells in drug discovery: emerging tools for high-throughput screening.* Assay Drug Dev Technol, 2011. **9**(2): p. 108-24.
47. Franca, R., et al., *Pharmacogenetics and induction/consolidation therapy toxicities in acute lymphoblastic leukemia patients treated with AIEOP-BFM ALL 2000 protocol.* Pharmacogenomics J, 2015.

CHAPTER 5

Phenotypic screening of cannabinoid receptor 2 ligands shows different sensitivity to genotype

Julia M. Hillger

Beau le Roy

Zi Wang

Thea Mulder-Krieger

Dorret I. Boomsma

P. Eline Slagboom

Erik H. J. Danen

Adriaan P. IJzerman

Laura H. Heitman

Biochem Pharmacol, 2017. **130**: p. 60-70
DOI: https://doi.org/10.1016/j.bcp.2017.01.014

Abstract

The Cannabinoid Receptor 2 (CB_2R) is a G protein-coupled receptor (GPCR) investigated intensively as therapeutic target, however no drug has reached the market yet. We investigated personal differences in CB_2R drug responses using a label-free whole-cell assay (xCELLigence) combined with cell lines (Lymphoblastoid Cell Lines) from individuals with varying CB_2R genotypes. Responses to agonists, partial agonists and antagonists of various chemical classes were characterized. Endogenous cannabinoids such as 2-AG induced cellular effects vastly different from all synthetic cannabinoids, especially in their time-profile.

Secondly, the Q63R polymorphism affected CB_2R responses in general. Agonists and especially partial agonists showed higher efficacy in a Q63R minor homozygote versus other genotypes. Non-classical cannabinoid CP55940 showed the most pronounced personal effects with highly reduced potency and efficacy in this genotype. Contrarily, aminoalkylindole compounds showed less individual differences.

In conclusion, a label-free whole-cell assay combined with personal cell lines is a promising vehicle to investigate personal differences in drug response originating from genetic variation in GPCRs. Such phenotypic screening allows early identification of compounds prone to personal differences (‘precision medicine’) or more suited as drugs for the general population.

Introduction

The Cannabinoid Receptor 2 (CB_2R) is a class A G Protein-Coupled Receptor (GPCR) which has been investigated intensively, for instance as therapeutic target for novel immunomodulators [1]. The Cannabinoid receptor family consists of CB_1R, CB_2R and as of late, the former orphan receptors GPR55 and GPR18. Together with their endogenous ligands, they form part of the endocannabinoid system which is involved in many physiological processes. CB_2R is a (predominantly) $G\alpha_i$-coupled receptor which is expressed mainly in cells of the immune system, such as T- and B-lymphocytes, as well as the central and peripheral nervous system and the gastrointestinal tract [1-3]. As such, the CB_2R is involved in a wide range of pathological conditions ranging from atherosclerosis [4], neuropathic pain [5], neurodegenerative diseases [6], osteoporosis [7] and autoimmune diseases [8] to cancer [9-11]. Hence, the CB_2R has been in the focus of drug development efforts for over a decade. However, no selective drug targeting the CB_2R has made it to the market as of yet. There can be several reasons as to why drugs fail in clinical trials, one of which is differences in individuals' responses to the drug. In fact, even the most widely prescribed and sold drugs, the so-called big 'blockbuster' drugs, only work in 35–75% of all patients [12], as individual drug response varies due to differences in genetics, lifestyle and environment. Therefore, personalized or precision medicine aims to personalize drug prescriptions based on a patient's individual characteristics, e.g. genetic information, and thereby decreases risks of ineffective dosing or side-effects [13, 14]. An abundant source of genetic variation in humans is Single Nucleotide Polymorphism (SNP), which can lead to an alteration in the amino acid sequence of a protein [15]. Many polymorphisms have been documented in the CB_2R, including three that change the amino acid sequence and occur highly frequently in the population, namely Q63R, Q66R and H316Y [16]. Of these, both Q63R and H316Y have been linked to various pathological conditions. Q63R is special, as it can be caused by a SNP (rs2501432) as well as a dinucleotide polymorphism (rs35761398). Q63R has been shown to be involved in schizophrenia and depression [17-19], alcoholism [20], eating disorders [21], early menarche in obesity [22] and various immune system related disorders [23-25], while H316Y has been associated with lowered bone mineral density [26].

We investigated personal differences in CB_2R drug responses using a sensitive *in vitro* assay, i.e. a label-free cellular assay using the xCELLigence system, in combination with personal cell lines. With the xCELLigence, whole-cell responses are measured non-invasively allowing for the investigation of drug responses in an unbiased way, i.e. without selecting one signaling pathway or effect. The personal cell lines used in this study were

Lymphoblastoid Cell Lines (LCLs) obtained from participants of the Netherlands Twin Register (NTR), which are derived from B-lymphocytes and thus endogenously express the CB_2R [27, 28]. Using LCLs from individuals with different CB_2R genotypes, we tested a number of ligands ranging from agonists and partial agonists to antagonists (**Fig. 1**), which have potential use in different pathological indications. Firstly, endogenous cannabinoids are fatty acid derivatives such as the eicosanoids 2-AG (2-Arachidonoylglycerol), the main endogenous ligand for CB_2R, and AEA (anandamide) [29, 30]. Synthetic cannabinoids can be divided into classical and non-classical, such as JWH133 and CP55940, respectively. Another large class of synthetic cannabinoid receptor ligands are the aminoalkylindoles, of which WIN55212-2 is the most studied agonist and AM630 is one of the most utilized CB_2R antagonists [1, 31]. Several classes also contain partial agonists, such as aminoalkylindole GW405833 or BAY59-3074, which belongs to a separate chemical class.

In this study, we show that the xCELLigence in combination with these personal cell lines can be successfully applied to investigate personal differences in drug response originating from, for instance, genetic variation in GPCRs. We furthermore demonstrate that while certain classes of CB_2R ligands show individual differences, others deliver consistent effects

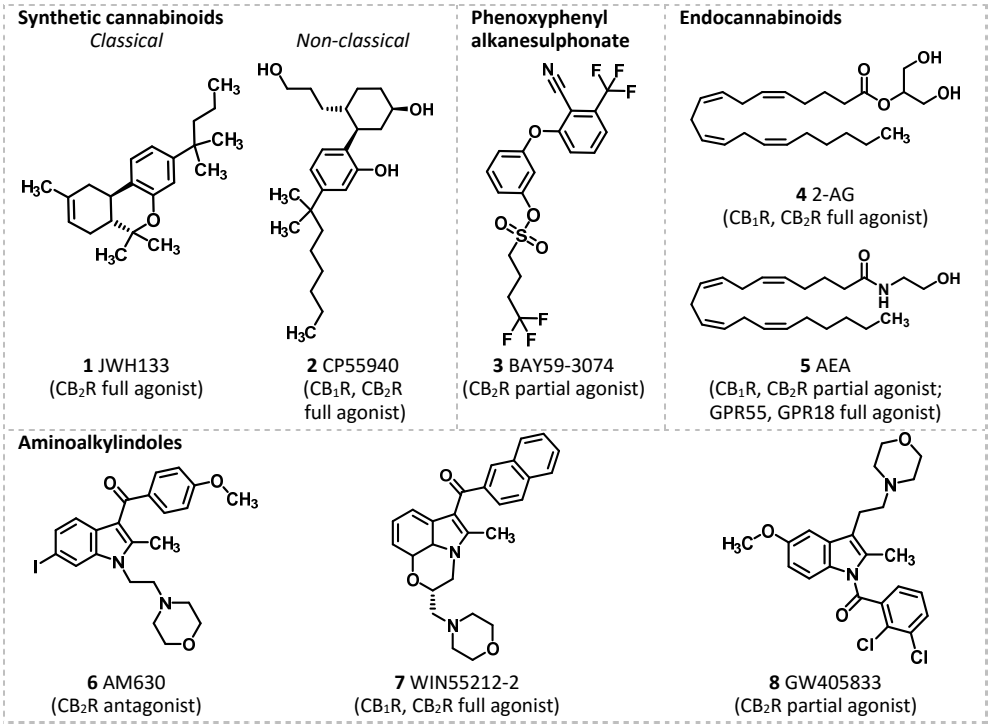

Figure 1. Chemical structures of CB_2R ligands characterized in this manuscript.

independent of genotype. Thus while taking personal medical effects into account, it is still possible to identify potential 'blockbuster' drugs by using such phenotypic screening methods with personal cell lines.

Material and methods

Chemicals and reagents

Fibronectin from bovine plasma, Roswell Park Memorial Institute (RPMI) 1640 cell culture medium (25 mM HEPES and NaHCO3) and Pertussis Toxin (PTX) were purchased from Sigma Aldrich (Zwijndrecht, NL). CB_2R ligands AM630, GW405833 and CP55940 were purchased from Sigma Aldrich, BAY59-3074, WIN55212-2 mesylate, JWH133 and AEA from Tocris Bioscience (Bristol, UK) and 2-AG from Cayman Chemicals (Ann Arbor, MI, USA). All other chemicals and reagents were of analytical grade and obtained from commercial sources, unless stated otherwise.

Lymphoblastoid cell line generation

For all participants of the Netherlands Twin Register (NTR, VU, Amsterdam, NL) [27] included in this study, lymphoblastoid cell lines (LCLs) were generated in accordance with Chapter 3 and 4 by the Rutgers University Cell and DNA Repository (Department of Genetics, Piscataway, NJ, USA). According to a standard transformation protocol [27], peripheral B-lymphocytes were transformed with Epstein-Barr Virus (EBV) by treatment with filtered medium from a Marmoset cell line in the presence of phytohemagglutinin during the first week of culture [32-34]. EBV transformed lymphocytes were expanded by culture for 8–12 weeks and subsequently cryopreserved.

Cell culture

LCLs from a family of four individuals, two parents (i.e. genetically unrelated; individual 2 and 3) and their monozygotic twin children (i.e. genetically equal; individual 4 and 5), as well as one other unrelated individual (individual 1) were used for the experiments presented in this manuscript. Individual 2 and 3 have been part of previous Chapter 3, where we investigated effects of JWH133, AM630 as well as PTX inhibition of JWH133. These data were incorporated in the current Chapter to allow direct comparison to effects of other compounds, individuals and genotypes. The LCLs were cultured as described previously (Chapter 3). In short, LCLs were cultured as suspension cells in RPMI 1640 (25 mM HEPES and NaHCO3) supplemented with 15% Fetal calf serum (FCS), 50 mg/ml streptomycin,

50 IU/ml penicillin, at 37 °C and 5% CO2. Cells were subcultured twice a week at a ratio of 1:5 on 10 cm ø plates and disposed after maximally 120 days.

qPCR

For qPCR analysis of receptor expression, RNA of three independent samples of each cell line was isolated by RNeasy Plus Mini (QIAGEN, Venlo, the Netherlands) and cDNA was randomly primed from 500 ng of total RNA using ReverstAid H Minus First Strand cDNA synthesis Kit (ThermoFisher, Breda, The Netherlands). The primer list is included in **Table 1**. Real-time qPCR was performed in triplicate for each sample using SYBR Green PCR (Applied Biosystems, part of ThermoFisher) on a 7500 Real-Time PCR System (Applied Biosystems). qPCR data were collected and analyzed using SDS2.3 software (Applied Biosystems). Household gene β-actin was used as internal control to normalize receptor expression and compare between individuals. Relative mRNA amounts after correction for β-actin control mRNA were expressed using the $2^{-\Delta\Delta Ct}$ method.

Table 1. Primers for qPCR.

Gene	Forward	Reverse
β-actin	ATTGCCGACAGGATGCAGAA	GCTGATCCACATCTGCTGGAA
CNR1	GAGAAGATGACTGCGGGAGA	GTTGTAAAATTCTGTAATGTTCACCTG
CNR2	CATGCTGTGCCTCATCAACT	GATCTCGGGGCTTCTTCTTT
GPR55	GGAAAGTGGAAAAATACATGTGC	CAGCGGGAAGAAGACCTTG
GPR18	AACGGGGGAGAACAGTTACA	AACTTTTTCTGCGCATGCTT

Label-free whole-cell analysis (xCELLigence RTCA system)

Instrumentation principle

Cellular assays using the xCELLigence RTCA system [35] were performed in accordance with previously published protocols (**Chapter 3**) and [36]. The real-time cell analyzer (RTCA) uses a detection system based on electrical impedance to measure the whole-cell responses. Cell attachment to gold electrodes embedded on the bottom of the microelectronic E-plates changes the local ionic environment at the electrode-solution interface, which generates impedance. Relative changes in impedance (Z) are recorded in real-time and summarized in the Cell Index (CI). This CI, which is a dimensionless parameter, is defined at any given time point as $(Z_i - Z_0)\ \Omega/15\ \Omega$. Z_i is the impedance at each individual time point, whereas Z_0 is defined as 0, as it represents the baseline impedance in the absence of cells measured prior to the start of the experiment. Impedance and the corresponding CI increase proportionally as cell adhere to the electrodes. The impedance profile directly reflects any changes in

degree of adhesion, cell number, viability and morphology [35, 37]. As such cellular parameters are also affected upon activation of GPCR signaling, this allows real-time monitoring of cellular signaling events [35].

General protocol

xCELLigence assays on LCLs were performed as described previously in **Chapter 3** with some minor modifications. Briefly, cells were seeded onto fibronectin-coated E-plates (10 µg/ml) at 50,000 cells/well, unless stated otherwise. Cell counts were performed with Trypan blue staining on a BioRad TC10 automated cell counter. E-plates were clicked in the xCELLigence recording station in an incubator (37 °C, 5% CO2). Impedance was measured overnight for 18 h, after which the cells were stimulated with a cannabinoid receptor agonist or vehicle control in 5 µl, unless specified otherwise. As compound solubility required addition of dimethylsulfoxide (DMSO) or acetonitrile (ACN), the final concentration upon ligand or vehicle addition was kept at 0.25% DMSO or respectively 1% ACN for all wells and assays.

For agonist screening purposes, cells were stimulated with agonist concentrations corresponding to approximately 100 × published pK_I values for hCB_2R [38, 39]. Agonist or partial agonist concentration-effect curves were generated by stimulating cells with increasing concentrations of the respective compound. For antagonist assays, cells were pre-incubated for 30 min with 5 µl of vehicle control or the respective antagonist at increasing concentrations. Subsequently, cells were challenged with a submaximal agonist concentration of reference full agonist JWH133 equal to the agonist's EC_{80} concentration (100 nM) or vehicle control. Of note, for partial agonist curves, fibronectin coating was increased (50 µg/ml) and cells were seeded at a higher density of 100,000 cells/well in order to achieve a sufficient window. To allow comparison, full agonist JWH133 was always tested alongside all partial agonists under equal conditions. For endocannabinoids, addition of the protease inhibitor phenylmethylsulfonyl fluoride (PMSF) to prevent possible degradation was tested, but as this did not change the responses or time-profile it was further omitted (*data not shown*).

For studies on $G\alpha_i$ coupling, cells were seeded in assay medium containing 100 ng/ml Pertussis Toxin (PTX) or vehicle control, and stimulated after 18 h with agonist at corresponding EC_{80} concentration or vehicle control.

Data analysis

Data were analyzed as described previously in **Chapter 3**. Experimental data were captured and processed with RTCA Software 1.2 (ACEA, San Diego, CA, USA), in which ligand responses

were normalized to the last time point prior to compound addition resulting in the Δ Cell Index (Delta Cell Index or Δ CI). Data were exported to GraphPad Prism 6.0 (GraphPad Software Inc., San Diego, CA, USA) for further analysis. Correction for any ligand-independent effects was achieved by subtracting vehicle control as baseline. Peak responses were defined as highest Δ CI (Max Δ CI) observed within 30 min after compound addition. For negative impedance responses of 2-AG, Max-Min Δ CI within 1 h was used, which is the amplitude between the highest and lowest Δ CI. Peak values and experimental Δ CI traces were used for construction of bar graphs or concentration–effect curves by nonlinear regression and calculation of IC_{50} (half maximal inhibitory concentration), EC_{50} (half maximal effective concentration) and EC_{80} (80% maximal effective concentration) values. E_{max} (maximum effect) values of compounds were derived from maximal responses within the analyzed timeframe. Agonist and partial agonist curves of all individuals as well as the derived E_{max} values were normalized to E_{max} of CB_2R-selective agonist JWH133 response on individual 1, first as this individual also showed the highest response for all agonists with the exception of CP55940, and secondly as this was also the only case of a single individual per genotype (only minor homozygote for Q63R, *Q63*).

All values obtained are means of at least three independent experiments performed in duplicate, unless stated otherwise. When comparing multiple means or multiple instances of two means, statistical significance was calculated using a two-way analysis of variance (ANOVA) with Fisher's LSD test, for example comparison of multiple EC_{50} values or antagonist inhibition of multiple compounds. Comparison of multiple means to one value was performed with a two-way ANOVA with Dunnett's post hoc test, for instance comparison of JWH133 Peak Δ CI response after pre-incubation with various antagonists.

Processing of SNPs and genetic data

As stipulated in the previous **Chapter 4**, SNP data for the NTR individuals included in this study were obtained from the Genomes of the Netherlands consortium (GoNL; *http://www.nlgenome.nl/*) of which the NTR is part of [40] and analyzed in-house using PLINK, an open-source whole genome association analysis toolset (PLINK v1.07, *http://pngu.mgh.harvard.edu.ezproxy.leidenuniv.nl:2048/purcell/plink/*) [41]. All SNPs within the boundaries of the *CNR2* gene (Ensembl gene: ENSG00000188822) as defined by human genome overview GRCh37 were analyzed further. Based on GRCh37 and dbSNP information (*http://www.ncbi.nlm.nih.gov.ezproxy.leidenuniv.nl:2048/SNP/*), SNPs were annotated according to position (e.g. coding sequence, exon) and SNP type (e.g. missense).

Data access

The LCLs used in this study were kindly provided within the framework of this collaboration [27] and are part of the Netherlands Twin Register (NTR; *http://www.tweelingenregister.org/en/*), and part of the Center for Collaborative Genomic Studies on Mental Disorders (NIMH U24 MH068457-06). Data and biomaterials (such as cell lines) are available to qualified investigators, and may be accessed by following a set of instructions stipulated on the National Institute of Mental Health (NIMH) website (*https://www.nimhgenetics.org/access_data_biomaterial.php*).

Results

LCLs predominantly express CB_2R

To confirm the suitability of LCLs for studies of CB_2R function alone, RNA expression levels of the four receptors belonging to the cannabinoid family were assessed by qPCR. These results showed that mRNA of all four cannabinoid receptors is present in LCLs to a similar degree, both compared between receptors and between individuals. There were however some differences. For instance, GPR18 was expressed higher in many individuals, though not statistically significant in all. The corresponding expression data are summarized in **Fig. 2**. We used the xCELLigence to further confirm the presence or absence of the different cannabinoid receptor subtypes, specifically CB_2R, by testing selective and non-selective cannabinoid agonists and antagonists using the LCL of one exemplary individual

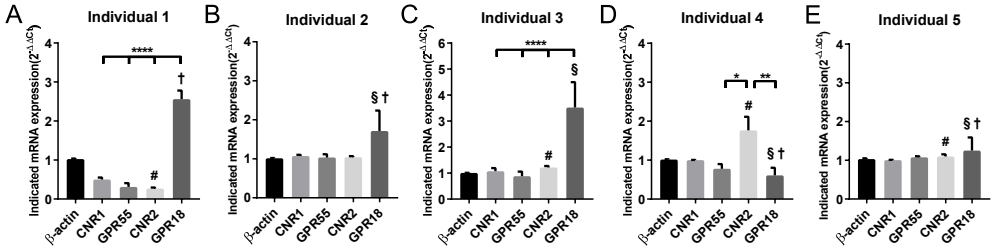

Figure 2. Cannabinoid receptor subtype mRNA expression in LCLs. Results of real-time qPCR (three independent samples measured in triplicate, mean ± SEM) show mRNA expression of four cannabinoid receptor genes per individual (**A–E** for individual 1–5, respectively). Significant differences in expression were determined with a two-way ANOVA Fisher's LSD test. * = $p < 0.05$, ** = $p < 0.01$, *** = $p < 0.001$, **** = $p < 0.0001$. Expression differences within each individual are indicated in the figure. Expression differences between individuals were for CNR2: # = individual 1 with *to 3,5 and ***to 4. For GPR18 these were: † = individual 1 with *to 2; **to 5; ****to 4 and § = individual 3 with ****to 2,4,5.

(individual 4). To ensure full receptor occupancy, we tested the compounds at concentrations corresponding to approximately 100× their K_i value at the respective receptor [38, 39]. The agonists tested included selective CB_2R agonist JWH133 as well as non-selective agonists CP55940 and WIN55212-2, which are both known to activate CB_1R as well as CB_2R. Neither of these three compounds are GPR18 agonists [42]. These agonists were also chosen as they represent three distinct chemical classes (**Fig. 1**). Ligand-induced changes in impedance were recorded in real-time, of which an example of resulting xCELLigence traces is shown in **Fig. 3**. A full real-time trace of a complete experiment is shown in **Fig. 3A**, and the corresponding vehicle-corrected compound responses are summarized in **Fig. 3B**. LCL seeding resulted in an initial quick increase in impedance related to cell adhesion, after which cells were allowed to proliferate and adjust for 18 h (**Fig. 3A**). Subsequent addition of the agonists induced an immediate increase of impedance to a peak which gradually decreased towards a plateau within 30 min (**Fig. 3B**). The responses of all three agonists were highly similar both in shape and height (**Fig. 3B, C**), indicating that the effects were mediated through the same receptor. AM251, which is known to be a GPR55 full agonist, partial GPR18 agonist and CB1R antagonist [42], gave little to no response. This indicates that the actual protein expression of these receptors is absent or too low to contribute to any of the compound responses measured here.

Furthermore, a CB_2R-selective antagonist, aminoalkylindole AM630 was tested as well to confirm that agonist responses were indeed CB_2R-mediated. While AM630 gave little to no response on its own, it was able to significantly block responses of all agonists at a concentration of 100 × K_i. The level of blockade did not differ significantly between agonists, irrespective of their receptor selectivity (**Fig. 3D**). Furthermore, comparable AM630 effects were observed on LCLs from other individuals. For instance, AM630 showed strong inhibition with a clear concentration-effect relationship that did not differ in potency between the five individuals tested and ranged from 6.76 ± 0.04 to 6.90 ± 0.05 (**Fig. 3E**).

Finally, the effect of pertussis toxin (PTX) pre-treatment was investigated to confirm downstream signaling through $G\alpha_i$. PTX caused a significant decrease in cellular responses of all three agonists for individual 4, which was to a similar degree as AM630 (**Fig. 3F**). In addition, inhibition of the agonist JWH133 by PTX was strong in all five individuals, with some differences in the level of remaining effects ranging from 7.6 ± 3.6% up to 35.5 ± 8.9% (**Fig. 3G**). Taken together, the agonist, antagonist and PTX effects confirm that CB_2R signaling can be measured sensitively and specifically in these LCLs.

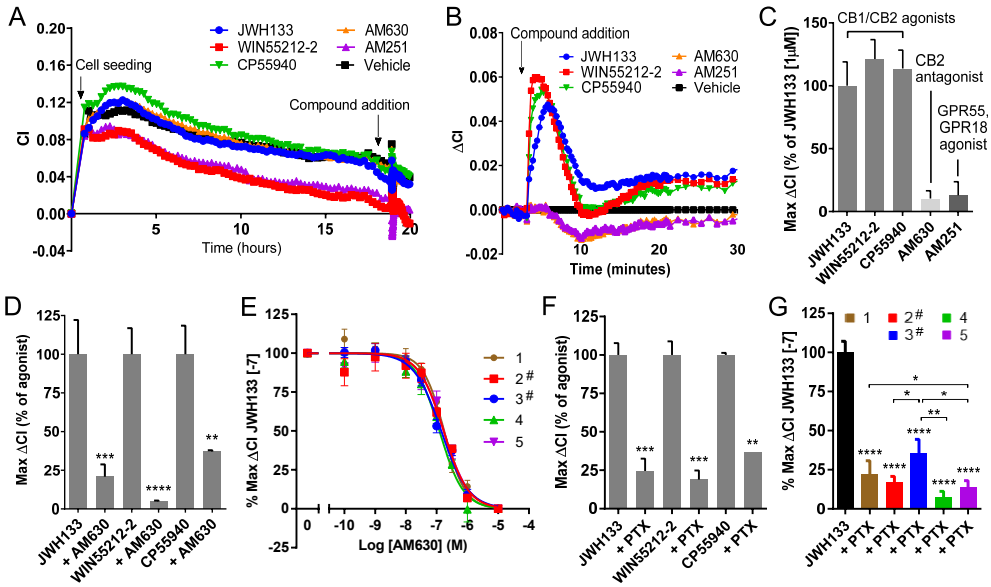

Figure 3. Cannabinoid receptor ligand screen to determine receptor subtype expression. Representative real-time traces of (**A**) a full experiment and (**B**) baseline-corrected responses in a screen of cannabinoid agonists and antagonist. (**C**) Corresponding maximal responses of the screen (Max Δ Cell Index or Max Δ CI), normalized to response to CB_2R-selective agonist JWH133. Concentrations used were JWH133 [1 μM], WIN55212-2 [10 μM], CP55940 [1 μM], AM630 [10 μM] and GPR55 agonist AM251 [10 μM]. All data shown were obtained with the LCLs of individual 4. (**D**) Inhibition of agonist effects by CB_2R specific antagonist AM630 in LCLs of individual 4, normalized to peak Δ CI of untreated agonist response. LCLs were pre-incubated with AM630 [10 μM] 30 min before stimulation with agonist at EC_{80} (JWH133 [100 nM], WIN55212-2 [10 nM], CP55940 [10 nM]). Degree of inhibition did not differ significantly between agonists, as determined by two-way ANOVA with Fisher's LSD post-hoc test. (**E**) Individual AM630 concentration-effect curve obtained from peak Δ CI of the baseline-corrected JWH133 response antagonized by increasing concentrations of AM630. Antagonist potency values were 6.76 ± 0.04, 6.77 ± 0.06, 6.85 ± 0.04, 6.90 ± 0.05 and 6.77 ± 0.04 for individuals 1–5, respectively. No statistically significant differences between individuals were observed as determined by two-way ANOVA with Fisher's LSD post-hoc test. (**F**) Inhibition of agonist-induced $G\alpha_i$ downstream signaling by pretreatment with PTX in LCLs of individual 4, normalized to peak Δ CI of untreated agonist response. LCLs were seeded in presence or absence of PTX [100 ng/ml] and treated with agonist at EC_{80} after 18 h growth. Degree of inhibition did not differ significantly between agonists, as determined by two-way ANOVA with Fisher's LSD post-hoc test. (**G**) Individual effect of $G\alpha_i$ inhibition by PTX on CB_2R response to agonist JWH133. Response in the presence of PTX versus JWH133 alone was highly significantly reduced within each individual (****). Statistical differences between individuals were determined by two-way ANOVA with Fisher's LSD post-hoc test. * = $p < 0.05$, ** = $p < 0.01$, *** = $p < 0.001$, **** = $p < 0.0001$. Data represent mean ± SEM obtained from three or four (**B, C, E, G**) independent experiments of performed in duplicate. For (**D, F**) data represent mean ± SD from two independent experiments performed in duplicate from individual 4, used as representative example here, while results on other individuals (2, 3, 5) were comparable (*data not shown*). #AM630 curves and PTX inhibition for individuals 2 and 3 had been previously established (**Chapter 3**) but were incorporated to allow direct comparison.

Individual differences in CB_2R synthetic agonist responses in LCLs

Following the confirmation that cellular effects were specifically CB_2R-related, agonist concentration-effect curves were studied on LCLs from five individuals. Individuals 2 and 3 are the parents of individuals 4 and 5, their monozygotic twin children, while individual 1 is unrelated. Examining their genotypes from DNA sequence data revealed that individual 1 is a homozygote for the minor allele (genotype *GG* thus *Q63*) for Q63R polymorphism (rs35761398), while individuals 2 and 3 are heterozygotes and individuals 4 and 5 are homozygotes for the major allele (genotype *AA* thus *Q63*) (see also **Table 2** and **Table 3**), representing the most common genotype among the human population (*http://www.ncbi.nlm.nih.gov.ezproxy.leidenuniv.nl:2048/SNP/*). First, full concentration-response curves were made for three compounds, typically referred to as full agonists, from different chemical classes, JWH133, WIN55212-2 and CP55940. Example xCELLigence traces of the JWH133 concentration-effect relationship are given in **Fig. 4A**. The resulting concentration-effect curves are summarized in **Fig. 4B–D**. Corresponding pEC_{50} values are summarized in **Table 2** while E_{max} values are given in **Table 3**.

As can be observed from the curves and pEC_{50} values (**Table 2**), potencies for the three agonists were similar for all individuals, with a notable exception for CP55940 on individual 1 (**Fig. 4D**). For this individual, who is the only minor homozygote for Q63R, CP55940 showed a significantly increased EC_{50} value of approximately 10-fold. In contrast, the efficacy of all three agonists was much more divergent on the different cell lines. Interestingly, WIN55212-2 which showed no significant differences in potency, showed a significant spread in efficacy corresponding to genotype (**Fig. 4C**, **Table 3**). WIN55212-2 had the lowest efficacy on the two heterozygous individuals 2 and 3, which in fact made it a partial agonist on these cell lines in comparison to JWH133 (**Table 3**). For the other three individuals, WIN55212-2 had a similar efficacy to JWH133, and both compounds had the highest efficacy on the LCLs of individual 1. The two synthetic cannabinoids JWH133 and CP55940 showed differences in efficacy that did not correlate with genotype. However, compared to JWH133, CP55940 had a lower efficacy in all individuals making it a partial agonist, with exception of individual 4. Even on individual 1 CP55940 was a partial agonist, where for all other tested agonists the highest efficacy was found. Taken together, CP55940 was the only synthetic agonist with clear individual differences related to genotype (i.e. a decreased potency and efficacy in presence of *Q63)*, while aminoalkylindole WIN55212-2 was the least prone to individual variation.

Endogenous agonist induces different cellular response than synthetic agonists

To test whether signaling caused by endogenous agonists also showed individual differences,

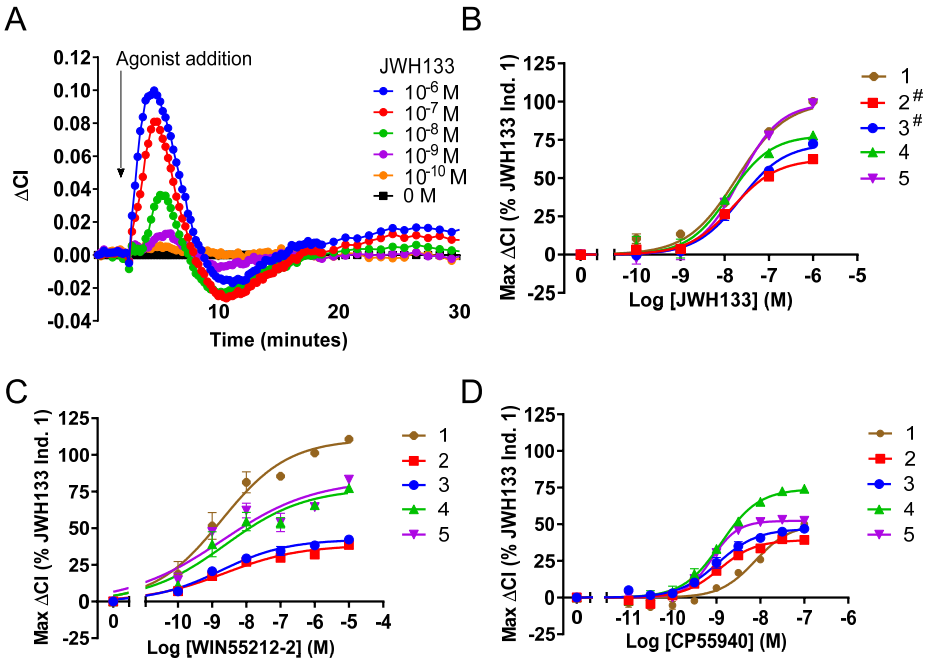

Figure 4. Individual CB_2R responses to full agonists of three distinct chemical classes. Cell lines were stimulated with different concentrations of full agonist JWH133, WIN55212-2 or CP55940 18 h after seeding (50,000 cells/well). (**A**) Representative graph of the baseline-corrected JWH133 response [1 µM – 100 pM] from individual 1. Concentration-effect curves of all individuals (1–5) of (**B**) classical cannabinoid JWH133 (**C**) aminoalkylindole WIN55212-2 and (**D**) non-classical cannabinoid CP55940 obtained from Max Δ CI, normalized to E_{max} of CB_2R-selective agonist JWH133 response on individual 1. Data represent mean ± SEM obtained from three or four independent experiments performed in duplicate. #JWH133 curves for individuals 2 and 3 have been previously established (**Chapter 3**) but were incorporated to allow direct comparison.

the response induced by the two main endogenous CB_2R ligands, eicosanoid 2-AG and AEA, known as full and partial CB_2R agonists respectively, were examined. In order to allow a sufficient response window to characterize partial agonist AEA, conditions were optimized by seeding more cells (100,000 cells/well) and coating with more fibronectin (50 µg/ml). Both full agonist JWH133 and 2-AG were also tested under these adjusted conditions, and the responses of JWH133 were used as reference compound to determine the level of partial agonism. Interestingly, the resulting real-time trace differed significantly from all synthetic agonists, as shown in **Fig. 5A, B**. While all synthetic agonists induced an immediate positive impedance change, which was characterized by a fast peak and subsequent decline to baseline in around 30 min, the endogenous 2-AG induced a negative change in impedance with a much slower onset after about 20 min, and a much more prolonged response that still

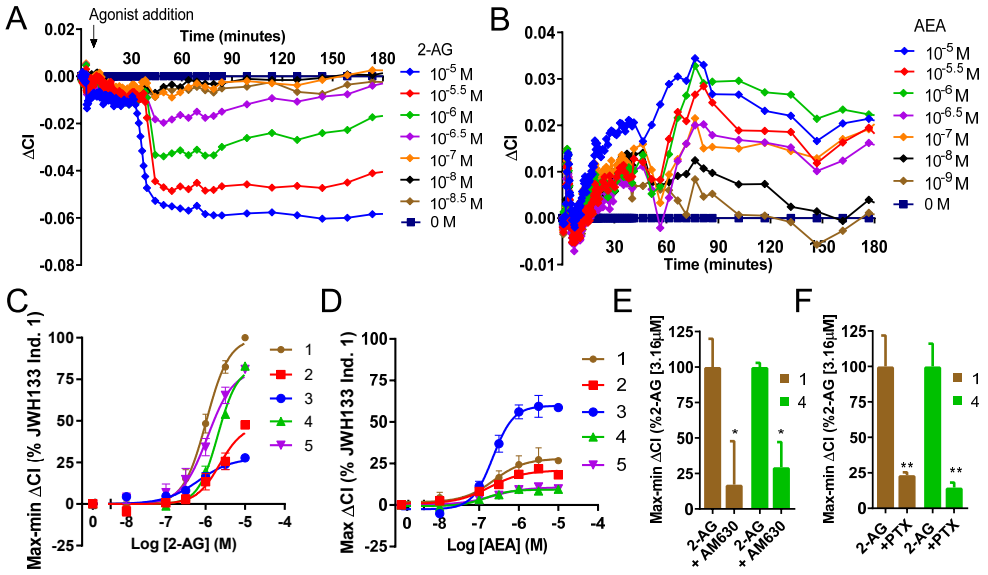

Figure 5. Individual CB_2R responses to endocannabinoids. Cell lines were stimulated with 2-AG (50,000 cells/well, fibronectin 10 µg/ml) or AEA (100,000 cells/well, fibronectin 50 µg/ml) 18 h after seeding. Representative graphs of the baseline-corrected (**A**) 2-AG [10 µM – 3.16 nM] and (**B**) AEA [10 µM – 1 nM] response from individual 1. (**C**) Concentration-effect curves of 2-AG were obtained from Max-Min Δ CI within 1 h of stimulation were normalized to E_{max} on individual 1. (**D**) Concentration-effect curves of AEA were obtained from Max Δ CI normalized to E_{max} of CB_2R-selective agonist JWH133 response on individual 1. Next, bar graphs show the inhibition of the 2-AG effect by (**E**) CB_2R-selective antagonist AM630 [10 µM] and (**F**) $G\alpha_i$-inhibitor PTX normalized to 2-AG's effect at EC_{80} (3.16 µM). Data represent the means ± SEM from three or four (**C, D**) or means ± SD of two (**E, F**) independent experiments performed in duplicate. Significance of inhibitor effect versus 2-AG response only was determined with a two-way ANOVA Fisher's LSD test * = $p < 0.05$, ** = $p < 0.01$. AM630 and PTX inhibition did not differ significantly between individuals 1 (*Q63*) and 4 (*Q63*) as determined using a two-way ANOVA with a Sidak post-hoc test.

persisted after 180 min (**Fig. 5A**). Interestingly, AEA showed a similar time-profile as 2-AG with slower onset and prolonged response, but induced a positive impedance change like the synthetic cannabinoids, albeit with a different shape (**Fig. 5B**). Thus, endogenous agonist signaling through CB_2R lead to vastly different cellular changes than any of the synthetic agonists. To confirm whether these effects were also CB_2R -mediated, we showed that the 2-AG response is blocked by CB_2R -selective antagonist AM630, similar to the synthetic agonists (**Fig. 5E**). Moreover, downstream signaling via $G\alpha_i$ was inhibited by PTX pre-treatment as well (**Fig. 5F**). Of note, AM630 blockade and PTX inhibition did not differ significantly between individuals, even with opposing Q63R genotype, as demonstrated in the LCLs of individuals 1 and 4 (**Fig. 5E, F**).

Furthermore, the concentration-effect relationship of 2-AG showed significant differences between the five individuals, which were within half a log-unit and therefore smaller than those observed for CP55940. However, these differences in potencies were not consistent with the presence of Q63R (**Fig. 5C**, **Table 2**). Interestingly, the differences in efficacy of 2-AG were consistent with genotype (**Table 3**), as the efficacy in heterozygous individuals 2 and 3 was significantly lower than for all other individuals. Any differences observed for AEA were not CB_2R genotype-related (**Fig. 5D**, **Table 2** and **Table 3**). In summary, especially signaling by the main CB_2R endogenous ligand 2-AG lead to different cellular changes as opposed to synthetic agonists, and showed a genotype effect on efficacy as it appeared to be highest in the *Q63* homozygote, but lowest in Q63R heterozygotes.

Partial agonist responses differ between individuals

Subsequently, two partial CB_2R agonists were tested on all five individuals to investigate the presence of any differences in individual effects possibly linked to the Q63R genotype. Once again, conditions were adjusted to more cells (100,000 cells/well) and fibronectin (50 µg/ml) to allow a sufficient response window for these partial agonists. JWH133 was also tested under these adjusted conditions as reference compound to determine the level of partial agonism. The two partial agonists tested were aminoalkylindole GW405833 and BAY59-3074, which belongs to a separate chemical class (**Fig. 1**). In all individuals, both agonists induced positive impedance responses like the synthetic full agonists, and demonstrated clear partial agonistic behavior in comparison to JWH133, irrespective of genotype (**Fig. 6A and B**). The concentration-effect curves are represented in **Fig. 6C and D**, while the resulting pEC_{50} and E_{max} values are summarized in **Tables 2 and 3**, respectively. GW405833 showed significant differences in potency which were within half a log-unit and were not entirely consistent with genotype. However, the individual potencies for BAY59-3074 showed a larger spread close to a full log-unit. The lowest potency was observed on individual 1, though this statistical difference was not genotype consistent. In terms of efficacy, BAY59-3074 had a higher efficacy than GW405833 for all individuals. Interestingly, the E_{max} value of GW405833 on the LCLs of individual 1 (i.e. presence of *Q63*) was significantly higher than that on all other individuals (**Table 3**), which was also observed for BAY59-3074. Taken together, the partial agonists showed personal differences in response, which (in part) appeared to be compound specific and less pronounced for the aminoalkylindole GW405833.

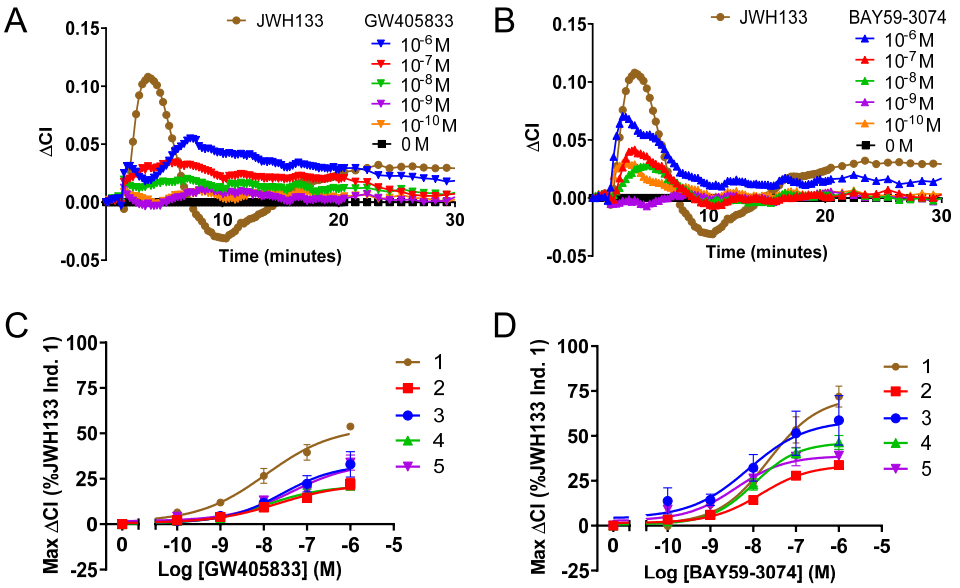

Figure 6. Individual CB_2R responses from two partial agonists. Cell lines were stimulated with agonist 18 h after seeding (100,000 cells/well, fibronectin 50 µg/ml). Representative graph of the baseline-corrected response to (**A**) GW405833 and (**B**) BAY59-3074 [1 µM – 100 pM] from individual 1. Resulting concentration-effect curves of (**C**) GW405833 and (**D**) BAY59-3074 obtained from peak Δ CI normalized to JWH133 [1 µM] effect on individual 1. Data represent mean ± SEM obtained from three independent experiments performed in duplicate.

Discussion

CB_2R is considered a potential therapeutic target for immune system related disorders such as multiple sclerosis and allergy [43], neuropathic pain [44], cancer and osteoporosis [1, 43]. As genetic differences between individuals can induce large variations in drug response, we studied such personal effects on a variety of CB_2R ligands with a panel of personal cell lines, the LCLs, from individuals with varying CB_2R genotypes. These included genetically unrelated individuals as well as monozygotic twins, who are deemed genetically identical. Hence, confirming the comparability of their responses is a standard way to control for genotype-unrelated effects [27, 45]. The individuals in this study represent all possible genotypes for the polymorphism Q63R. Even though this polymorphism is present in roughly half of the population and thus is extremely common, it has also been associated with various pathological disorders [17-19, 22-25]. This makes characterizing the impact of this polymorphism on drug responses an important issue for CB_2R drug discovery.

We characterized the genotype-effect on responses of several individuals by applying label-free cellular assay technology, namely the impedance-based xCELLigence apparatus.

Such technologies allow sensitive non-invasive assays that enable the investigation of GPCRs in endogenous cell systems, including LCLs for which we previously established an optimized protocol (**Chapter 3**). The combination of such a non-invasive assay with a personal cell line offers many advantages over traditional GPCR methodologies. In general, potencies of all CB_2R compounds tested in our research on the LCLs were within one log-unit range of previously published values (**Table 2**) [38, 39]. Notable exceptions were 2-AG and GW405833, which differed from published pEC_{50} values by up to 17-fold (pEC_{50} of 6.91 by Gonsiorek *et al*. [46]) and 43-fold (pEC_{50} of 9.19 ± 0.09 by Valenzano *et al*. [47]), respectively. This discrepancy is most likely due to differences in cell lines and assay type. Valenzano *et al.* [47] used a typical endpoint cAMP accumulation assay in combination with a CHO-K1 system overexpressing recombinant CB_2R, while LCLs represent a more physiological cell system with endogenous receptor expression. Furthermore, rather than just being a human cell line with endogenous expression, LCLs are even one step closer to the physiological situation as they are directly derived from individual persons. The use of a label-free whole-cell assay is preferable over typical endpoint assays to minimize bias [48], especially when investigating a GPCR with functional selectivity such as the CB_2R, in which multiple pathways can be activated to a different extent [49, 50].Before starting CB_2R functional investigations in LCLs, we studied expression levels and screened functional responses to confirm receptor subtype presence. All cannabinoid receptors are expressed in LCLs at mRNA level (**Fig. 2**) with some differences between individuals. However, these did not correspond to the general differences we observed in compound potency or efficacy (**Table 2** and **Table 3**). For example for CB_2R, mRNA expression differed for individual 1, especially as opposed to individual 4. However, both individuals were among the highest responders on average for CB_2R compounds (**Table 3**). Furthermore, most individuals showed high GPR18 mRNA levels, but AM251 which targets GPR18 and GPR55 but not CB_2R, showed no response (**Fig. 3**) [46]. This indicates that functional GPR18 levels were in fact not high, if at all present in these LCLs, which shows that mRNA expression levels do not necessarily correlate with functional protein expression on the cellular membrane, a feature well appreciated in literature [51, 52]. Taken together, the data shown in **Fig. 3** prove that CB_2R is in fact the major receptor responsible for compound responses, which is in accordance with previous literature that states CB_2R is the highest expressed receptor in LCLs [28]. Of note, any of the full agonists tested in this manuscript such as WIN5512-2, JWH133, CP55940 and 2-AG are not known as agonists of GPR18 [42].

After confirming that CB_2R is well expressed in LCLs and that CB_2R signaling can be measured sensitively and specifically in LCLs (**Fig. 2** and **Fig. 3**), we characterized responses

Table 2. Individual potencies of all CB_2R (partial) agonists. Statistically significant differences between individuals were determined by two-way ANOVA with Fisher's LSD post-hoc test. * = p < 0.05; ** = p < 0.01; **** = p < 0.0001.

Individual	JWH133	WIN55212-2	CP55940	2-AG	AEA	GW405833	BAY59-3074
	pEC_{50} ± SEM	*pEC_{50} ± SEM*	*pEC_{50} ± SEM*	*pEC_{50} ± SEM*	*pEC_{50} ± SEM*	*pEC_{50} ± SEM*	*pEC_{50} ± SEM*
1 *(Unrelated; R63)*	7.73 ± 0.06	8.73 ± 0.09	8.12 ± 0.06 *****to all*	5.98 ± 0.02 **to 2,4*	6.76 ± 0.08	7.99 ± 0.09 **to 2 **to 3*	7.67 ± 0.09 **to 4* *****to 2,5*
2 *(Parent 1; Q/R63)*	7.82 ± 0.07 [a]	8.65 ± 0.12	8.93 ± 0.05 *****to 1*	5.65 ± 0.06 **to 1,5* *****to 3*	6.91 ± 0.09 **to 3*	7.69 ± 0.09 **to 1,5*	8.27 ± 0.10 **to 4,5 **to 3* *****to 1*
3 *(Parent 2; Q/R63)*	7.71 ± 0.04 [a]	8.75 ± 0.11	8.97± 0.05 *****to 1*	6.19 ± 0.09 *****to 2,4*	6.64 ± 0.05 **to 2*	7.56 ± 0.15 ***to 1,5*	7.92 ± 0.08 ***to 2,* *****to 5*
4 *(Twin 1; Q63)*	7.90 ± 0.08 **to 5*	8.62 ± 0.18	8.90 ± 0.04 *****to 1*	5.69 ± 0.02 **to 1,5* *****to 3*	6.75 ± 0.07	7.76 ± 0.08	8.00 ± 0.04 **to 1,2* *****to 5*
5 *(Twin 2; Q63)*	7.67 ± 0.05 **to 4*	8.72 ± 0.23	9.11 ± 0.03 *****to 1*	5.95 ± 0.05 **to 2,4*	6.76 ± 0.16	7.95 ± 0.13 **to 2 **to 3*	8.54 ± 0.12 **to 2* ***** to 1,3,4*

[a] JWH133 curves for individuals 2 and 3 have been previously established (**Chapter 3**) and data were incorporated to allow direct comparison.

Table 3. Individual efficacies of all CB_2R (partial) agonists. All efficacies are in reference to the standard CB_2R-selective agonist JWH133 tested on the individual that was the only minor homozygote for Q63R (*Q63*), individual 1, with exception of 2-AG which was normalized to maximal 2-AG effect on individual 1 as explained in text. Statistically significant differences between individuals were determined by two-way ANOVA with Fisher's LSD post-hoc test. * = p < 0.05; ** = p < 0.01; *** = p < 0.001, **** = p < 0.0001.

Individual	JWH133	WIN55212-2	CP55940	2-AG	AEA [a]	GW405833 [a]	BAY59-3074 [a]
	Emax ± SEM	*Emax ± SEM*	*Emax ± SEM*	*Emax ± SEM*	*Emax ± SEM*	*Emax ± SEM*	*Emax ± SEM*
1 *(Unrelated; R63)*	**100 ± 4.2**	110.1 ± 5.4	50.1 ± 3.2	100 ± 13.2	26.8 ± 2.3	53.8 ± 1.5	71.9 ± 5.9
	**to 4 **to 3 ***to 2*	**to 4,5 ****to 2,3*	**to 4*	*****to 2,3*	***to 3*	**to 2,4,5 **to 3*	**to 2,4 **to 3,5*
2 *(Parent 1; Q/R63)*	62.4 ± 1.8 [b]	38.5 ± 5.3	39.3 ± 6.3	47.5 ± 7.1	18.2 ± 2.1	28.4 ± 6.0	50.5 ± 11.9
	****to 1,5*	****to 4 ****to 1,5*	****to 4*	***to 5 ***to 4 ****to 1*	****to 3*	**to 1*	**to 1*
3 *(Parent 2; Q/R63)*	72.5 ± 7.7 [b]	42.4 ± 4.3	47.0 ± 5.8	27.8 ± 3.1	58.7 ± 9.4	24.9 ± 3.1	39.2 ± 1.3
	***to 1,5*	****to 4 ****to 1,5*	***to 4*	*****to 1,4,5*	***to 1 ***to 2 ****to 4,5*	***to 1*	***to 1*
4 *(Twin 1; Q63)*	77.9 ± 4.1	77.3 ± 9.9	74.1 ± 6.8	82.9 ± 4.4	9.5 ± 2.3	27.6 ± 3.9	46.4 ± 3.8
	**to 1,5*	**to 1 ***to 2,3*	**to 1,5 **to 3 ***to 2*	****to 2 ****to 3*	*****to 3*	**to 1*	**to 1*
5 *(Twin 2; Q63)*	98.8 ± 10.9	83.2 ± 13.3	52.4 ± 10.9	81.0 ± 18.4	9.8 ± 1.7	26.9 ± 1.7	38.9 ± 3.5
	**to 4 **to 3 ***to 2*	**to 1 ****to 2,3*	**to 4*	***to 2 ****to 3*	*****to 3*	**to 1*	***to 1*

[a] As opposed to the full agonists, experiments with partial agonists AEA, GW405833 and BAY59-3074 were performed with more coating (Fibronectin 50 µg/ml) and higher cell density (100,000 cells/well) in order to obtain a sufficient window.

[b] JWH133 curves for individuals 2 and 3 have been previously established (**Chapter 3**), data were incorporated to allow direct comparison.

of five individuals to various CB_2R ligand types and classes (**Fig. 1**) which revealed that certain chemical classes of compounds were more sensitive to genotype than others (**Fig. 4, Fig. 5** and **Fig. 6**, **Table 2** and **Table 3**). All tested aminoalkylindole compounds as well as the classical cannabinoid JWH133 showed the least differences between individuals, in comparison to compounds of other chemical classes. The notion that aminoalkylindole compounds showed the least genotype-related effects was strengthened by testing three pharmacological types of ligands of this chemical class. Similar to the aminoalkylindole agonist, no individual differences were observed for the CB_2R -selective antagonist AM630 (**Fig. 3D**). Even a partial agonist of this class (GW405833) was less prone to individual differences than a partial agonist of another class. It has been suggested that partial agonists are more sensitive to system-related differences in receptor function, for instance receptor expression or downstream coupling, than full agonists or antagonists [53]. Consequently, they may be more prone to genotype-related effects. In fact, we have demonstrated in a previous Chapter that a partial agonist on the adenosine A_{2A} receptor showed a clear genotype-related difference in LCLs, while full agonists did not (**Chapter 4**). The two synthetic partial agonists for the CB_2R that we tested here exhibited similar sensitivity (**Fig. 6**, **Table 2** and **Table 3**). In efficacy, they showed the clearest genotype-related effect as it was only significantly elevated for the *Q63* individual, as opposed to the full agonists where more individuals differed.

Overall, CP55940 showed the most pronounced personal effects with highly reduced potency and efficacy in presence of *Q63*, while all other agonists and partial agonists showed the highest efficacy in presence of this genotype. Interestingly, Q63R has been reported to cause diminished WIN55212-2 efficacy in HEK293h CB_2R cells while CP55940 was not affected [54]. Our results contradict these findings, which may be due to the difference in model systems used. HEK293 cells are recombinant and receptor-overexpressing, whereas LCLs are personal cell lines with endogenous levels of receptor expression, and therefore may represent a more physiologically relevant system.

When investigating genotype effects on endogenous cannabinoid response, we noted that 2-AG showed vastly different cellular effects than any other ligand tested here, despite being clearly CB_2R -mediated (**Fig. 5**). Another endocannabinoid, AEA, showed a similarly changed time-profile as 2-AG, even though the direction of impedance change was more similar to synthetic cannabinoids. These differences in cellular effects between endogenous and synthetic cannabinoids may originate from downstream signaling differences resulting in a different cellular response as measured by xCELLigence. For instance, Shoemaker *et al.* [49] found that 2-AG was a more potent activator of MAPK whereas synthetic ligands

more potently inhibited adenylyl cyclase activity. Moreover, our experiments with 2-AG do not suggest that Q63R influences its responses, which contrasts with previous reports of Carrasquer *et al.* [54] and Ishiguro *et al.* [17], where recombinant overexpressing cell systems, HEK293 and CHO cells, were used. However, our findings are confirmed by Sipe *et al.* [8] who used a more physiological setting of T-lymphocytes, as is the case in this study. Taken all of the above together, this once more highlights the importance of using primary or derived (i.e. endogenous immortalized) cell systems that offer more physiological relevance versus recombinant systems.

There are several mechanisms by which a polymorphism may influence receptor signaling. Q63R in the CB_2R results from a dinucleotide conversion of AA to GG that exchanges a glutamine for an arginine at position 63 in the intracellular loop 1, and as such it is not in proximity of the putative CB_2R ligand binding site [54, 55]. Therefore, its position suggests that Q63R does not directly influence ligand binding. Rather, its effects on drug responses may originate from differences in downstream signaling [17, 54]. CB_2R has been shown to signal through multiple pathways such as cAMP, β-arrestin, pERK and GIRK, to which various agonists may be differently biased [30, 56, 57]. Moreover, it has been well established that agonists can activate the various G protein-dependent and –independent pathways modulated by CB_2R to a different extent [49, 50]. In our LCLs, all CB_2R agonists signaled strongly through $G\alpha_i$ coupling as was demonstrated by potent inhibition through PTX (**Fig. 3** and **Fig. 5**), which on some instances showed differences in the levels of remaining response (**Fig. 3D**). While $G\alpha_i$ signaling therefore clearly represents the predominant signaling pathway for CB_2R in all individuals, the varying remaining responses could indicate individual differences in coupling to other signaling pathways. Hence, Q63R related differences observed between CP55940 and other agonists may be related to their specific bias. Q63R could potentially affect coupling to one signaling pathway more than others, an effect which is then only noted for agonists that preferably and potently activate that pathway, in this case CP55940. Alternatively, Q63R could affect the bias of a particular ligand as CP55940 towards different signaling pathways.

Another interesting genotype-related effect was that in overall efficacy (**Table 3**), *Q63* homozygous individual 1 generally ranked highest. Q63R heterozygotes (ind. 2 and 3) appeared to have the lowest efficacy for CB_2R agonists, even compared to Q63 homozygotes (ind. 4 and 5), rather than an intermediate or mixed cellular effect. This was most pronounced for WIN55212-2 and 2-AG (**Table 3**). The effect could arise from, for instance, a difference in signaling pathway bias between the two receptor forms. In a heterozygote, where both receptor forms are present that each have different efficiencies

in pathway-coupling, the overall signaling and cellular effect may be lower as opposed to either receptor form as homozygote, that works synergistically.

In conclusion, our results demonstrate that aminoalkylindole compounds exhibited the least sensitivity to genotypes while non-classical cannabinoid CP55940 showed the most. *Q63* genotype influenced CB_2R ligand effects leading to higher efficacy of agonists and especially partial agonists, but decreased potency and efficacy of the non-classical cannabinoid CP55940, which was also the most pronounced 'personal' effect measured here. The LCLs, as personal cell lines, in combination with the sensitive label-free impedance-based technology have the potential to represent a more physiologically relevant model system to investigate individual differences in drug response. Their combination provided novel insights into the impact of CB_2R polymorphism on drug response, which demonstrates on the one hand the ability of this phenotypic screening method to identify 'blockbuster' drug candidates that are less prone to individual differences. On the other hand, this approach may advance precision medicine and stratify patient groups. Altogether, this will help in reducing attrition rates of drugs in clinical trials.

Acknowledgements

We thank Dr. A. Brooks (Department of Genetics, Rutgers University, Piscataway, NJ, USA) for preparation of the lymphoblastoid cell lines. Funding for the GoNL was provided by the Netherlands Organization for Scientific Research (184021007) to BBMRI-NL.

The research presented in this manuscript was supported by the Center for Collaborative Genomic Studies on Mental Disorders (NIMH U24 MH068457-06).

References

1. Malfitano, A.M., et al. *What we know and do not know about the cannabinoid receptor 2 (CB2)*. in *Seminars in immunology*. 2014. Elsevier.
2. Maresz, K., et al., *Direct suppression of CNS autoimmune inflammation via the cannabinoid receptor CB1 on neurons and CB2 on autoreactive T cells.* Nature medicine, 2007. **13**(4): p. 492-497.
3. Derocq, J.-M., et al., *Cannabinoids enhance human B-cell growth at low nanomolar concentrations.* FEBS letters, 1995. **369**(2): p. 177-182.
4. Rajesh, M., et al., *CB2 cannabinoid receptor agonists attenuate TNF-α-induced human vascular smooth muscle cell proliferation and migration.* British journal of pharmacology, 2008. **153**(2): p. 347-357.
5. Malan, T.P., et al., *Inhibition of pain responses by activation of CB 2 cannabinoid receptors.* Chemistry and physics of lipids, 2002. **121**(1): p. 191-200.
6. Koppel, J., et al., *CB2 receptor deficiency increases amyloid pathology and alters tau processing in a transgenic mouse model of Alzheimer's disease.* Molecular Medicine, 2013. **19**(1): p. 357.
7. Idris, A.I., et al., *Regulation of bone mass, osteoclast function, and ovariectomy-induced bone loss by the type 2 cannabinoid receptor.* Endocrinology, 2008. **149**(11): p. 5619-5626.
8. Sipe, J.C., et al., *Reduced endocannabinoid immune modulation by a common cannabinoid 2 (CB2) receptor gene polymorphism: possible risk for autoimmune disorders.* Journal of leukocyte biology, 2005. **78**(1): p. 231-238.
9. Guzman, M., *Cannabinoids: potential anticancer agents.* Nature Reviews Cancer, 2003. **3**(10): p. 745-755.
10. Sánchez, C., et al., *Inhibition of glioma growth in vivo by selective activation of the CB2 cannabinoid receptor.* Cancer Research, 2001. **61**(15): p. 5784-5789.
11. McKallip, R.J., et al., *Targeting CB2 cannabinoid receptors as a novel therapy to treat malignant lymphoblastic disease.* Blood, 2002. **100**(2): p. 627-634.
12. Carey, J. *Making personalized medicine pay*. BusinessWeek 2010 [cited 2015 24.06.2015]; Available from: *http://www.bloomberg.com/bw/magazine/content/10_05/b4165058407403.htm*.
13. Mansour, J.C. and R.E. Schwarz, *Molecular mechanisms for individualized cancer care.* J Am Coll Surg, 2008. **207**(2): p. 250-8.
14. van't Veer, L.J. and R. Bernards, *Enabling personalized cancer medicine through analysis of gene-expression patterns.* Nature, 2008. **452**(7187): p. 564-70.
15. Kruglyak, L. and D.A. Nickerson, *Variation is the spice of life.* Nature Genetics, 2001. **27**(3): p. 234-236.
16. Ishiguro, H., et al., *Cannabinoid Receptor Gene Variations in Neuropsychiatric Disorders*, in *Endocannabinoids: Molecular, Pharmacological, Behavioral and Clinical Features*, E. Murillo-Rodríguez, Editor 2013, Bentham Science Publishers. p. 3-24.
17. Ishiguro, H., et al., *Brain cannabinoid CB2 receptor in schizophrenia.* Biological psychiatry, 2010. **67**(10): p. 974-982.

18. Tong, D., et al., *Association of single-nucleotide polymorphisms in the cannabinoid receptor 2 gene with schizophrenia in the Han Chinese population.* J Mol Neurosci, 2013. **51**(2): p. 454-60.
19. Onaivi, E.S., et al., *Brain neuronal CB2 cannabinoid receptors in drug abuse and depression: from mice to human subjects.* PLoS One, 2008. **3**(2): p. e1640.
20. Ishiguro, H., et al., *Involvement of cannabinoid CB2 receptor in alcohol preference in mice and alcoholism in humans.* Pharmacogenomics J, 2007. **7**(6): p. 380-5.
21. Ishiguro, H., et al., *A nonsynonymous polymorphism in cannabinoid CB2 receptor gene is associated with eating disorders in humans and food intake is modified in mice by its ligands.* Synapse, 2010. **64**(1): p. 92-6.
22. Bellini, G., et al., *The Cannabinoid Receptor 2 Q63R Variant Modulates the Relationship between Childhood Obesity and Age at Menarche.* PLoS One, 2015. **10**(10): p. e0140142.
23. Bellini, G., et al., *Association between cannabinoid receptor type 2 Q63R variant and oligo/polyarticular juvenile idiopathic arthritis.* Scand J Rheumatol, 2015. **44**(4): p. 284-7.
24. Mahmoud Gouda, H. and N.R. Mohamed Kamel, *Cannabinoid CB2 receptor gene (CNR2) polymorphism is associated with chronic childhood immune thrombocytopenia in Egypt.* Blood Coagul Fibrinolysis, 2013. **24**(3): p. 247-51.
25. Rossi, F., et al., *The cannabinoid receptor type 2 Q63R variant increases the risk of celiac disease: implication for a novel molecular biomarker and future therapeutic intervention.* Pharmacol Res, 2012. **66**(1): p. 88-94.
26. Woo, J.H., et al., *Cannabinoid receptor gene polymorphisms and bone mineral density in Korean postmenopausal women.* Menopause, 2015. **22**(5): p. 512-519.
27. Willemsen, G., et al., *The Netherlands Twin Register biobank: a resource for genetic epidemiological studies.* Twin Res Hum Genet, 2010. **13**(3): p. 231-45.
28. Vincent, M., et al., *Genome-wide transcriptomic variations of human lymphoblastoid cell lines: insights from pairwise gene-expression correlations.* Pharmacogenomics, 2012. **13**(16): p. 1893-904.
29. Basu, S., A. Ray, and B.N. Dittel, *Cannabinoid receptor 2 is critical for the homing and retention of marginal zone B lineage cells and for efficient T-independent immune responses.* J Immunol, 2011. **187**(11): p. 5720-32.
30. Howlett, A.C., et al., *International Union of Pharmacology. XXVII. Classification of cannabinoid receptors.* Pharmacol Rev, 2002. **54**(2): p. 161-202.
31. Ross, R.A., et al., *Agonist-inverse agonist characterization at CB1 and CB2 cannabinoid receptors of L759633, L759656 and AM630.* British journal of pharmacology, 1999. **126**(3): p. 665-672.
32. Sugimoto, M., et al., *Steps involved in immortalization and tumorigenesis in human B-lymphoblastoid cell lines transformed by Epstein-Barr virus.* Cancer research, 2004. **64**(10): p. 3361-4.
33. Sie, L., S. Loong, and E.K. Tan, *Utility of lymphoblastoid cell lines.* J Neurosci Res, 2009. **87**(9): p. 1953-9.
34. Miller, G. and M. Lipman, *Release of infectious Epstein-Barr virus by transformed marmoset leukocytes.* Proceedings of the National Academy of Sciences of the United States of America, 1973. **70**(1): p. 190-4.

35. Yu, N., et al., *Real-time monitoring of morphological changes in living cells by electronic cell sensor arrays: an approach to study G protein-coupled receptors.* Anal Chem, 2006. **78**(1): p. 35-43.
36. Guo, D., et al., *Functional efficacy of adenosine A(2)A receptor agonists is positively correlated to their receptor residence time.* British journal of pharmacology, 2012. **166**(6): p. 1846-59.
37. Fang, Y., *Label-Free Receptor Assays.* Drug Discov Today Technol, 2011. **7**(1): p. e5-e11.
38. Abood M., B.F., Bonner T.I., Cabral G., Casellas P., Cravatt B.F., Devane W.A., Elphick M.R., Felder C.C., Herkenham M., Howlett A.C., Kunos G., Mackie K., Martin B.R., Mechoulam R., Pertwee R.G. *Cannabinoid receptors: CB2 receptor. Last modified on 16/03/2016. Accessed on 08/07/2016.* . 2016 Last modified on 16/03/2016; Available from: *http://www.guidetopharmacology.org/GRAC/ObjectDisplayForward?objectId=57.*
39. IUPHAR. *GPR18, GPR55 and GPR119: GPR55. Last modified on 16/03/2016. Accessed on 08/07/2016.* 2016 Last modified on 16/03/2016; Available from: *http://www.guidetopharmacology.org/GRAC/ObjectDisplayForward?objectId=109*.
40. Boomsma, D.I., et al., *The Genome of the Netherlands: design, and project goals.* Eur J Hum Genet, 2014. **22**(2): p. 221-7.
41. Purcell, S., et al., *PLINK: a tool set for whole-genome association and population-based linkage analyses.* Am J Hum Genet, 2007. **81**(3): p. 559-75.
42. McHugh, D., et al., *Delta(9) -Tetrahydrocannabinol and N-arachidonyl glycine are full agonists at GPR18 receptors and induce migration in human endometrial HEC-1B cells.* Br J Pharmacol, 2012. **165**(8): p. 2414-24.
43. Yang, P., L. Wang, and X.Q. Xie, *Latest advances in novel cannabinoid CB(2) ligands for drug abuse and their therapeutic potential.* Future Med Chem, 2012. **4**(2): p. 187-204.
44. Gilron, I. and A.H. Dickenson, *Emerging drugs for neuropathic pain.* Expert Opin Emerg Drugs, 2014. **19**(3): p. 329-41.
45. Silventoinen, K., et al., *The CODATwins Project: The Cohort Description of Collaborative Project of Development of Anthropometrical Measures in Twins to Study Macro-Environmental Variation in Genetic and Environmental Effects on Anthropometric Traits.* Twin Res Hum Genet, 2015. **18**(4): p. 348-60.
46. Gonsiorek, W., et al., *Endocannabinoid 2-arachidonyl glycerol is a full agonist through human type 2 cannabinoid receptor: antagonism by anandamide.* Mol Pharmacol, 2000. **57**(5): p. 1045-50.
47. Valenzano, K.J., et al., *Pharmacological and pharmacokinetic characterization of the cannabinoid receptor 2 agonist, GW405833, utilizing rodent models of acute and chronic pain, anxiety, ataxia and catalepsy*. Neuropharmacology, 2005. **48**(5): p. 658-72.
48. Rocheville, M., et al., *Mining the potential of label-free biosensors for seven-transmembrane receptor drug discovery.* Oligomerization and Allosteric Modulation in G-Protein Coupled Receptors, 2012. **115**: p. 123.
49. Shoemaker, J.L., et al., *Agonist-directed trafficking of response by endocannabinoids acting at CB2 receptors.* Journal of Pharmacology and Experimental Therapeutics, 2005. **315**(2): p. 828-838.

50. Atwood, B.K., et al., *Functional selectivity in CB2 cannabinoid receptor signaling and regulation: implications for the therapeutic potential of CB2 ligands.* Molecular pharmacology, 2012. **81**(2): p. 250-263.
51. Guo, Y., et al., *How is mRNA expression predictive for protein expression? A correlation study on human circulating monocytes.* Acta Biochim Biophys Sin (Shanghai), 2008. **40**(5): p. 426-36.
52. Vogel, C. and E.M. Marcotte, *Insights into the regulation of protein abundance from proteomic and transcriptomic analyses.* Nat Rev Genet, 2012. **13**(4): p. 227-32.
53. van Tilburg, E.W., et al., *2,8-Disubstituted adenosine derivatives as partial agonists for the adenosine A2A receptor.* Bioorganic & medicinal chemistry, 2003. **11**(10): p. 2183-92.
54. Carrasquer, A., et al., *Functional consequences of nonsynonymous single nucleotide polymorphisms in the CB2 cannabinoid receptor.* Pharmacogenetics and genomics, 2010. **20**(3): p. 157-166.
55. Feng, Z., et al., *Modeling, molecular dynamics simulation, and mutation validation for structure of cannabinoid receptor 2 based on known crystal structures of GPCRs.* J Chem Inf Model, 2014. **54**(9): p. 2483-99.
56. Felder, C.C., et al., *Comparison of the pharmacology and signal transduction of the human cannabinoid CB1 and CB2 receptors.* Mol Pharmacol, 1995. **48**(3): p. 443-50.
57. Dhopeshwarkar, A. and K. Mackie, *CB2 Cannabinoid Receptors as a Therapeutic Target-What Does the Future Hold?* Molecular Pharmacology, 2014. **86**(4): p. 430-437.

CHAPTER 6

Personal lymphoblastoid cell lines reveal E354Q polymorphism effects on GIP receptor signaling

Julia M. Hillger

Maartje J. Sprietsma

Jaqueline S. Gerritsen

Zi Wang

Thea Mulder-Krieger

Dorret I. Boomsma

P. Eline Slagboom

Adriaan P. IJzerman

Laura H. Heitman

Manuscript in preparation

Abstract

The glucose-dependent insulinotropic polypeptide receptor (GIPR) is a G protein-coupled receptor that plays an important role in whole-body metabolism. One missense Single Nucleotide Polymorphism (SNP) rs1800437 coding for amino acid change E354Q in the GIPR, has been associated with several diseases including diabetes and the risk of bone fractures. We investigated the functional effects of this SNP in personal cell lines from a panel of individuals with different genotypes for the polymorphism. Genotype effects were measured using a sensitive *in vitro* assay, i.e. a label-free cell morphology-based assay (xCELLigence), in combination with personal lymphoblastoid cell lines (LCLs) derived from Netherlands Twin Register participants. Responses to the endogenous agonist GIP showed enhanced potency in *Q354* homozygous individuals, while heterozygotes showed mixed effects. A mutational study of the E354 residue in recombinant HEK293 cells expressing GIPR did not show differences in potency, but revealed a reduced duration of effect for *Q354*, which was not observed in LCLs. Taken together, this study provides more insight into E354Q-related physiological changes as they occur in the human individual, and thereby contributes to precision medicine for GIPR-related pathologies.

Introduction

The glucose-dependent insulinotropic polypeptide receptor (GIPR) is a class B G protein-coupled receptor (GPCR) which is part of the glucagon receptor family [1]. It plays an important role in whole-body metabolism, such as glucose homeostasis and particularly insulin secretion, lipid uptake and bone density [2-4]. In the emerging era of precision medicine, it is becoming apparent that genetic differences between individuals can affect both drug action and susceptibility to disease. Several of such examples for GPCR polymorphisms already exist [5-8]. For the GIPR, previous research has linked Single Nucleotide Polymorphisms (SNPs) to various pathological conditions including obesity and diabetes [9-12]. One SNP of particular interest is rs1800437, which is a missense SNP that changes a glutamic acid to a glutamine at amino acid 354 of the receptor (E354Q). This E354Q is the only frequent one of 227 known GIPR missense variants that occurs in more than 1% of the population, namely with a Minor Allele Frequency (MAF) of 16% [13, 14]. Interestingly, several studies have associated this SNP with insulin resistance, type II diabetes, cardiovascular disease and the risk of bone fractures [3, 12, 15, 16]. Furthermore, a number of functional studies have indicated roles for this polymorphism in for instance receptor (in)activation [17] and desensitization [3].

This polymorphism could therefore play an important role in disease susceptibility of, as well as influence drug treatment. Mapping and understanding the effects of this polymorphism not only in the overall population, but in the individual patient is therefore paramount [18]. However, the E354Q polymorphism has so far been the subject of either cohort or candidate gene studies, or of functional studies in which its effect was analyzed in mouse cell lines or recombinant cell systems with artificially introduced mutations [3, 12, 15, 16, 19]. Despite their merits such cellular systems are further away from the physiological condition in humans. To better understand the influence of polymorphisms on receptor response in an individual, an ideal set-up would therefore be to use patient-derived material as a model system.

One example of such are lymphoblastoid cell lines (LCLs), which are commonly used to store a person's genetic material, as is done by many large scale genetic consortia such as the International HapMap and 1000 genomes projects [20-24]. We recently published a methodology that allows measurement of GPCR function in such LCLs, with which we were able to detect the effect of polymorphisms in two other GPCRs, the adenosine A_{2A} receptor and cannabinoid receptor 2 (**Chapter 4, 5**). Responses were measured using the xCELLigence,

a newly developed, highly sensitive label-free cellular assay technology. This assay measures changes in cell morphology in real-time as opposed to techniques traditionally employed in GPCR research such as ligand binding or second messenger accumulation assays, which use static, one-molecule-detection [25-28].

In the current study we have applied this real-time morphological assay to assess effects of the GIPR polymorphism E354Q in LCLs. We characterized GIPR responses in a selection of individuals from the Netherlands Twin Register (NTR) [29]. Subsequently, we performed an E354 mutational study in HEK293 cells using the same cellular assay technology as a functional read-out to provide a direct comparison to the effects observed in the LCLs.

Material and methods

Chemicals and reagents

Fibronectin from bovine plasma, ATP, unsupplemented Roswell Park Memorial Institute (RPMI) 1640 cell culture medium (25 mM HEPES and $NaHCO_3$) and Dulbecco's Modified Eagles Medium – high glucose (DMEM) were purchased from Sigma Aldrich (Zwijndrecht, The Netherlands). Fetal calf serum (FCS) was obtained from Thermo Fisher Scientific (Breda, The Netherlands). GIP was purchased from Tebu-Bio (Heerhugowaard, The Netherlands), while (Pro^3)GIP was obtained from American Peptide Company Inc (Sunnyvale, CA, USA). All other chemicals and reagents were of analytical grade and obtained from commercial sources, unless stated otherwise.

Lymphoblastoid cell line generation

For all 78 individuals of the Netherlands Twin Register (NTR, VU, Amsterdam, NL) [29] included in this study, lymphoblastoid cell lines (LCLs) were generated in accordance with previous Chapters (eg. **Chapter 3**) by the Rutgers Institute (Department of Genetics, Piscataway, NJ, USA). Briefly, peripheral B-lymphocytes were transformed with Epstein-Barr Virus (EBV) using a standard transformation protocol [29] and subsequently cryopreserved.

Cell culture

LCLs were cultured as suspension cells in RPMI 1640 (25 mM HEPES and $NaHCO_3$) supplemented with 15% FCS, 50 mg/mL streptomycin, 50 IU/mL penicillin, at 37°C in a humidified 5% CO_2 incubator, as described previously (**Chapter 3**). Cells were subcultured twice a week at a ratio of 1:5 on 10 cm ø plates and disposed after maximally 120 days.

HEK293 cells were grown in culture medium consisting of DMEM supplemented with

10% FCS, 50 mg/mL streptomycin and 50 IU/mL penicillin at 37°C in a humidified 7% CO_2 incubator. Cells were subcultured twice a week at a ratio of 1:10 to 1:30 on 10 cm ø plates.

DNA constructs and mutant generation

cDNA encoding the human GIPR (ORF: NM_000164) with an N-terminal FLAG-tag cloned into the pcDNA3.1(+) vector was purchased from GenScript (Hong Kong, China). Primers to generate the E354Q mutant were designed using the online QuickChange Primer Design tool [30] and produced by Eurogentec (Maastricht, The Netherlands). Primer sequences were forward: GCTGGGTGTCCACCAGGTGGTGTTTGC, and reverse: GCAAACACCACCTGGTGGACACCCAGC (5'–3'). The GIPR mutant was generated based on the QuikChange site-directed mutagenesis method (Agilent Technologies, La Jolla, CA, USA) [31] using pfu polymerase (Promega, Madison, WI, USA) in an 18-cycle mutagenic PCR. Subsequently, template DNA was digested by *DpnI* (New England Biolabs, Ipswich, MA, USA) treatment. PCR products were transformed into chemically competent DH5α cells (Life Technologies, Carlsbad, CA, USA) and purified using a standard Qiagen Miniprep kit (QIAGEN Benelux B.V., Venlo, The Netherlands). DNA concentration and purity were determined by NanoDrop 2000 (Thermo Fisher Scientific) and mutations were confirmed through double stranded DNA sequencing by the Leiden Genome Technology Center (LUMC, Leiden, The Netherlands).

HEK293 transfection

hGIPR constructs were transiently transfected into HEK293 cells. HEK293 cells were cultured in supplemented DMEM as stipulated above as a monolayer on 10-cm ø culture plates to 80–90% confluency. Transfections were performed using Lipofectamine 2000 (Thermo Fisher Scientific) and 8 µg of plasmid per 10-cm ø culture plate, in accordance with the manufacturer's instructions. As per these instructions, both plasmid and lipofectamine were diluted in unsupplemented OptiMEM (Thermo Fisher Scientific), subsequently mixed and incubated for 20 min at room temperature. Medium of HEK293 cells was exchanged to unsupplemented OptiMEM, after which the plasmid-lipofectamine mixture was deposited on the cells. After 6 hours of incubation with this mixture, cells were used for experiments.

Label-free whole-cell analysis (xCELLigence RTCA system)

Instrumentation principle

Cellular assays using the xCELLigence RTCA system [25] were performed in accordance with

previously published protocols (**Chapter 3, 4**) [32]. The detection principle of this real-time cell analyzer (RTCA) is based on electrical impedance. Gold electrodes are embedded on the bottom of the microelectronic E-plates. When cells attach to these, they alter the local ionic environment at the electrode-solution interface, thereby generating impedance. Relative changes in impedance (Z) are recorded in real-time and summarized in the dimensionless parameter Cell Index (CI). The CI at any given time point is defined as $(Z_i\text{-}Z_0)$ Ω /15 Ω, where Z_i is the impedance at each individual time point. Z_0 is defined as 0, as it represents the baseline impedance in the absence of cells. The resulting time-resolved impedance profile directly reflects any changes in degree of adhesion, cell number, viability and morphology, which are also the typical cellular parameters that are affected by GPCR signaling [25, 26].

General protocol

Prior to any experiment, background impedance (Z_0) was measured after adding 45 µL, or in case of antagonist experiments 40 µL, of the respective culture media to the E-plate wells. Subsequently, cells were harvested, centrifuged at 200g for 5min and resuspended in their corresponding fresh medium. xCELLigence assays on LCLs were performed as described previously (**Chapter 3**) with some minor modifications. Briefly, LCLs were harvested and seeded onto fibronectin-coated glass-bottom E-plates (50 µg/ml) at 100,000 cells/well. Transiently transfected HEK293 cells were harvested 4-6 hours following transfection by trypsinization, spun down once and seeded onto uncoated PET E-plates at 80,000 cells/well. Cell counts were performed with Trypan blue staining on a BioRad TC10 automated cell counter. After cell seeding, E-plates were clicked in the xCELLigence recording station in an incubator (37°C, 5% CO_2). Impedance was measured overnight for 18 hours, after which the cells were stimulated with a GPCR agonist or vehicle control in (5 µl), unless specified otherwise. For GIP concentration-response curves in LCLs, ATP [100 µM] was taken along to provide a receptor-independent reference of response height. As GIP and (Pro^3)GIP were stored as aliquots in Phosphate Buffered Saline (PBS), as per vendor instructions, PBS was used as vehicle control. The final PBS concentration upon ligand or vehicle addition was kept constant at 0.5 % PBS for all wells and assays. Agonist concentration-response curves were generated by stimulating cells with increasing concentrations of GIP. For the (Pro^3)GIP assay, cells were pre-incubated for 30 minutes with 5 µl of vehicle control or a high concentration of (Pro^3)GIP [1 µM]. Subsequently, cells were challenged with vehicle control or a submaximal agonist concentration of GIP corresponding to its EC_{80} value (concentration causing 80% of maximal effect) of *E354* and *Q354*, respectively (31.6 nM and 3.16 nM). All compound responses were recorded for at least 3 hours following agonist or vehicle addition.

ELISA

HEK293 cells were transiently transfected with the hGIPR E354, Q354 variant or mock as described above. Flat-bottom sterile 96 wells plates were coated with 50 µl poly-D-lysine (20 mg/L) (Sigma Aldrich) for 10 minutes. Cells were harvested, counted and seeded at 80,000 cells/well as described under the xCELLigence protocol, and medium was exchanged to normal culture medium. Cells were grown overnight at 37°C and 7% CO_2. Twenty-four hours post transfection, cells were washed once with PBS, fixed with 3,7% formaldehyde for 10 minutes and incubated in Tris-buffered saline (TBS) with 2% bovine serum albumin (BSA) for 30 minutes at room temperature. Cells were then incubated with 1:1000 anti-Q1-FLAG monoclonal antibody (Sigma Aldrich) and 1:1250 goat-anti-mouse HRP conjugated IgG antibody (Thermo Fisher Scientific) subsequently. Immunoreactivity was visualized by addition of 3,3',5,5'-tetramethylbenzidine (Sigma Aldrich). After 5 minutes the reaction was stopped by addition of 0.2M H_2SO_4. Absorbance was measured at 450 nm using a Victor plate reader (Perkin Elmer, Groningen, The Netherlands).

qPCR

qPCR on LCLs was performed as described previously (**Chapter 5**). Briefly, for each cell line RNA of three independent samples was isolated with RNeasy Plus Mini (QIAGEN, Venlo, the Netherlands). cDNA was randomly primed from 500 ng of total RNA using ReverstAid H Minus First Strand cDNA synthesis Kit (ThermoFisher, Breda, The Netherlands). The primers for GIPR were CGTCTGCTGGGACTATGCTG forward and TCTCCAAAGTCCCCATTGGC reverse. Household gene β-actin was used as internal control to enable comparison between individuals, and the primers for this were ATTGCCGACAGGATGCAGAA forward and GCTGATCCACATCTGCTGGAA reverse. Real-time qPCR was performed in triplicate for each sample using SYBR Green PCR (Applied Biosystems, part of ThermoFisher) on a 7500 Real-Time PCR System (Applied Biosystems). qPCR data were collected and analyzed using SDS2.3 software (Applied Biosystems). The $2^{-\Delta\Delta Ct}$ method was used to express relative mRNA amounts after correction for β-actin control mRNA.

Data analysis

xCELLigence

xCELLigence data were analyzed as described previously (**Chapter 3**). Experimental data were captured with RTCA Software 1.2 (ACEA, San Diego, CA, USA). Ligand responses were normalized to the last time point prior to compound addition resulting in a Normalized Cell Index (NCI). For HEK293, this was done directly in the RTCA program, while for the LCLs the

NCI was calculated in GraphPad Prism as the small (and sometimes negative) growth curves of LCLs hindered this calculation in the RTCA program. The NCI corrects for non-receptor-related variations that could for instance arise from a slight difference in seeding density, individual differences in proliferation rate and well-plate 'edge effects'. Data were exported to GraphPad Prism 6.0 (GraphPad Software Inc., San Diego, CA, USA) for further analysis. The lowest concentration of GIP was subtracted as baseline to correct for ligand-independent effects. Responses after compound addition were analyzed using AUC within 30 minutes for GIP and 60 minutes for ATP in LCLs, and 4 hours for GIP in HEK293hGIPR, due to the differences in duration of response. For analysis of the duration of response in HEK293hGIPR, responses were defined as highest NCI (Max NCI) observed at specific time points after compound addition. Peak values, AUC and experimental ΔCI or NCI traces were used for construction of bar graphs or concentration–effect curves by nonlinear regression and calculation of EC_{50} (concentration causing half maximal effect) and EC_{80} (concentration causing 80% of maximal effect) values. E_{max} (maximum effect) values of compounds were derived from maximal responses within the analyzed timeframe. All E_{max} values were normalized to the *E354* variant (individual E4 for LCLs).

Statistics

All values obtained are means of at least three independent experiments performed in duplicate on the same cell line, unless stated otherwise. When comparing multiple means or multiple instances of two means, statistical significance was calculated using a one-way analysis of variance (ANOVA) with Fisher's least significant difference (LSD) test, for example comparison of multiple pEC_{50} values for LCLs or percentage of response at certain time points for HEK293 cells. Comparison of two values was done with Student's t-test, for instance pEC_{50} values of HEK293 cells.

Processing of SNPs and genetic data

As described in previous Chapter 4, the SNP data of the individuals included in the current study were obtained from the Genomes of the Netherlands consortium (GoNL, *http://www.nlgenome.nl/*) [33], in which the NTR takes part. The SNP data were analyzed in-house using PLINK, an open-source whole genome association analysis toolset [34, 35]. For the current study, SNPs within the boundaries of the *GIPR* gene (Ensembl gene: ENSG00000010310) as defined by the human genome overview GRCh37 (*http://grch37.ensembl.org/index.html*) were extracted. Subsequently, SNPs were annotated

according to position (e.g. coding sequence, exon) and SNP type (e.g. missense) based on GRCh37 and dbSNP (*http://www.ncbi.nlm.nih.gov/SNP/*).

Results

Genotypes and NTR study

To study the effect of GIPR polymorphisms using LCLs of the NTR, we first determined the GIPR genotypes in the NTR population. This constituted a selection of in total related and unrelated 78 individuals of the NTR for whom both genetic information and corresponding LCLs were available. **Table 1** provides an overview of the SNPs present in the GIPR gene of this NTR population. We found a total of 23 SNPs with varying location, type and frequency. None were rare as all occurred in more than 10% of this NTR population, but two SNPs were extremely frequent as they were found in more than 40% of the NTR individuals (i.e. SNPs no. 22 and 23, rs9749225 and rs2238689, respectively). Of note, frequencies of most SNPs within this population were similar to the global MAF, with some exceptions that were found more frequently (e.g. SNP 22, rs9749225) or less frequently (e.g. SNP no. 14, rs35568293). Most commonly, SNPs were located within introns, with the exception of three. Two of those were located in other non-coding regions, namely the 3'-UTR. Finally, there was only one missense variant, rs1800437, which is in fact the polymorphism causing E354Q by changing a codon from GAG to CAG. Approximately 21% of the NTR individuals carried the minor allele of this SNP (i.e. CAG), which therefore provided sufficient individuals to perform a study on the effect of this polymorphism.

The preference for any genetic study is to include multiple unrelated individuals of each genotype, and if possible of both genders. Here, we also used the unique family set-up of the NTR for selecting individuals for inclusion into our study. The individuals from NTR included in GoNL comprised of trio's, with two genetically unrelated individuals, the parents, and an offspring. In a small number of families, two children, which were monozygotic or dizygotic twins, were included. As summarized in **Table 2**, we selected individuals to include: 1) one family with two monozygotic twins (family 1), whose comparability of response is a basic requirement to allow any conclusions from the experiments presented here in association with genotype; 2) one family in which the parents were opposing homozygotes and their offspring thus a heterozygote (family 2), where this special genetic relationship allowed further conclusions on genotype-related effects, and 3) three additional individuals to be able to study several unrelated individuals of each genotype. Of note, the maximum number

Table 1. SNPs found in GIPR gene in NTR individuals. Publicly annotated SNPs according to the dbSNP (*http://www.ncbi.nlm.nih.gov/SNP/)* within the *GIPR* gene in the selected NTR population, ordered based on increasing frequency in the NTR. Locations and gene boundaries were as defined by human genome overview GRCh37 (gene boundaries 19: 46171502 – 19:46186982). Type and global MAF are from the respective dbSNP pages (*http://www.ncbi.nlm.nih.gov/SNP/*).

Nr	SNP	Location	Minor Allele	Major Allele	Minor Allele count (NTR)	Type (dbSNP)	Global MAF (dbSNP)
1	rs11671664	19:46172278	A	G	0.114	Intron variant	A=0.1552
2	rs34089191	19:46176723	C	G	0.114	Intron variant, upstream variant 2KB	C=0.2171
3	rs55669001	19:46177235	C	T	0.114	Intron variant, upstream variant 2KB	C=0.1528
4	rs58304657	19:46176405	C	G	0.114	Intron variant, upstream variant 2KB	C=0.2192
5	rs9749185	19:46175416	A	G	0.114	Intron variant	A=0.1534
6	rs61373376	19:46183586	T	C	0.1579	Intron variant	T=0.0887
7	rs10423928	19:46182304	A	T	0.2105	Intron variant	A=0.1719
8	rs11672660	19:46180184	T	C	0.2105	Intron variant, upstream variant 2KB	T=0.1595
9	rs1800437	19:46181392	C	G	0.2105	Downstream variant 500B, missense, nc transcript variant	C=0.1611
10	rs2238690	19:46178886	A	G	0.2105	Intron variant, upstream variant 2KB	A=0.2512
11	rs2238691	19:46179043	A	G	0.2105	Intron variant, upstream variant 2KB	A=0.1603
12	rs2302382	19:46172569	A	C	0.2105	Intron variant	A=0.1627
13	rs34783010	19:46180414	T	G	0.2105	Intron variant	T=0.1595
14	rs35568293	19:46179110	C	T	0.2105	Intron variant, upstream variant 2KB	C=0.3155
15	rs7250736	19:46184012	G	C	0.2105	Intron variant	G=0.2514
16	rs7250754	19:46184061	A	C	0.2105	Intron variant	A=0.2514
17	rs2334255	19:46186150	T	G	0.2193	Downstream variant 500B, utr variant 3 prime	T=0.2606
18	rs12709891	19:46185217	A	C	0.2281	Nc transcript variant, utr variant 3 prime	A=0.2602
19	rs10404234	19:46183476	G	C	0.2368	Intron variant	G=0.2103
20	rs4803846	19:46180150	A	G	0.2368	Intron variant, upstream variant 2KB	A=0.2119
21	rs2878163	19:46183954	G	T	0.2456	Intron variant	G=0.2103
22	rs9749225	19:46175445	A	T	0.4035	Intron variant	T=0.2145
23	rs2238689	19:46178661	C	T	0.4211	Intron variant, downstream variant 500B, upstream variant 2KB	C=0.4880

Nc = non-coding; utr = untranslated region

Table 2. Selected set of NTR individuals studied for the E354Q GIPR polymorphism.

Identity				E354Q	
Group	Individual	Gender	Code	Genotype	Amino acid
Family 1	Father 1	Male	E1	GG	E
	Mother 1	Female	E2	GG	E
	Twin 1A	Female	E3	GG	E
	Twin 1B	Female	E4	GG	E
Family 2	Father 2	Male	E5	GG	E
	Mother 2	Female	Q1	CC	Q
	Twin 2A	Male	EQ1	CG	E/Q
Additional	Additional 1	Female	EQ2	CG	E/Q
	Additional 2	Female	EQ3	CG	E/Q
	Additional 3	Male	Q2	CC	Q

of *Q354* individuals was investigated, as only two of such were available in the NTR population. Moreover, both genders were represented in each group. Thus in total, we studied responses of LCLs of 10 individuals (**Table 2**).

GIPR signaling can be measured sensitively in LCLs using xCELLigence

To confirm the suitability of LCLs for studying GIPR effects, we first performed an initial qPCR as well as a response screen on the xCELLigence. The qPCR on a set of *E354* and *Q354* homozygous individuals revealed that mRNA of the GIPR was present in all individuals (**Fig. 1F**). mRNA levels were not consequently linked to genotype as significant differences were observed between individuals both with the same or different genotypes, and even between monozygotic twins E3 and E4.

Subsequently, we assessed GIPR responses on the xCELLigence in comparison with responses to ATP. The latter was used as a reference ligand as it is known to target GPCRs that are highly expressed and activation of these leads to cellular responses in LCLs (**Chapter 3**) [36, 37]. In **Fig. 1A** an exemplary experiment on the LCLs is presented, where cellular growth and responses were recorded in real-time. LCL seeding resulted in an initial increase in impedance related to cell adhesion, growth and division. Subsequent addition of a GPCR agonist such as ATP or GIP induced an immediate increase of impedance to a peak level of similar height, which gradually decreased towards a plateau. However, the duration

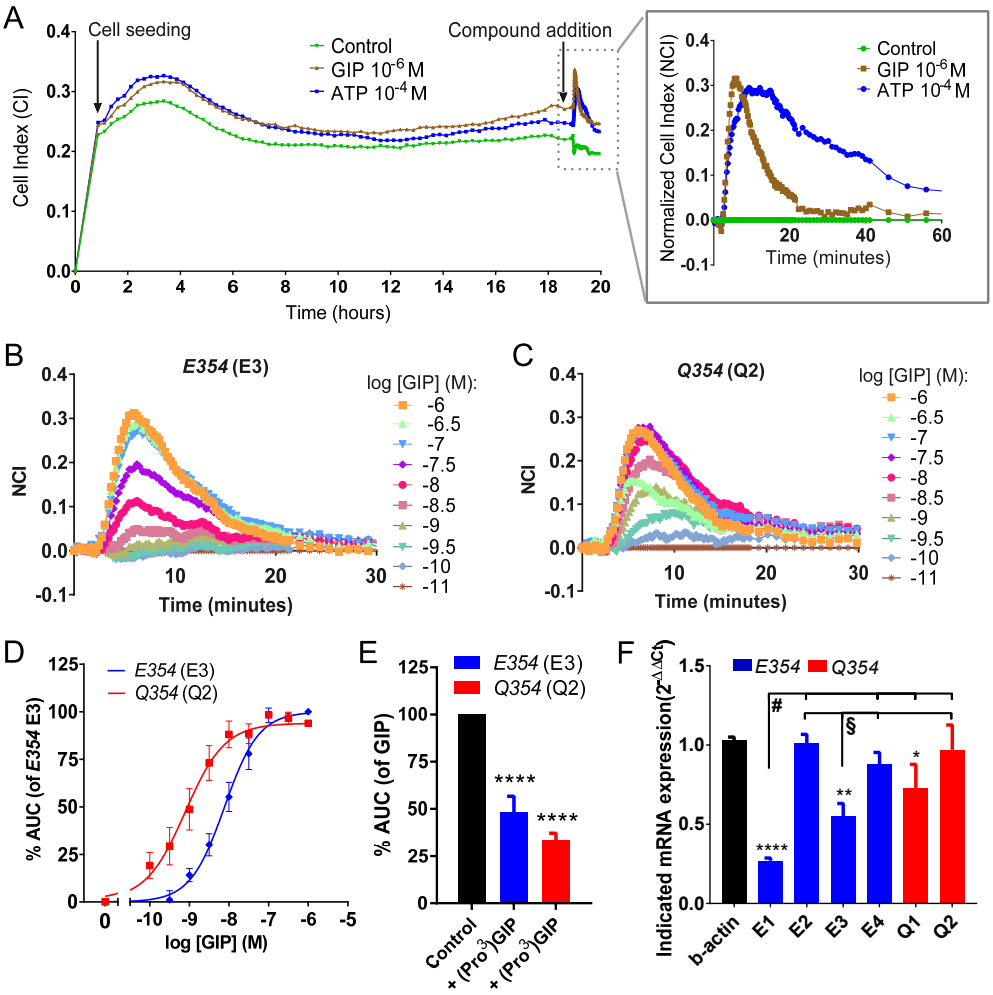

Figure 1. Characterization of GIPR response in LCLs with varying E354Q genotypes. (**A**) Representative example of a full real-time impedance plot and baseline-corrected responses of LCLs from one individual (E3) to GIP [1 µM] and ATP [100 µM]. Representative examples of baseline-corrected real-time impedance plot for one *E354* (E3, **B**) and one *Q354* (Q2, **C**) homozygous individual as a function of different concentrations of the endogenous agonist GIP ranging from 1 µM to 10 pM. (**D**) GIP concentration-response curves derived from AUC of NCI within 30 minutes after agonist addition, normalized to *E354* (E3). pEC_{50} and E_{max} values are summarized in *Table 3*. (**E**) Inhibitory effect of (Pro^3)GIP [1 µM] on response to a submaximal dose of GIP ([3.16 nM] for *Q354* and [31.6 nM] for *E354*). (**F**) Results of real-time qPCR show mRNA expression of GIPR in 6 selected individuals with *E354* or *Q354* genotype. Statistic differences were determined by one-way ANOVA with Fisher's LSD test. *p≤0.05, **p≤0.01, ***p≤0.001, ****p≤0.0001. For **F**, differences to β-actin are indicated with asterisk. Expression differences between individuals were # = E1 **** to E2, *** to E4 and Q2, ** to Q1. § = E3 ** to E2 and Q2, * to E4. In figures **A**, **B** and **C**, representative traces are shown. In figures **D**, **E** and **F** means ± SEM of three or more separate experiments performed in duplicate (**D** and **E**) or triplicate (**F**) are shown.

of response caused by ATP or GIP differed. For GIP, the response returned to baseline levels within a period of 30 minutes, where ATP induced cellular changes lasting over 60 minutes. This showed that LCL responses to GPCR agonists are receptor specific with regard to shape and duration as measured using the xCELLigence technology.

Finally, we tested inhibition of GIP signaling effects in LCLs using the only commercially available GIPR selective antagonist, (Pro^3)GIP, which did not elicit a response on its own upon addition to the LCLs (**Supplemental Fig. S1**). As shown in **Fig. 1E**, (Pro^3)GIP was able to (partly) diminish GIP responses.

Together, these results show that GIPR signaling in LCLs can be measured sensitively and specifically using the xCELLigence methodology.

E534Q alters endogenous agonist potency of GIPR in personal cell lines

Subsequently, LCL responses of the selection of E354Q individuals by the endogenous agonist GIP were determined. The resulting concentration-effect curves are summarized in **Fig. 1B-D**. GIP efficacy and potency values for the entire set of 10 individuals are summarized in **Table 3**. Responses between the monozygotic twins E3 and E4 were highly comparable, confirming that the LCLs are a suitable model system to study genetic effects on the GIPR.

Shown in **Fig. 1B and 1C** are representative examples of the real-time baseline-corrected responses of two unrelated individuals representing the two possible E354Q homozygous genotypes, i.e. one *E354* and one *Q354* homozygous individual, respectively. Irrespective of genotype, these LCLs showed similar responses to GIP which did not differ significantly in overall shape or duration. However, differences in GIP effects were observed, especially in potency as can be seen in **Fig. 1D** where the concentration-response curves of these two individuals are given. Furthermore, both *E354* and *Q354* homozygous individuals showed highly similar effects in potency within their respective group of individuals with the same genotype, but these groups differed significantly from each other. Specifically, pEC_{50} values of GIP on *E354* individuals ranged from 7.90 ± 0.07 (E4) to 8.34 ± 0.08 (E2), while the same values on LCLs of *Q354* individuals were 8.96 ± 0.25 (Q1) and 9.12 ± 0.08 (Q2). Therefore, GIP potency was significantly higher (i.e. 4-17-fold) in LCLs from *Q354* homozygous individuals (Q1 and Q2), as opposed to the *E354* homozygotes. Interestingly, the LCLs of heterozygotes showed mixed effects, as their potency values showed a large spread with a range of 7.91 ± 0.11 (EQ2) to 9.32 ± 0.14 (EQ1). Heterozygotes thus also differed significantly from each other by 4- to 26-fold, which was similar to the difference between *Q354* and *E354* homozygous individuals. In general, heterozygotes were closer in potency to *Q354*

Table 3. Endogenous agonist GIP potency and efficacy per individual's LCL.. Data represent means ± SEM for three or more different experiments performed in duplicate. E_{max} was corrected for growth curve height by NCI and normalized to the individual with the highest response. Statistically significant differences between individuals were determined by one-way ANOVA with Fisher's LSD post-hoc test. Significant differences are highlighted by blue = to *E354* individuals, red = to *Q354* individuals and green = to E354Q heterozygotes. Individual p-values are given in *Supplemental table S1*.

Group	Individual	pEC_{50} ± SEM	pEC_{50} Significantly different	E_{max} ± SEM	E_{max} Significantly different
Family 1	E1	8.14 ± 0.07	to all Q; to all E/Q except EQ2	87.3 ± 25.6	to all Q; to EQ2, E2, E3
	E2	8.34 ± 0.08	to all Q; to all E/Q; to E4	26.6 ± 7.1	to E1, E4, E5; to all E/Q except EQ2
	E3	8.11 ± 0.05	to all Q; to all E/Q except EQ2	43.5 ± 4.0	to E1, E4
	E4	7.90 ± 0.07	to all Q; to all E/Q except EQ2; to E2	100.0 ± 22.6	to all Q; to EQ2, E2, E3
	E5	8.14 ± 0.12	to all Q; to all E/Q except EQ2	79.8 ± 11.3	to all Q; to EQ2, E2
Family 2	Q1	8.96 ± 0.25	to all E; to all E/Q except EQ3	17.2 ± 7.3	to E1, E4, E5; to all E/Q except EQ2
Additional	EQ1	9.32 ± 0.14	to all E; to all E/Q; to Q1	76.7 ± 14.5	to E2, EQ2, Q1
	EQ2	7.91 ± 0.11	to all Q; to all E/Q; to E2	33.2 ± 4.2	to all E/Q; to E1, E4, E5
	EQ3	8.73 ± 0.08	to all E; to all E/Q; to Q2	74.7 ± 11.1	to all Q; to EQ2, E2
	Q2	9.12 ± 0.08	to all E; to all E/Q except EQ1	40.9 ± 5.5	to E1, E4, E5, EQ3

(EQ1, EQ3) than to *E354* individuals (EQ2 only). This was irrespective of gender, and not smaller between related family members. In fact, in family 2 who encompassed a *E354* father and *Q354* mother, GIP potency in LCLs of their child was not in between the two but instead much closer to *Q354*.

Besides potency, we also assessed GIP efficacy for which we did not observe a genotype-related trend, despite a wide range of efficacies with many significant differences (**Table 3**). The individuals with the highest efficacy were three *E354* homozygotes, followed by two heterozygotes. Both *Q354* individuals showed lower efficacy, with Q1 the lowest of all. The trend was however not consistent, as other *E354* homozygotes such as E2 showed efficacies lower than some *Q354*. Furthermore, the monozygotic twin pair E3 and E4 differed largely in efficacy. Thus, GIP efficacies were not consistent with genotype. Of note, GIP efficacy was not related to gender either, as for instance for *E354* the individuals with highest and lowest efficacy were both female. Finally, there was also no clear relationship to GIPR mRNA levels, as for example the two cell lines with the highest E_{max}, E4 and E1, differed greatly in their mRNA levels (**Fig. 1F**).

In conclusion, the responses of the NTR individuals' LCLs revealed that the E354Q polymorphism increased the potency of endogenous agonist GIP in *Q354* homozygotes, while heterozygotes showed mixed effects with respect to GIP potency. The efficacy of GIP was not affected by this polymorphism.

Mutational study E354 in HEK293 cells shows differences in duration of effect

To provide a more direct comparison to our personal cell lines, we performed a mutational study using transiently transfected HEK293 cells and measured their responses upon GIP addition using the xCELLigence. An example of the real-time readout of cellular growth and responses to GIP for HEK293 cells transiently transfected with mock, *E354* and *Q354* is presented in **Fig. 2A**. Addition of GIP to mock-transfected HEK293 cells did not induce significant changes in impedance, while it resulted in an immediate effect in *E354* or *Q354* transfected cells. In both cases, impedance increased to a peak level within 120 minutes and subsequently declined towards baseline, which it did not reach though, even after 240 minutes. Thus, the GIP response dynamics of HEK293hGIPR cells are different from LCLs, especially in response duration.

Fig. 2B and **2C** display examples of the respective real-time traces of *E354* and *Q354* HEK293hGIPR cells responses to GIP from which concentration-effect curves were constructed by analyzing the AUC over 4 hours of response (**Fig. 2D**). The overall effect of GIP in this time period did not differ significantly between *E354* and *Q354* with respect to potency

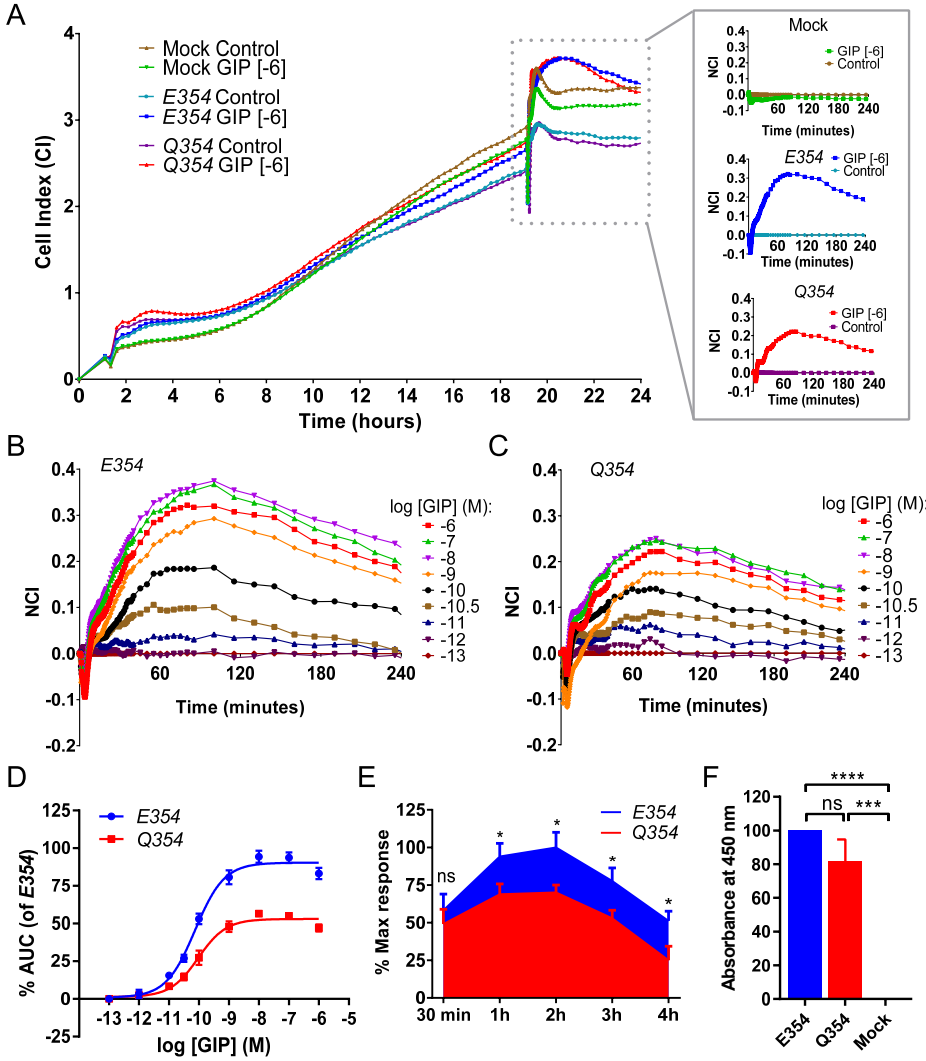

Figure 2. Characterization for hGIPR response in HEK293 cells transiently transfected with *E354* or *Q354* variant. Representative example of a full real-time impedance plot and baseline-corrected responses of mock, *E354* and *Q354* transiently transfected HEK293 cells (**A**) and real-time baseline-corrected concentration-responses curves for (**B**) *E354* and (**C**) *Q354* transfected HEK293 cells. (**D**) Concentration-response curves derived of AUC from NCI within 4 hours after GIP addition for *E354* and *Q354* transfected HEK293 cells. pEC_{50} values were 10.25 ± 0.06 and 10.18 ± 0.08, while E_{max} values were 100 ± 2.9 % and 56.9 ± 6.4 %, respectively. Potency was not significantly different, while E_{max} differed by **** as determined by Student's t-test. (**E**) Percentage highest baseline-corrected response to GIP [1 µM] of *Q354* versus *E354* at several time points. The overall highest response of *E354* was set to 100%. (**F**) Cell-surface expression of *E354* and *Q354* over mock transfected HEK293 cells as determined by FLAG-tag ELISA, which was not significantly different between the two variants. All data are presented as means ± SEM of three or more separate experiments performed in duplicate. Statistic differences were determined by two-way (**E**) or one-way (**F**) ANOVA with Fisher's LSD test. *p≤0.05, **p≤0.01, ***p≤0.001, ****p≤0.0001.

(pEC_{50} of 10.25 ± 0.06 and 10.18 ± 0.08, respectively). Efficacy, however, defined as the maximally achieved overall AUC, was significantly altered (E_{max} of 100 ± 2.9 % and 56.9 ± 6.4 %, respectively). Thus, the overall cellular effect through *Q354* was lower than through *E354*, which was mostly due to how the height of the cellular effect diverged over time (**Fig. 2E**). Specifically, at 30 minutes after agonist addition *E354* and *Q354* showed virtually the same height of response to GIP, while the effect on *Q354* declined towards baseline more rapidly after that time. At 4 hours after GIP addition, the effect on *Q354* was only 49 % of *E354*.
Finally, we confirmed that any differences between *E354* and *Q354* receptor variants transiently transfected in HEK293 cells were not due to differences in cell surface expression by performing ELISA (**Fig. 2F**). In conclusion, the mutational study of E354Q in transiently transfected HEK293 cells showed no differences in potency. In contrast, significant differences were found in efficacy as the height as well as duration of response were decreased in *Q354*.

Discussion

Genetic differences between individuals can affect both drug action and susceptibility to diseases, as is increasingly recognized under the concept of personalized or precision medicine [38]. The GIPR missense SNP E354Q has been associated with diseases including diabetes and bone-fracture risk [12, 15, 16] and shown to have functional effects in mouse cell lines or recombinant cell systems [3, 16, 19]. However, results from such animal and recombinant cells may not be directly translatable to the human individual. Additionally, several of these studies yielded conflicting results. To provide a better link with the physiological situation we studied the effect of this SNP in personal cell lines, i.e. LCLs of a set of individuals from the NTR [29].

The E354Q was present in 21% of NTR individuals, which was in accordance with its global MAF [14]. Most of the other SNPs in the *GIPR* gene (**Table 1**) were located in introns, as is common for intron-containing GPCRs due to the evolutionary conservation of the different regions [39, 40]. Thus for functional studies in LCLs, we selected 10 individuals including two or more unrelated individuals of both genders for each of the three E354Q genotypes (**Table 2**). The set of monozygotic twins used as control for genotype-unrelated effects [29, 41] showed highly comparable responses to the endogenous agonist GIP (**Fig. 1, Table 3**), confirming LCLs are a suitable model system. Remarkably, E354Q affected GIP potency consistently over all individuals, while being independent on gender and family-relation. GIP had higher potency in all *Q354* versus *E354* homozygotes, while heterozygotes

showed a wide spread in potency, differing between each other and from both homozygotes (**Fig. 1, Table 3**). Interestingly, precisely this heterozygous variant but not the homozygous *Q354* has been associated with cardiovascular disease [15]. Conversely, only *Q354* homozygotes were associated with reduced serum C-peptide concentrations, a parameter related to insulin levels [16]. Finally, Torekov *et al.* found minor allele carriers had lowered bone mineral density, but only *Q354* homozygotes had increased risk for certain fractures [12]. The effect of E354Q heterozygosity is therefore not straightforward, and could vary depending on disease. Thus, investigating heterozygosity is imperative for deciphering E354Q pharmacology.

In our study, the E354Q SNP showed clear (genotype-related) effects in LCLs of NTR individuals, mainly on the potency of the endogenous ligand GIP. For instance, GIP potency was highly comparable in the monozygous twins E3 and E4 (**Table 3**). In contrast, the efficacy was not genotype-related (**Table 3**), as for example the same monozygous twins E3 and E4 differed greatly in their E_{max}. Efficacy was also not related to other characteristics such as gender (**Table 2**, **Table 3**) or GIPR mRNA levels (**Fig. 1F**). For example, E4 and E1 were the two cell lines with the highest E_{max}. Contrarily, E4 had high GIPR mRNA levels while E1 exhibited the lowest of all individuals. It has to be kept in mind that mRNA expression levels do not necessarily correlate with functional protein expression on the cellular membrane, a feature well-known in literature [42, 43]. Thus, it appears that neither differences in mRNA levels or E_{max} reveal any E354Q-related effects on functional GIPR expression. Notably, the maximal effects of both GIP and another ligand which targets a completely different set of GPCRs, namely ATP, showed a similar ranking of individuals (*data not shown*). Hence it is possible that the differences in maximal effects reflect each individual's overall cell properties such as viability, proliferation rate and adherence to electrodes, which are not specifically GPCR-related but are known to affect xCELLigence readout [25-28].

Overall, the E354Q SNP showed outspoken effects in LCLs of NTR individuals. It has been suggested that E354, based on functionality of the same $E^{6.48}$ in other class B GPCRs, has a potentially important role in ligand binding and receptor (in)activation [17]. It was shown that mutation to an alanine caused a loss of hydrogen bonding network interactions, resulting in a constitutively active mutant with higher GIP affinity and potency, but unchanged efficacy [17]. Mutation to glutamine may have similar effects by reducing interaction strength, thus causing increased potency yet similar efficacy for agonists, which is in accordance with the observations in LCLs. However, several studies examining functional effects of E354Q in mouse cell lines or recombinant cell systems yielded conflicting results. For instance, Fortin *et al.* noted that *Q354* reduced induction of cAMP production in

recombinant HEK293 cells, while neither Almind *et al.* nor Mohammad *et al.* found any effect on cAMP formation in CHO cells or mouse adipocytes, respectively [3, 16, 19]. A similar discrepancy was observed for antagonism of GIPR in LCLs, which is considered a potential treatment for GIPR-related metabolic abnormalities such as diabetes [44]. When we tested (Pro^3)GIP, the only commercially available GPR antagonist, in LCLs, it partly inhibited GIP activation (**Fig. 1E**) in correspondence to its reported low potency [45]. Interestingly, in our hands (Pro^3)GIP merely acted as an antagonist (**Supplemental Fig. S1**), while Sparre-Ulrich *et al*. reported it to be a full or partial agonist [46]. It stands to notice that the above findings were established in recombinant or non-human cell systems. On the other hand, LCLs are a completely human system that endogenously expresses hGIPR. Lastly, all of these observations were obtained using typical endpoint or second messenger assays, which focus on one part of a cellular response only. Systems such as the xCELLigence offer the advantage of measuring whole-cell responses in real-time as opposed to a static, one-molecule-detection [25-28]. Hence, such label-free whole-cell assays are preferable over typical endpoint assays to minimize bias [47].

To further investigate the influence of the model system used, we measured E354Q mutational effects in a common recombinant system, namely transiently transfected HEK293 cells, using the exact same xCELLigence assay to provide direct comparison. As in LCLs, *E354* and *Q354* were not differentially expressed and we observed a receptor-specific impedance signal (**Fig. 2A, F**). Interestingly, HEK293hGIPR cells showed a response duration vastly different from LCLs (30 minutes for LCLs versus over 240 minutes for HEK293hGIPR). In addition, overall GIP potency was at least 5-fold higher than in LCLs. However, previously published potencies also span a wide range, even within the same cell type. GIP potencies on transiently transfected HEK293hGIPR cells expressing *E354* range from 0.9 pM [19] to 490 ± 30 pM [17], and even 3.63 nM on CHO cells [16], all of which values that were determined in cAMP-based assays.

Besides differences in GIP effects in general, E354Q specifically showed divergent pharmacological effects in HEK293hGIPR and LCLs. Specifically, E354Q did not affect potency in HEK293hGIPR, but had a significant influence on efficacy in terms of height and duration of cellular effects, which were both lower for *Q354* than for *E354* (**Fig. 2**). This is in accordance with findings by Mohammad *et al*. in the same cell type, who established that *Q354* slowed receptor recycling to the cell surface following agonist stimulation [3]. This could lead to a decreased availability of receptors to mediate the cellular effects as measured by the xCELLigence, thus lower and declining more rapidly over time.

It is well-established that the behavior of GPCRs is dependent on the cellular context [48, 49]. HEK293 cells are a prototypical recombinant system prone to receptor overexpression, whereas LCLs are personal cell lines with endogenous levels of receptor expression. This emphasizes the importance of using primary or derived (i.e. endogenous immortalized) human cell systems that offer more physiological relevance to confirm any effects established in other cell systems.

Irrespective of the model system, it is essential to consider findings in the light of physiological and pathological conditions. Consumption of meals induces GIP blood concentrations to approx. 100 pM, which return to previous levels around 20 pM within 3 to 4 h [3, 50-52]. It is clear that such physiological concentrations of GIP cannot reach a maximal effect in *E354* LCLs, where potencies are around 10 nM (Table 3). However, GIP potency on *Q534* LCLs was higher and in the pM range. This makes potency differences extremely relevant for physiological effects, as receptors with increased potency such as the *Q354* variant could mediate a larger response. If this variant additionally shows a shorter effect duration or slower recycling to the surface after GIP stimulation, as pointed at by our results and those of Mohammad *et al.* in HEK293 cells [3], the combination could contribute to lowered GIP sensitivity and, for instance, increasing the risk of insulin resistance. Replicating these findings in cell types directly involved in the physiological functions of GIP, such as adipocytes from patients versus healthy volunteers containing both E354Q GIPR forms, could offer more conclusive results.

In conclusion, our study with personal cell lines that endogenously express E354Q shows that this polymorphism has a strong effect on receptor response, namely by increasing GIP potency, which can affect the physiological function of the receptor. Furthermore, a mutational study in recombinant HEK293 cells revealed a reduced effect duration for *Q354*, which was not observed in LCLs. Thus, the effects of E354Q differ depending on the model system used. By studying E354Q effects in personal cell lines, we aimed to increase the link with the real-life situation and to provide more insight into physiological changes as they occur in the human individual, and thereby contribute to precision medicine for GIPR-related pathologies.

Data Access

The LCLs used in this study were kindly provided within the framework of this collaboration [29] and are part of the Netherlands Twin Register (NTR; *http://www.tweelingenregister.org/en/*), and part of the Center for Collaborative Genomic

Studies on Mental Disorders (NIMH EQ34 MH068457-06). Data and biomaterials (such as cell lines) are available to qualified investigators, and may be accessed by following a set of instructions stipulated on the National Institute of Mental Health (NIMH) website (*https://www.nimhgenetics.org/access_data_biomaterial.php*).

Acknowledgements

We thank Dr. A. Brooks (Department of Genetics, Rutgers University, Piscataway, NJ, USA) for preparation of the lymphoblastoid cell lines. The research presented in this manuscript was supported by the Center for Collaborative Genomic Studies on Mental Disorders (NIMH EQ34 MH068457-06). Funding for the GoNL was provided by the Netherlands Organization for Scientific Research (184021007) to BBMRI-NL. The NTR acknowledges support from the Netherlands Organization for Scientific Research (grant NWO 480-15-001/674: Netherlands Twin Registry Repository: researching the interplay between genome and environment).

References

1. Usdin, T.B., et al., *Gastric inhibitory polypeptide receptor, a member of the secretin-vasoactive intestinal peptide receptor family, is widely distributed in peripheral organs and the brain.* Endocrinology, 1993. **133**(6): p. 2861-70.
2. Irwin, N. and P.R. Flatt, *Therapeutic potential for GIP receptor agonists and antagonists.* Best Pract Res Clin Endocrinol Metab, 2009. **23**(4): p. 499-512.
3. Mohammad, S., et al., *A naturally occurring GIP receptor variant undergoes enhanced agonist-induced desensitization, which impairs GIP control of adipose insulin sensitivity.* Mol Cell Biol, 2014. **34**(19): p. 3618-29.
4. Holst, J.J., et al., *Searching for the physiological role of glucose-dependent insulinotropic polypeptide.* J Diabetes Investig, 2016. **7 Suppl 1**: p. 8-12.
5. Davies, M.A., et al., *Pharmacologic analysis of non-synonymous coding h5-HT2A SNPs reveals alterations in atypical antipsychotic and agonist efficacies.* Pharmacogenomics J, 2006. **6**(1): p. 42-51.
6. Docherty, S.J., et al., *A genetic association study of DNA methylation levels in the DRD4 gene region finds associations with nearby SNPs.* Behav Brain Funct, 2012. **8**: p. 31-44.
7. Ishiguro, H., et al., *Brain cannabinoid CB2 receptor in schizophrenia.* Biol Psychiatry, 2010. **67**(10): p. 974-82.
8. Sadee, W., et al., *Genetic variations in human G protein-coupled receptors: implications for drug therapy.* AAPS pharmSci, 2001. **3**(3): p. 54-80.
9. Sauber, J., et al., *Association of variants in gastric inhibitory polypeptide receptor gene with impaired glucose homeostasis in obese children and adolescents from Berlin.* Eur J Endocrinol, 2010. **163**(2): p. 259-64.
10. Vogel, C.I., et al., *Gastric inhibitory polypeptide receptor: association analyses for obesity of several polymorphisms in large study groups.* BMC Med Genet, 2009. **10**: p. 19.
11. Saxena, R., et al., *Genetic variation in GIPR influences the glucose and insulin responses to an oral glucose challenge.* Nat Genet, 2010. **42**(2): p. 142-8.
12. Torekov, S.S., et al., *A functional amino acid substitution in the glucose-dependent insulinotropic polypeptide receptor (GIPR) gene is associated with lower bone mineral density and increased fracture risk.* J Clin Endocrinol Metab, 2014. **99**(4): p. E729-33.
13. NCBI. *GIPR, http://www.ncbi.nlm.nih.gov/gene/2696, Accessed 21.07.2016*. 2016 03.07.2016 21.07.2016].
14. dbSNP. *http://www.ncbi.nlm.nih.gov/projects/SNP/snp_ref.cgi?rs=1800437 ; Accessed 21.07.2016*. 2016 21.07.2016].
15. Nitz, I., et al., *Association analyses of GIP and GIPR polymorphisms with traits of the metabolic syndrome.* Mol Nutr Food Res, 2007. **51**(8): p. 1046-52.
16. Almind, K., et al., *Discovery of amino acid variants in the human glucose-dependent insulinotropic polypeptide (GIP) receptor: the impact on the pancreatic beta cell responses and functional expression studies in Chinese hamster fibroblast cells.* Diabetologia, 1998. **41**(10): p. 1194-8.
17. Cordomi, A., et al., *Functional elements of the gastric inhibitory polypeptide receptor: Comparison between secretin- and rhodopsin-like G protein-coupled receptors.* Biochem Pharmacol, 2015. **96**(3): p. 237-46.

18. Venkatakrishnan, A.J., et al., *Molecular signatures of G-protein-coupled receptors.* Nature, 2013. **494**(7436): p. 185-94.
19. Fortin, J.P., et al., *Pharmacological characterization of human incretin receptor missense variants.* J Pharmacol Exp Ther, 2010. **332**(1): p. 274-80.
20. Sie, L., S. Loong, and E.K. Tan, *Utility of lymphoblastoid cell lines.* J Neurosci Res, 2009. **87**(9): p. 1953-9.
21. Sugimoto, M., et al., *Steps involved in immortalization and tumorigenesis in human B-lymphoblastoid cell lines transformed by Epstein-Barr virus.* Cancer research, 2004. **64**(10): p. 3361-4.
22. Abecasis, G.R., et al., *A map of human genome variation from population-scale sequencing.* Nature, 2010. **467**(7319): p. 1061-73.
23. Welsh, M., et al., *Pharmacogenomic discovery using cell-based models.* Pharmacological reviews, 2009. **61**(4): p. 413-29.
24. Wheeler, H.E. and M.E. Dolan, *Lymphoblastoid cell lines in pharmacogenomic discovery and clinical translation.* Pharmacogenomics, 2012. **13**(1): p. 55-70.
25. Yu, N., et al., *Real-time monitoring of morphological changes in living cells by electronic cell sensor arrays: an approach to study G protein-coupled receptors.* Anal Chem, 2006. **78**(1): p. 35-43.
26. Fang, Y., *Label-Free Receptor Assays.* Drug Discov Today Technol, 2011. **7**(1): p. e5-e11.
27. Rocheville, M., et al., *Mining the potential of label-free biosensors for seven-transmembrane receptor drug discovery.* Progress in molecular biology and translational science, 2013. **115**: p. 123-42.
28. Fredholm, B.B., et al., *International Union of Basic and Clinical Pharmacology. LXXXI. Nomenclature and classification of adenosine receptors--an update.* Pharmacol Rev, 2011. **63**(1): p. 1-34.
29. Willemsen, G., et al., *The Netherlands Twin Register biobank: a resource for genetic epidemiological studies.* Twin Res Hum Genet, 2010. **13**(3): p. 231-45.
30. Program, Q.P.D. *http://www.genomics.agilent.com/primerDesignProgram.jsp?toggle=uploadNow&mutate=true&_requestid=1185053*. [cited 2015 November 3].
31. Liu, H. and J.H. Naismith, *An efficient one-step site-directed deletion, insertion, single and multiple-site plasmid mutagenesis protocol.* BMC Biotechnol, 2008. **8**: p. 91.
32. Guo, D., et al., *Functional efficacy of adenosine A(2)A receptor agonists is positively correlated to their receptor residence time.* British journal of pharmacology, 2012. **166**(6): p. 1846-59.
33. *Whole-genome sequence variation, population structure and demographic history of the Dutch population.* Nature genetics, 2014. **46**(8): p. 818-25.
34. Purcell, S., et al., *PLINK: a tool set for whole-genome association and population-based linkage analyses.* Am J Hum Genet, 2007. **81**(3): p. 559-75.
35. Purcell, S., *PLINK v1.07, http://pngu.mgh.harvard.edu/purcell/plink/*.
36. Jacob, F., et al., *Purinergic signaling in inflammatory cells: P2 receptor expression, functional effects, and modulation of inflammatory responses.* Purinergic signalling, 2013. **9**(3): p. 285-306.

37. Lee, D.H., et al., *Expression of P2 receptors in human B cells and Epstein-Barr virus-transformed lymphoblastoid cell lines.* BMC immunology, 2006. **7**: p. 22-33.
38. Lu, Y.F., et al., *Personalized medicine and human genetic diversity.* Cold Spring Harb Perspect Med, 2014. **4**(9).
39. Kruglyak, L. and D.A. Nickerson, *Variation is the spice of life.* Nature Genetics, 2001. **27**(3): p. 234-236.
40. Small, K.M., et al., *Gene and protein domain-specific patterns of genetic variability within the G-protein coupled receptor superfamily.* Am J Pharmacogenomics, 2003. **3**(1): p. 65-71.
41. Silventoinen, K., et al., *The CODATwins Project: The Cohort Description of Collaborative Project of Development of Anthropometrical Measures in Twins to Study Macro-Environmental Variation in Genetic and Environmental Effects on Anthropometric Traits.* Twin Res Hum Genet, 2015. **18**(4): p. 348-60.
42. Guo, Y., et al., *How is mRNA expression predictive for protein expression? A correlation study on human circulating monocytes.* Acta Biochim Biophys Sin (Shanghai), 2008. **40**(5): p. 426-36.
43. Vogel, C. and E.M. Marcotte, *Insights into the regulation of protein abundance from proteomic and transcriptomic analyses.* Nat Rev Genet, 2012. **13**(4): p. 227-32.
44. McClean, P.L., et al., *(Pro(3))GIP[mPEG]: novel, long-acting, mPEGylated antagonist of gastric inhibitory polypeptide for obesity-diabetes (diabesity) therapy.* British journal of pharmacology, 2008. **155**(5): p. 690-701.
45. Gault, V.A., et al., *Characterization of the cellular and metabolic effects of a novel enzyme-resistant antagonist of glucose-dependent insulinotropic polypeptide.* Biochemical and biophysical research communications, 2002. **290**(5): p. 1420-6.
46. Sparre-Ulrich, A.H., et al., *Species-specific action of (Pro3)GIP - a full agonist at human GIP receptors, but a partial agonist and competitive antagonist at rat and mouse GIP receptors.* British journal of pharmacology, 2016. **173**(1): p. 27-38.
47. Rocheville, M., et al., *Mining the potential of label-free biosensors for seven-transmembrane receptor drug discovery.* Oligomerization and Allosteric Modulation in G-Protein Coupled Receptors, 2012. **115**: p. 123.
48. Butcher, A.J., et al., *Differential G-protein-coupled receptor phosphorylation provides evidence for a signaling bar code.* J Biol Chem, 2011. **286**(13): p. 11506-18.
49. Tobin, A.B., A.J. Butcher, and K.C. Kong, *Location, location, location...site-specific GPCR phosphorylation offers a mechanism for cell-type-specific signalling.* Trends Pharmacol Sci, 2008. **29**(8): p. 413-20.
50. Jorde, R., et al., *Effect of gastrin on fasting and postprandial plasma GIP release in man.* Digestion, 1982. **25**(2): p. 81-7.
51. Lyssenko, V., et al., *Pleiotropic effects of GIP on islet function involve osteopontin.* Diabetes, 2011. **60**(9): p. 2424-33.
52. Tseng, C.C., et al., *Postprandial stimulation of insulin release by glucose-dependent insulinotropic polypeptide (GIP). Effect of a specific glucose-dependent insulinotropic polypeptide receptor antagonist in the rat.* J Clin Invest, 1996. **98**(11): p. 2440-5.

Supporting information

Supplemental Table S1. Significant differences in endogenous agonist GIP potency and efficacy per individual's LCL. Data represent pEC_{50} ± SEM and E_{max} ± SEM of at least three experiments performed in duplicate. Statistical analysis was performed by one-way ANOVA with Fisher's LSD post-hoc test. For pEC_{50}, a large difference between GG genotypes (*E354*) the CC genotype (*Q354*) compared to GG genotypes and a mixed effect for the heterozygote genotype. The E_{max} showed little differences that were not consistent with genotype. ns = not significant; *p≤0.05, **p≤0.01, ***p≤0.001, ****p≤0.0001.

Individuals	pEC_{50}		E_{max}	
	Summary	P Value	Summary	P Value
E1 vs. E2	ns	0.1670	**	0.0027
E1 vs. E3	ns	0.8819	*	0.0250
E1 vs. E4	ns	0.1156	ns	0.4986
E1 vs. E5	ns	0.9651	ns	0.7103
E1 vs. Q1	****	<0.0001	**	0.0015
E1 vs. EQ1	****	<0.0001	ns	0.6019
E1 vs. EQ2	ns	0.1278	**	0.0067
E1 vs. EQ3	***	0.0002	ns	0.4815
E1 vs. Q2	****	<0.0001	*	0.0103
E2 vs. E3	ns	0.1278	ns	0.3722
E2 vs. E4	**	0.0049	***	0.0004
E2 vs. E5	ns	0.2149	*	0.0128
E2 vs. Q1	***	0.0005	ns	0.6423
E2 vs. EQ1	****	<0.0001	*	0.0183
E2 vs. EQ2	**	0.0056	ns	0.7262
E2 vs. EQ3	*	0.0100	*	0.0105
E2 vs. Q2	****	<0.0001	ns	0.4081
E3 vs. E4	ns	0.1518	**	0.0048
E3 vs. E5	ns	0.8562	ns	0.0803
E3 vs. Q1	****	<0.0001	ns	0.2008
E3 vs. EQ1	****	<0.0001	ns	0.1078
E3 vs. EQ2	ns	0.1670	ns	0.5847
E3 vs. EQ3	***	0.0001	ns	0.0860
E3 vs. Q2	****	<0.0001	ns	0.8790
E4 vs. E5	ns	0.1330	ns	0.3210
E4 vs. Q1	****	<0.0001	***	0.0003
E4 vs. EQ1	****	<0.0001	ns	0.2546
E4 vs. EQ2	ns	0.9569	**	0.0011
E4 vs. EQ3	****	<0.0001	ns	0.1617
E4 vs. Q2	****	<0.0001	**	0.0015
E5 vs. Q1	****	<0,0001	**	0.0066
E5 vs. EQ1	****	<0.0001	ns	0.8877
E5 vs. EQ2	ns	0.1456	*	0.0272
E5 vs. EQ3	***	0.0006	ns	0.7947
E5 vs. Q2	****	<0.0001	*	0.0447
Q1 vs. EQ1	*	0.0406	**	0.0094

Q1 vs. EQ2	****	<0.0001	ns	0.4320
Q1 vs. EQ3	ns	0.1318	**	0.0054
Q1 vs. Q2	ns	0.2966	ns	0.2129
EQ1 vs. EQ2	****	<0.0001	*	0.0381
EQ1 vs. EQ3	***	0.0004	ns	0.9185
EQ1 vs. Q2	ns	0.1690	ns	0.0630
EQ2 vs. EQ3	****	<0.0001	*	0.0251
EQ2 vs. Q2	****	<0.0001	ns	0.6547
EQ3 vs. Q2	**	0.0041	*	0.0415

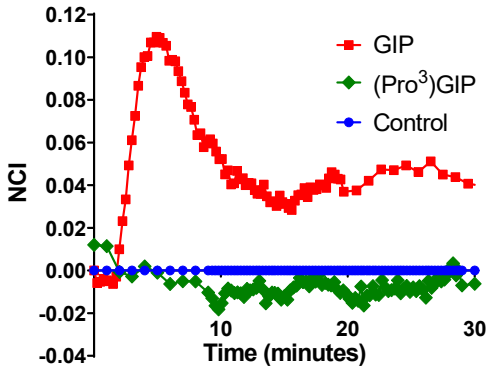

Supplemental Figure S1. (Pro^3)GIP response in LCLs. Representative example of a baseline-corrected responses to either (Pro^3)GIP [1 µM] or GIP [31.6nM] of LCLs from one *E354* individual, E3. Data is representative for three or more separate experiments performed in duplicate.

CHAPTER 7

Conclusions and future perspective

This thesis delves into examining the influence of genetic variation on GPCR function within the human individual. In this concluding chapter, insights gained from case studies at three different GPCRs are elaborated on, and suggestions for future investigations around precision medicine for GPCRs are presented.

Conclusions

Assay methodology and model systems

GPCRs are traditionally investigated in reporter-based assays performed on heterologous cell lines, which offer only limited translational value [1-6]. Physiologically more appropriate model systems and assays are thus required (Chapter 2). LCLs, which are among the most frequently biobanked samples used for storing genetic material [7-13], could form a highly valuable resource for investigating genetic effects on drug action and receptor function. In addition, label-free cellular assays offer increased physiological relevance over the assays used traditionally in GPCR research, as discussed in Chapter 1 and 2 [4, 13-15]. Unfortunately, these were originally deemed incompatible with suspension cells such as LCLs due to the detection mechanism positioned at the bottom of the well [16]. In this thesis I present a methodology with increased translational value by employing personal cell lines (the LCLs) as a model system, in combination with a physiologically more appropriate label-free cellular assay (the xCELLigence) to investigate GPCR function (Chapter 3). Adaptation to suspension cells drastically widens the realm of application for label-free assays, while investigating GPCR functionality in LCLs opens up an avenue for exploring precision medicine for GPCRs.

Genetic variation in GPCRs

Genetic variants in drug targets affect pathology and drug action [17]. Despite GPCRs being the largest group of drug targets to-date [18], studies on their genetic variation are sporadic, often only statistically associative and focus on one single target. Investigations generally work with one consensus form of a receptor, the so-called Wild-type, hereby ignoring the naturally occurring genetic variation in the population. However, other receptor variants may be more relevant for certain diseases or drug effects. Three separate cases of common polymorphisms that affect GPCR signaling are presented in this thesis, each revealing different properties including the sensitivity to agonist type, chemical scaffold and variant position in the gene.

Throughout this thesis I present examples that show genetic variations at different positions in GPCRs can be of influence. Logically, single nucleotide polymorphisms (SNPs)

most likely to have profound effects on receptor function are those that alter the amino acid sequence of the receptor, the so-called non-synonymous SNPs. Indeed, the variants that affected the Cannabinoid Receptor 2 (CB_2R) and the glucose-dependent insulinotropic polypeptide receptor (GIPR), Q63R and E354Q respectively, both changed an amino acid (**Chapter 5** and **6**). In fact, many cases presented in the literature fall into this category [2, 19, 20]. However, changing amino acid sequence is not the only way in which a receptor can be affected by polymorphisms. **Chapter 4** presents the case of the Adenosine A_{2A} receptor, in which responses differ between individuals in the absence of any non-synonymous SNPs. Genotype comparison revealed differences in two intron SNPs, one of which associated with caffeine-induced sleep disorders [21-23]. Such SNPs could have regulatory potential, for instance in affecting receptor expression which in turn may affect G protein coupling efficiency [23, 24].

Interestingly, this particular $A_{2A}R$ SNP altered partial agonist potency, but not that of full agonists or antagonists (**Chapter 4**). In a similar manner, the partial agonists for the CB_2R showed higher efficacy in a Q63R minor homozygote (**Chapter 5**). While either potency or efficacy of partial agonists can be affected, it overall appears that partial agonists may be more receptive to polymorphism-induced changes. This concurs with the theory that deems partial agonists more sensitive to system-related differences in receptor function, for instance in receptor expression or downstream coupling, than full agonists or antagonists [25]. The nature of the ligand thus influences its sensitivity to e.g. polymorphisms. In addition, the chemical scaffold of a ligand is likewise important. **Chapter 5** presents how compounds of different chemical classes show more or less modulation due to CB_2R genetic variation. Non-classical cannabinoid CP55940 showed the most pronounced personal effects, while aminoalkylindole compounds showed fewer individual differences. Taking both ligand nature and chemical scaffold effects into account could allow early identification of compounds prone to personal differences ('precision medicine') or compounds that would be more suited as drugs for the general population.

Besides affecting drug action, SNPs can also alter the physiological function of a receptor with potentially pathological consequences. **Chapter 6** focusses on the investigation of the GIPR, in which E354Q influenced endogenous agonist effects, in particular with respect to potency in LCLs and duration of response when the receptor was expressed in recombinant HEK293 cells. This SNP has previously been linked with various pathologies including insulin resistance, diabetes and cardiovascular disease [26-29]. Interestingly, endogenous agonists are not necessarily more sensitive to receptor polymorphisms than synthetic ligands, as the study of adenosine on the $A_{2A}R$ and various endocannabinoids on CB_2R show (**Chapter 4** and

5). While some SNPs are of pathological consequence, others may be more relevant for drug effects. For instance, the $A_{2A}R$ SNP has been associated with caffeine effects and pharmacotherapy-related toxicities in acute lymphoblastic leukemia as well as pathological conditions including anxiety in autism [21-24]. Similarly, Q63R in the CB_2R has been linked to various pathological disorders [5, 30-35] as well as synthetic ligand effects (Chapter 5, [36]). It is important to note that if a polymorphism affects an endogenous agonist, this may not directly leading to pathology. However it can still drastically alter a system's sensitivity to drug treatment, even if the synthetic compounds are not directly affected themselves. In conclusion, it is undoubtedly necessary to take physiology and pathology into account when selecting ligands and conditions to study the influence of GPCR polymorphisms.

Finally, it could be argued that SNPs with profound effects on receptor function are likely less frequent in the population due to evolutionary pressure. It is a common misconception that a frequent SNP has likely little effect [2]. The frequencies of the SNPs in this thesis however tell a different story, as the SNPs in the GIPR and CB_2R with a global Minor Allele Frequency of approx. 35% and 16%, respectively [37-39], are in fact quite frequent, regardless of any functional effects. Many disease-related SNPs are quite rare, but some common SNPs are also known to contribute to or cause certain disease phenotypes [2, 17].

In summary, the cases presented in this thesis demonstrate that for every GPCR, there appears to be at least one polymorphism candidate to affect receptor function. The particularities of each polymorphism can however differ, depending on the nature of the ligand such as endogenous vs. synthetic, partial vs. full agonist, chemical scaffold as well as the number of individuals potentially affected.

LCLs as model system for genetic effects on GPCRs

The examples summarized in this thesis (Chapter 3-6) demonstrate that LCLs are a suitable model system to study genetic effects on GPCRs, and the applied methodology facilitates phenotypic measurements of personal responses. LCLs thus enable direct measurement of polymorphism effects in a physiological environment, without having to generate and introduce a receptor mutant into a heterologous cell line as is generally done in the GPCR field. Any such alterations can affect receptor pharmacology and decrease translatability (Chapter 2). It is therefore unsurprising that the results presented in this thesis agree with previous investigations to some degree, while contradicting others. In chapter 5 for instance, Q63R influences on CB_2R contrasted previous reports obtained in recombinant overexpressing cell systems, while confirming findings in a more physiological cell type [5, 36, 40, 41]. E354Q effects on GIPR differed between LCLs and HEK293 cells even in our hands

(Chapter 6), and results of either cell type were both in accordance and contrast with previous studies [28, 29, 42]. Overall, it appears that LCLs are a well-suited system to measure personal polymorphism effects on GPCRs in a physiological setting, and enable explorations into the realm of GPCR precision medicine. While they increase translatability in comparison to traditional cell systems, the relevance of effects established in this thesis depends on further replication in e.g., more individuals for genotype effects, and/or primary cell types directly involved in pathology.

Future perspectives

Altogether a variety of impact factors for GPCR research including model systems, assay technology and genetic variation have been detailed throughout this thesis. The following section will discuss the future perspectives precision medicine for GPCRs involving some of these findings and additional aspects for further consideration.

Genetic variation landscape in druggable GPCRs

With the rise of personalized or precision medicine concepts, it is increasingly recognized that genetic differences between individuals can affect both drug action and susceptibility to diseases [17]. Examples of influential genetic variants of various types, frequencies and physiological consequences are accumulating. However, which variants are pathogenic, collateral of inconsequential is still largely undefined and subject of tremendous ongoing research efforts.

When regarding any two unrelated individuals, 99% of their genomic DNA sequences are identical. The other 1%, however, signifies in fact 38 million different genomic variations. In turn, 90% of these variations are formed by SNPs, which makes these the most common source of genetic variation in the human population [12, 32]. On average, around one SNP occurs per 300 bases, meaning that each GPCRs should contain several SNPs, which occur more or less frequently in the population [2, 43]. During our annotation process of SNPs in druggable GPCRs (Chapter 1, Fig. 3), we noted several trends.

First, the total amount of SNPs is related to gene size (Fig. 1). The largest GPCR genes, which belong mostly to Class C and Adhesion GPCRs, generally have the most genetic variation. Table 1 shows the top and bottom 5 genes with most or least SNPs. Based on these, SNPs of any kind occur within a GPCR gene on average around every 140 bp in the largest genes and every 413 bp in the shortest genes. This increased distance in shorter genes is unsurprising as, the shorter a gene, the larger the relative part that is coding sequence, which is more evolutionary conserved.

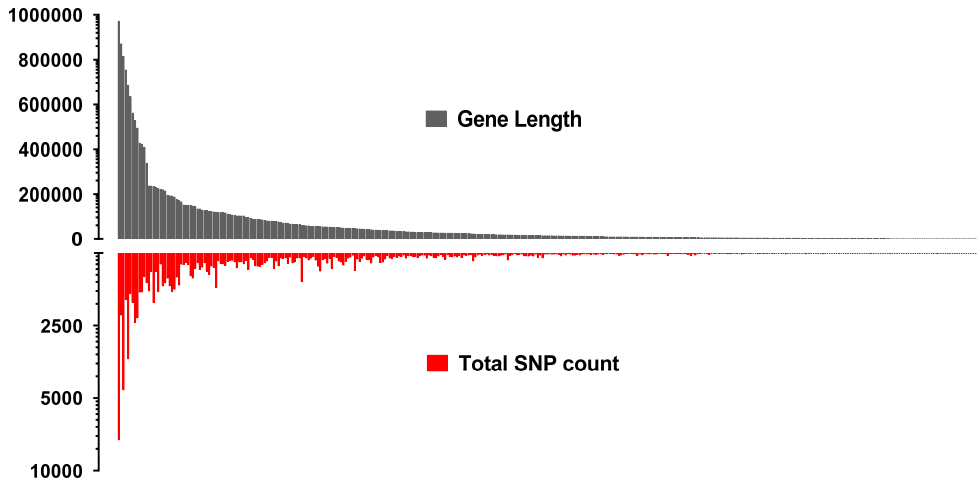

Figure 1. Total SNP count vs gene length for all 370 druggable GPCRs. A list of all druggable non-olfactory GPCRs was downloaded from the IUPHAR database. The gene length and SNP information were exported from Ensembl Biomart archived page (April 2013, version 71) corresponding to genome build GCRh37.p10.

Secondly, most SNPs are located in non-coding regions and/or do not affect amino acid sequence in any way. Non-synonymous SNPs only represented 0.7% of all SNPs found in druggable GPCRs (total 152.000 SNPs on 370 GPCR genes). Synonymous SNPs which are located in the coding region but do not change the amino acid sequence made up 25%. Hence, GPCRs contain an abundance of SNPs predominantly in non-coding regions, with 42.5% in UTR and intron regions. This is common for any intron-containing GPCR due to the evolutionary conservation of the different regions [43, 44].

Finally, SNPs with possibly profound effects on receptor function i.e. by altering the amino acid sequence of the receptor, are more abundantly occurring than one might expect. While the overall amount of SNPs increases with gene size (**Fig. 1**), on average each druggable GPCR contains at least 1-5 non-synonymous SNPs, independent of gene size (**Table 1**). The bottom line is that for each GPCR, there appear to be genetic differences which may impact receptor and drug functionality. Hence it is paramount not to ignore the potentially influential natural variation occurring in any GPCR or drug target for future pharmacological research.

Although SNPs form the major source, there are other types of genetic variants present in the human genome. These include bi-allelic short insertions or deletions, large deletions, short repeats such as micro- and minisatellites, and copy number variants (CNV) which can extend to repeats of entire genes [32]. While most have no detrimental clinical

Table 1. GPCR genes with the top five most and least SNPs in total. The gene length and SNP information were exported from Ensembl Biomart archived page (April 2013, version 71) corresponding to genome build GCRh37.p10. The column labelled altering SNPs entails the number of SNPs that are either missense-, start and stop codon, or frameshift variants for the respective receptor.

Gene	GPCR class	Receptor type	Gene lenght (bp)	Average SNP distance (bp)	SNPs	
					Total	Altering
GRM7	Class C	Metabotropic glutamate receptor 7	971527	118	8216	2
LPHN2	Adhesion	Latrophilin receptor 2	686275	126	5430	5
LPHN3	Adhesion	Latrophilin receptor 3	871208	160	5430	2
GRM8	Class C	Metabotropic glutamate receptor 8	814696	151	5388	5
BAI3	Adhesion	Brain-specific angiogenesis inhibitor	754144	144	5248	2
TAS2R16	Taste	Type 2 taste receptor 16	995	332	3	2
GPR32	Class A	Orphan receptor	1268	423	3	1
CHRM4	Class A	Muscarinic acetylcholine receptor 4	1467	489	3	0
MC3R	Class A	Melanocortin receptor 3	1083	361	3	1
FFAR1	Class A	Free fatty acid receptor 1	922	461	2	1

consequences, some form a pathological risk. For instance, several repeat polymorphisms in the Arginine vasopressin receptor 1A have been associated with altered social, sexual and reproductive behavior [45-47]. Also, the TAS2R receptor family that detects bitter taste of compounds such as caffeine contains about 25 GPCRs, but the exact number per individual varies due to copy number variation. Individual experiences of bitterness are altered by genetic variation in these receptors [48, 49]. Finally, duplication of orphan receptor GPR101 has been shown to lead to X-linked acrogigantism [50]. Thus next to SNPs, it would be an important addition to study other forms of genomic variations too, as these can also account for a difference in GPCR response [51].

Of note, the Netherlands Twin Registry (NTR; *http://www.tweelingenregister.org/en/*) [7] from which the collection of LCLs utilized in this study originated, has served as data source for many genetic studies, including SNPs as well as CNVs already [52-55]. Given the appropriate samples are available, utilizing the set-up of LCLs and label-free technology could offer additional insights into the functional influences of such other types of variants too.

LCLs and emerging cellular model systems for drug research

Two of the major challenges in today's drug development are the lack of understanding inter-individual variability in drug effectiveness, and the translatability of preclinical results. Inappropriate model systems have contributed to both issues, and consequently to lack of reproducibility in preclinical research, lack of clinical effectiveness and high attrition rates [6, 56].

In this thesis I have presented a methodology utilizing LCLs from the NTR [7] as a model system to investigate genetic effects on GPCR functionality. Applications of LCLs are however by no means limited to the three exemplary GPCR cases discussed in this thesis (Chapter 4-6), as LCLs express many more GPCRs as well as other drug targets [11, 57, 58].

In general, renewable *in vitro* cell sources have been essential in facilitating drug discovery and pharmacogenomic studies. In fact, much of our understanding of the influences of genetic variation in humans is based on studies utilizing LCLs [59]. LCLs are already easily available in large variety as LCL repositories exist in abundance, some representing specific disease populations or ethnicities [7-11, 59-61]. Hence they are utilized in many aspects of pharmacogenomics, and examples include general genotype-phenotype association, many genome-wide association studies (GWAS) for drug-induced phenotypes and even follow-up studies of clinical findings [11, 57].

Notwithstanding the convenience and usefulness of LCLs as a cellular model system, there are concerns that their immortalization and cell line maintenance could obscure genetic findings [59, 62-64]. Certainly, it is well known that a large number of genes are differentially expressed between primary cells and cell lines [59]. Opposed to this, primary cells express signaling pathways and retain many cellular functions that are seen *in vivo*, thus providing a more relevant context (Chapter 2). Over the past decades, numerous biobanks have been set up to support medical research by programmed storage of biological material and corresponding data. These biomaterials include LCLs as well as primary material such as tissues, (stem) cells and blood, all of which are actively used from translational and personalized medicine to target and drug discovery [65, 66]. Several approaches applying label-free technology to utilize patient primary cells as model system are discussed in Chapter 2. While such cell types have increased translational value, the materials are often limited due to culture and sampling issues. On the other hand, LCLs are a renewable source that is already widely available, and offer genotypic and phenotypic information and stability that is absent in many other renewable sources. How appropriate either model system is depends largely on the application and question at hand.

An alternative that could incorporate renewability, primary tissue properties and patient origin are stem cells, which offer great potential as physiologically more relevant models. In particular induced pluripotent stem cells (iPSC), which can maintain the disease genotype and phenotype indefinitely, provide a source of models for an expansive range of adult differentiated cells, possibly even for each individual patient. The ability to reprogram cells of patients into disease-relevant cell types could provide more representative and predictive cellular models for both disease modelling and drug discovery [60], and has the potential to personalize pharmacological research [67, 68]. iPSC have already been used for drug screening and disease modelling, particular as neural cells, haematopoietic cell types, hepatocytes and cardiomyoctes [69, 70]. For some of such cell types, hiPSC-cardiomyocytes in particular, there are also examples of their application in label-free assays (Chapter 2, Table 1) [71-73]. Interestingly, iPSC can be derived from a variety of cellular sources, including LCLs. This taps into the invaluable resources of the already available, vast collections of LCLs. iPSC derived from LCLs retain their disease mutation, exhibit identical characteristics as iPSC derived from more common sources such as fibroblasts, and can be differentiated into various cell types including neurons and even intestinal organoids [60, 61]. Organoids constitute near-physiological 3D models of an organ with realistic micro-anatomy, and as such enable more accurate study of many physiological processes [74]. Furthermore, iPSC from LCLs even recover their donor-specific gene expression signature [59, 60]. While it is unlikely that the lack of donor signature on gene expression in LCLs themselves would cause false-positive findings of genetic influence, such as the ones presented in this thesis in Chapter 3-6, regaining this signature in iPSC increases the ability to study inter-individual differences in gene expression [59].

In summary, as these developments show, LCLs offer an enormous bioresource for both drug discovery and disease modelling [60, 61].

Comeback of phenotypic assays for drug research

In addition to the need for more representative model systems, a preference is emerging for minimally invasive, time-resolved and thus pharmacologically more relevant assays. As principal criteria, new assay approaches for pharmaceutical drug discovery are to be more efficient and multidimensional [19]. Amongst these are label-free cellular assays. As discussed in Chapter 2, these assays offer a wide range of applications and have similarly been applied to many important classes of drug targets, which include besides GPCRs also receptor tyrosine kinases and nuclear receptors [75-78]. Their realm of application is large and constantly expanding.

This preference is part of a general trend back towards phenotypic screening. Phenotypic screens were in fact the norm for drug discovery prior to the 1980s. Following the advent of molecular cloning then, target-based screening became the standard approach for drug discovery. This strategy includes cloning and functional expression of potential drug targets in recombinant cell lines for study and screening of drug candidates (**Fig. 2**). While this approach has delivered many drug candidates over the years, there were relatively few new drugs. One reason is that this approach may work very well for monogenic diseases, however, most human diseases are likely multifactorial. Rather than caused by a single genetic change, they are complex diseases originating through an interplay of a multitude of genetic and environmental factors. Hence they may require engagement of multiple targets to achieve clinical efficacy [79-82].

In such instances, target-agnostic approaches as utilized in phenotypic screening assays can offer advantages. In fact, significantly more small-molecule first-in-class drugs were discovered through phenotypic screening than target-based approaches [83]. Instead of focusing on engaging a specific target, phenotypic assays rely on finding molecules with a particular biological effect in cell-based or animal models (**Fig. 2**) [80-82]. This approach does however have its own hurdles to overcome, which include the need to identify a phenotypic

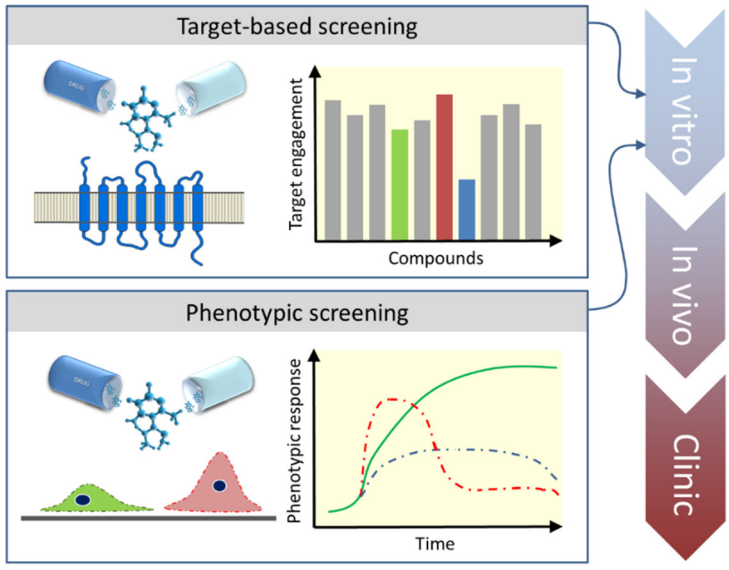

Figure 2. Phenotypic assays versus target-based approach. Target-based drug discovery approach focuses on engaging a specific target, often using molecular cloning and recombinant techniques. Phenotypic assays identify molecules with a particular biological effect in cell-based or animal models. Phenotypic assays can provide context that is closer to the clinical situation.

endpoint appropriately associated with the disease of interest. Label-free assay technologies offer additional advantages here, as they do not require assumptions about molecular mechanisms and pathways but rather allow for a multidimensional and less biased investigation [80]. In summary, label-free assay technology provides phenotypic assays that are able to acquire molecular-level understanding of complex biological processes in their native environment [6, 84]. When combined with the appropriate cellular model systems, as discussed in this thesis in e.g. **Chapter 2**, the combination offers a powerful approach for pharmaceutical research in general and precision medicine in particular.

Precision medicine prospective for GPCRs

The human genome mapping, the resulting pharmacogenetic discoveries and the ongoing movement towards precision medicine have influenced drug development in general, and hence also for GPCRs. It is increasingly recognized among the GPCR research community that tailoring a drug candidate for a particular genetic variant of a GPCR could offer various benefits [19] (**Fig. 3**). There are numerous examples of genetic variants in GPCRs altering pharmacology or pathology. In 2001, Sadee *et al.* published an exemplary catalogue of genetic GPCR variants and possible implications for drug therapy [64]. More than a decade later, the tailoring of GPCR targeting drugs based on genetic variation in patients is still deemed to be in the early stages of feasibility [34]. To name a particular example, the α_{2A} adrenergic receptor antagonist yohimibine improved insulin secretion in type II diabetes patients that were carriers of a particular SNP in this receptor [20]. Other forms of genetic variation besides SNPs have also been found to be of influence, for instance GPCR expression

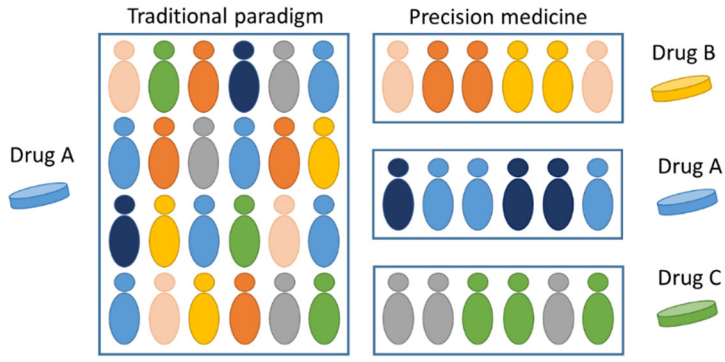

Figure 3. Precision medicine versus traditional treatment paradigm. Tailoring a drug (candidate) to patient characteristics such as genetic information can offer several benefits including decreased risks of ineffective treatment, of inappropriate dosing or of side effects [91-93].

as a biomarker for the clinical efficacy of the A_3 adenosine receptor agonist IB-MECA, or the conversion of $P2Y_{12}$ receptor prodrug Plavix being impaired by the 2C16 isoform of CYP450 enzymes [85, 86] .

The progress in precision medicine for GPCRs has come in large part through pharmacogenomic advances. Over the past two decades, the Human Genome Project, HapMap project and 1000 Genomes project have been instrumental in identifying human genetic variants contributing to common diseases [8, 79, 87]. The emergence of GWAS in 2005 has led to a surge in the successful identification of numerous disease-associated genetic loci. However useful, with GWAS genetic variants are mostly associated, not necessarily correlated with disease, as there is no clue to the underlying mechanism [79, 88]. Finally, in the past couple of years, whole-exome sequencing experiments which specifically focus on coding regions related to proteins have become available [79]. The costs of such techniques are decreasing, while patient willingness to participate is on the rise [79, 89]. Continuing these trends, first personalized whole-genome sequencing and finally, with gaining the appropriate pharmacological understanding, various forms of precision medicine may become standard clinical practice (**Fig. 3**). Before this becomes clinical reality however, there are hurdles to be overcome such as the existing skepticism by clinicians, mostly related to ethical concerns about privacy and potential discrimination of patients [79, 90]. First and foremost however remains the appropriate identification of disease-related genetic variants and corresponding implications for medical treatment. To deliver the required molecular-level understanding of genetic influences on pathology and pharmacology, more representative model systems and assay techniques are becoming available. Now is the time to employ these tools to become more familiar with the key contributing factors, establish the necessary key concepts, integrate these into target discovery and drug development and hereby lay the path towards precision medicine for GPCRs, drug targets and patients in general.

Final Notes

Altogether a novel cellular approach towards studying genetic effects on GPCR function has been explored and detailed throughout this thesis. Several GPCRs and different types of genetic variations were investigated, demonstrating together that personal cell lines in combination with label-free technology are an appropriate tool to enable GPCR pharmacogenetic studies. Incorporating aspects such as genetic variation in drug targets,

representative model systems and appropriate assay technology are important factors for advancing GPCR drug discovery. The data presented in this thesis contributes towards the progress of applying precision medicine concepts to this class of drug targets.

References

1. Docherty, S.J., et al., *A genetic association study of DNA methylation levels in the DRD4 gene region finds associations with nearby SNPs.* Behav Brain Funct, 2012. **8**: p. 31-44.
2. Sadee, W., et al., *Genetic variations in human G protein-coupled receptors: implications for drug therapy.* AAPS pharmSci, 2001. **3**(3): p. 54-80.
3. Eglen, R. and T. Reisine, *Primary cells and stem cells in drug discovery: emerging tools for high-throughput screening.* Assay Drug Dev Technol, 2011. **9**(2): p. 108-24.
4. Yu, N., et al., *Real-time monitoring of morphological changes in living cells by electronic cell sensor arrays: an approach to study G protein-coupled receptors.* Anal Chem, 2006. **78**(1): p. 35-43.
5. Ishiguro, H., et al., *Brain cannabinoid CB2 receptor in schizophrenia.* Biological psychiatry, 2010. **67**(10): p. 974-982.
6. Moller, C. and M. Slack, *Impact of new technologies for cellular screening along the drug value chain.* Drug Discov Today, 2010. **15**(9-10): p. 384-90.
7. Willemsen, G., et al., *The Netherlands Twin Register biobank: a resource for genetic epidemiological studies.* Twin Res Hum Genet, 2010. **13**(3): p. 231-45.
8. Abecasis, G.R., et al., *A map of human genome variation from population-scale sequencing.* Nature, 2010. **467**(7319): p. 1061-73.
9. Welsh, M., et al., *Pharmacogenomic discovery using cell-based models.* Pharmacological reviews, 2009. **61**(4): p. 413-29.
10. Dausset, J., et al., *Centre d'etude du polymorphisme humain (CEPH): collaborative genetic mapping of the human genome.* Genomics, 1990. **6**(3): p. 575-7.
11. Wheeler, H.E. and M.E. Dolan, *Lymphoblastoid cell lines in pharmacogenomic discovery and clinical translation.* Pharmacogenomics, 2012. **13**(1): p. 55-70.
12. Nicola Daniele, M.C., Claudio Pellegrini, Entela Shkëmbi and F. Zinno, *Biobanks and Clinical Research: An "Interesting" Connection.* Peertechz Journal of Cytology and Pathology, 2016. **1**(1): p. 034-043.
13. Rocheville, M., et al., *Mining the potential of label-free biosensors for seven-transmembrane receptor drug discovery.* Progress in molecular biology and translational science, 2013. **115**: p. 123-42.
14. Fang, Y., *Label-Free Receptor Assays.* Drug Discov Today Technol, 2011. **7**(1): p. e5-e11.
15. Stallaert, W., et al., *Impedance responses reveal beta(2)-adrenergic receptor signaling pluridimensionality and allow classification of ligands with distinct signaling profiles.* PLoS One, 2012. **7**(1): p. e29420.
16. Lieb, S., et al., *Label-free analysis of GPCR-stimulation: The critical impact of cell adhesion.* Pharmacological research : the official journal of the Italian Pharmacological Society, 2016. **108**: p. 65-74.
17. Lu, Y.F., et al., *Personalized medicine and human genetic diversity.* Cold Spring Harb Perspect Med, 2014. **4**(9).
18. Overington, J.P., B. Al-Lazikani, and A.L. Hopkins, *How many drug targets are there?* Nat Rev Drug Discov, 2006. **5**(12): p. 993-6.
19. Jacobson, K.A., *New paradigms in GPCR drug discovery.* Biochem Pharmacol, 2015. **98**(4): p. 541-55.

20. Tang, Y., et al., *Genotype-based treatment of type 2 diabetes with an alpha2A-adrenergic receptor antagonist.* Sci Transl Med, 2014. **6**(257): p. 3009934.
21. Bodenmann, S., et al., *Polymorphisms of ADORA2A modulate psychomotor vigilance and the effects of caffeine on neurobehavioural performance and sleep EEG after sleep deprivation.* Br J Pharmacol, 2012. **165**(6): p. 1904-13.
22. Childs, E., et al., *Association between ADORA2A and DRD2 polymorphisms and caffeine-induced anxiety.* Neuropsychopharmacology : official publication of the American College of Neuropsychopharmacology, 2008. **33**(12): p. 2791-800.
23. Freitag, C.M., et al., *Adenosine A(2A) receptor gene (ADORA2A) variants may increase autistic symptoms and anxiety in autism spectrum disorder.* European child & adolescent psychiatry, 2010. **19**(1): p. 67-74.
24. Franca, R., et al., *Pharmacogenetics and induction/consolidation therapy toxicities in acute lymphoblastic leukemia patients treated with AIEOP-BFM ALL 2000 protocol.* Pharmacogenomics J, 2015.
25. van Tilburg, E.W., et al., *2,8-Disubstituted adenosine derivatives as partial agonists for the adenosine A2A receptor.* Bioorganic & medicinal chemistry, 2003. **11**(10): p. 2183-92.
26. Nitz, I., et al., *Association analyses of GIP and GIPR polymorphisms with traits of the metabolic syndrome.* Mol Nutr Food Res, 2007. **51**(8): p. 1046-52.
27. Torekov, S.S., et al., *A functional amino acid substitution in the glucose-dependent insulinotropic polypeptide receptor (GIPR) gene is associated with lower bone mineral density and increased fracture risk.* J Clin Endocrinol Metab, 2014. **99**(4): p. E729-33.
28. Mohammad, S., et al., *A naturally occurring GIP receptor variant undergoes enhanced agonist-induced desensitization, which impairs GIP control of adipose insulin sensitivity.* Mol Cell Biol, 2014. **34**(19): p. 3618-29.
29. Almind, K., et al., *Discovery of amino acid variants in the human glucose-dependent insulinotropic polypeptide (GIP) receptor: the impact on the pancreatic beta cell responses and functional expression studies in Chinese hamster fibroblast cells.* Diabetologia, 1998. **41**(10): p. 1194-8.
30. Tong, D., et al., *Association of single-nucleotide polymorphisms in the cannabinoid receptor 2 gene with schizophrenia in the Han Chinese population.* J Mol Neurosci, 2013. **51**(2): p. 454-60.
31. Onaivi, E.S., et al., *Brain neuronal CB2 cannabinoid receptors in drug abuse and depression: from mice to human subjects.* PLoS One, 2008. **3**(2): p. e1640.
32. Bellini, G., et al., *The Cannabinoid Receptor 2 Q63R Variant Modulates the Relationship between Childhood Obesity and Age at Menarche.* PLoS One, 2015. **10**(10): p. e0140142.
33. Mahmoud Gouda, H. and N.R. Mohamed Kamel, *Cannabinoid CB2 receptor gene (CNR2) polymorphism is associated with chronic childhood immune thrombocytopenia in Egypt.* Blood Coagul Fibrinolysis, 2013. **24**(3): p. 247-51.
34. Rossi, F., et al., *The cannabinoid receptor type 2 Q63R variant increases the risk of celiac disease: implication for a novel molecular biomarker and future therapeutic intervention.* Pharmacol Res, 2012. **66**(1): p. 88-94.
35. Bellini, G., et al., *Association between cannabinoid receptor type 2 Q63R variant and oligo/polyarticular juvenile idiopathic arthritis.* Scand J Rheumatol, 2015. **44**(4): p. 284-7.

36. Carrasquer, A., et al., *Functional consequences of nonsynonymous single nucleotide polymorphisms in the CB2 cannabinoid receptor.* Pharmacogenetics and genomics, 2010. **20**(3): p. 157-166.
37. NCBI. *GIPR, http://www.ncbi.nlm.nih.gov/gene/2696, Accessed 21.07.2016*. 2016 03.07.2016 21.07.2016].
38. dbSNP. *http://www.ncbi.nlm.nih.gov/projects/SNP/snp_ref.cgi?rs=1800437 ; Accessed 21.07.2016*. 2016 21.07.2016].
39. dbSNP. *https://www.ncbi.nlm.nih.gov/projects/SNP/snp_ref.cgi?rs=2501432; Accessed 29.05.2017*. 2017 29.05.2017].
40. Sipe, J.C., et al., *Reduced endocannabinoid immune modulation by a common cannabinoid 2 (CB2) receptor gene polymorphism: possible risk for autoimmune disorders.* Journal of leukocyte biology, 2005. **78**(1): p. 231-238.
41. Valenzano, K.J., et al., *Pharmacological and pharmacokinetic characterization of the cannabinoid receptor 2 agonist, GW405833, utilizing rodent models of acute and chronic pain, anxiety, ataxia and catalepsy.* Neuropharmacology, 2005. **48**(5): p. 658-72.
42. Fortin, J.P., et al., *Pharmacological characterization of human incretin receptor missense variants.* J Pharmacol Exp Ther, 2010. **332**(1): p. 274-80.
43. Kruglyak, L. and D.A. Nickerson, *Variation is the spice of life.* Nature Genetics, 2001. **27**(3): p. 234-236.
44. Small, K.M., et al., *Gene and protein domain-specific patterns of genetic variability within the G-protein coupled receptor superfamily.* Am J Pharmacogenomics, 2003. **3**(1): p. 65-71.
45. Prichard, Z.M., et al., *AVPR1A and OXTR polymorphisms are associated with sexual and reproductive behavioral phenotypes in humans. Mutation in brief no. 981. Online.* Human mutation, 2007. **28**(11).
46. Walum, H., et al., *Genetic variation in the vasopressin receptor 1a gene (AVPR1A) associates with pair-bonding behavior in humans.* Proceedings of the National Academy of Sciences of the United States of America, 2008. **105**(37): p. 14153-6.
47. Meyer-Lindenberg, A., et al., *Genetic variants in AVPR1A linked to autism predict amygdala activation and personality traits in healthy humans.* Molecular psychiatry, 2009. **14**(10): p. 968-75.
48. Nozawa, M., Y. Kawahara, and M. Nei, *Genomic drift and copy number variation of sensory receptor genes in humans.* Proceedings of the National Academy of Sciences of the United States of America, 2007. **104**(51): p. 20421-6.
49. Lipchock, S.V., et al., *Caffeine Bitterness is Related to Daily Caffeine Intake and Bitter Receptor mRNA Abundance in Human Taste Tissue.* Perception, 2017. **46**(3-4): p. 245-256.
50. Iacovazzo, D., et al., *Germline or somatic GPR101 duplication leads to X-linked acrogigantism: a clinico-pathological and genetic study.* Acta Neuropathol Commun, 2016. **4**(1): p. 016-0328.
51. Redon, R., et al., *Global variation in copy number in the human genome.* Nature, 2006. **444**(7118): p. 444-54.
52. Scheet, P., et al., *Twins, tissue, and time: an assessment of SNPs and CNVs.* Twin research and human genetics : the official journal of the International Society for Twin Studies, 2012. **15**(6): p. 737-45.

53. Ehli, E.A., et al., *De novo and inherited CNVs in MZ twin pairs selected for discordance and concordance on Attention Problems.* Eur J Hum Genet, 2012. **20**(10): p. 1037-43.
54. Vink, J.M., et al., *Polygenic risk scores for smoking: predictors for alcohol and cannabis use?* Addiction, 2014. **109**(7): p. 1141-51.
55. Middeldorp, C.M., et al., *Anxiety and depression in children and adults: influence of serotonergic and neurotrophic genes?* Genes Brain Behav, 2010. **9**(7): p. 808-16.
56. Freedman, L.P., et al., *Reproducibility: changing the policies and culture of cell line authentication.* Nature methods, 2015. **12**(6): p. 493-7.
57. Sie, L., S. Loong, and E.K. Tan, *Utility of lymphoblastoid cell lines.* J Neurosci Res, 2009. **87**(9): p. 1953-9.
58. Vincent, M., et al., *Genome-wide transcriptomic variations of human lymphoblastoid cell lines: insights from pairwise gene-expression correlations.* Pharmacogenomics, 2012. **13**(16): p. 1893-904.
59. Thomas, S.M., et al., *Reprogramming LCLs to iPSCs Results in Recovery of Donor-Specific Gene Expression Signature.* PLoS genetics, 2015. **11**(5): p. e1005216.
60. Barrett, R., et al., *Reliable generation of induced pluripotent stem cells from human lymphoblastoid cell lines.* Stem cells translational medicine, 2014. **3**(12): p. 1429-34.
61. Rajesh, D., et al., *Human lymphoblastoid B-cell lines reprogrammed to EBV-free induced pluripotent stem cells.* Blood, 2011. **118**(7): p. 1797-800.
62. Choy, E., et al., *Genetic analysis of human traits in vitro: drug response and gene expression in lymphoblastoid cell lines.* PLoS genetics, 2008. **4**(11): p. e1000287.
63. Plagnol, V., et al., *Extreme clonality in lymphoblastoid cell lines with implications for allele specific expression analyses.* PLoS One, 2008. **3**(8): p. e2966.
64. Stark, A.L., et al., *Heritable and non-genetic factors as variables of pharmacologic phenotypes in lymphoblastoid cell lines.* The pharmacogenomics journal, 2010. **10**(6): p. 505-12.
65. Artene, S.A., et al., *Biobanking in a constantly developing medical world.* ScientificWorldJournal, 2013. **2013**: p. 343275.
66. Ministers, C.o.E.a.C.o., *Recommendation Rec 4 of the Committee of Ministers to Member States on Research on Biological Materials of Human Origin*, S. European Commission, France, Editor 2006.
67. Hosoya, M. and K. Czysz, *Translational Prospects and Challenges in Human Induced Pluripotent Stem Cell Research in Drug Discovery.* Cells, 2016. **5**(4).
68. Rony, I.K., et al., *Inducing pluripotency in vitro: recent advances and highlights in induced pluripotent stem cells generation and pluripotency reprogramming.* Cell proliferation, 2015. **48**(2): p. 140-56.
69. Robinton, D.A. and G.Q. Daley, *The promise of induced pluripotent stem cells in research and therapy.* Nature, 2012. **481**(7381): p. 295-305.
70. Bellin, M., et al., *Induced pluripotent stem cells: the new patient?* Nature reviews. Molecular cell biology, 2012. **13**(11): p. 713-26.
71. Doherty, K.R., et al., *Structural and functional screening in human induced-pluripotent stem cell-derived cardiomyocytes accurately identifies cardiotoxicity of multiple drug types.* Toxicol Appl Pharmacol, 2015. **285**(1): p. 51-60.

72. Zhang, X., et al., *Multi-parametric assessment of cardiomyocyte excitation-contraction coupling using impedance and field potential recording: A tool for cardiac safety assessment.* J Pharmacol Toxicol Methods, 2016. **81**: p. 201-16.
73. Gamal, W., et al., *Real-time quantitative monitoring of hiPSC-based model of macular degeneration on Electric Cell-substrate Impedance Sensing microelectrodes.* Biosensors and Bioelectronics, 2015. **71**: p. 445-455.
74. Fatehullah, A., S.H. Tan, and N. Barker, *Organoids as an in vitro model of human development and disease.* Nat Cell Biol, 2016. **18**(3): p. 246-254.
75. Atienza, J.M., et al., *Label-free and real-time cell-based kinase assay for screening selective and potent receptor tyrosine kinase inhibitors using microelectronic sensor array.* Journal of biomolecular screening, 2006. **11**(6): p. 634-43.
76. Zhuang, G., et al., *Phosphoproteomic analysis implicates the mTORC2-FoxO1 axis in VEGF signaling and feedback activation of receptor tyrosine kinases.* Science signaling, 2013. **6**(271): p. ra25.
77. Tanaka, H., et al., *Nuclear envelope-localized EGF family protein amphiregulin activates breast cancer cell migration in an EGF-like domain independent manner.* Biochemical and biophysical research communications, 2012. **420**(4): p. 721-6.
78. Varisli, L., et al., *Androgen regulated HN1 leads proteosomal degradation of androgen receptor (AR) and negatively influences AR mediated transactivation in prostate cells.* Molecular and cellular endocrinology, 2012. **350**(1): p. 107-17.
79. Li, A. and D. Meyre, *Jumping on the Train of Personalized Medicine: A Primer for Non-Geneticist Clinicians: Part 1. Fundamental Concepts in Molecular Genetics.* Current Psychiatry Reviews, 2014. **10**(2): p. 91-100.
80. Priest, B.T. and G. Erdemli, *Phenotypic screening in the 21st century.* Frontiers in pharmacology, 2014. **5**: p. 264.
81. Swinney, D.C., *Phenotypic vs. target-based drug discovery for first-in-class medicines.* Clinical pharmacology and therapeutics, 2013. **93**(4): p. 299-301.
82. Zheng, W., N. Thorne, and J.C. McKew, *Phenotypic screens as a renewed approach for drug discovery.* Drug Discov Today, 2013. **18**(21-22): p. 1067-73.
83. Swinney, D.C. and J. Anthony, *How were new medicines discovered?* Nature reviews. Drug discovery, 2011. **10**(7): p. 507-19.
84. Kojima, R., D. Aubel, and M. Fussenegger, *Novel theranostic agents for next-generation personalized medicine: small molecules, nanoparticles, and engineered mammalian cells.* Curr Opin Chem Biol, 2015. **28**: p. 29-38.
85. Silverman, M.H., et al., *Clinical evidence for utilization of the A3 adenosine receptor as a target to treat rheumatoid arthritis: data from a phase II clinical trial.* The Journal of rheumatology, 2008. **35**(1): p. 41-8.
86. Beitelshees, A.L. and H.L. McLeod, *Clopidogrel pharmacogenetics: promising steps towards patient care?* Arterioscler Thromb Vasc Biol, 2006. **26**(8): p. 1681-3.
87. Consortium, T.I.H., *The International HapMap Project.* Nature, 2003. **426**(6968): p. 789-96.
88. Visscher, P.M., et al., *Five years of GWAS discovery.* Am J Hum Genet, 2012. **90**(1): p. 7-24.
89. Hood, L. and S.H. Friend, *Predictive, personalized, preventive, participatory (P4) cancer medicine.* Nature reviews. Clinical oncology, 2011. **8**(3): p. 184-7.

90. Hindorff, L.A., et al., *Potential etiologic and functional implications of genome-wide association loci for human diseases and traits.* Proceedings of the National Academy of Sciences of the United States of America, 2009. **106**(23): p. 9362-7.
91. van't Veer, L.J. and R. Bernards, *Enabling personalized cancer medicine through analysis of gene-expression patterns.* Nature, 2008. **452**(7187): p. 564-70.
92. Mirnezami, R., J. Nicholson, and A. Darzi, *Preparing for precision medicine.* The New England journal of medicine, 2012. **366**(6): p. 489-91.
93. Katsanis, S.H., G. Javitt, and K. Hudson, *Public health. A case study of personalized medicine.* Science, 2008. **320**(5872): p. 53-4.

Summary

The traditional medical treatment paradigm focuses on prescribing one drug to treat all patients with a specific disease or condition, so called 'one-size-fits-all'. However, it has been shown increasingly that differences between persons, such as in lifestyle or genes, can change both the course of a disease and effect of a drug. In order to adapt medical treatment and drug development to that, a concept know as precision medicine, it is essential to study which and how genetic differences, i.e. polymorphisms, affect drug response. In this thesis I studied of the influences of genetic variation on a specific class of drug targets, the G protein-coupled receptors (GPCRs), by using a combination of personal cellular models and novel label-free assay technology.

Chapter 1 introduces the main subjects and concepts around precision medicine, GPCRs and genetic variation discussed in this thesis. Chapter 2 continues with discussing the concept of using patient-derived cell lines as model systems and highlights the advantages of label-free technology assays to investigate these. To better understand drug action and pathological processes in the human individual, physiologically more appropriate model systems are needed. For this, patient-derived cells can offer specific advantages. Traditional GPCR assays are often label-based, which has disadvantages when aiming to represent the physiological situation as closely as possible. Novel label-free cellular assays enable the study of complex biological processes in their native environment. Examples and advantages of the combination of these two are discussed in chapter 2.

Chapter 3 describes the optimization and application of an impedance-based label-free assay methodology, the xCELLigence, to a type of personal cell line, the lymphoblastoid cell lines (LCLs) from individuals of the Netherlands Twin Registry (NTR), to allow direct measurement of cellular effects of GPCR signaling. Generally, this label-free assay technology was deemed only compatible with adherent cell lines, while LCLs are suspension cells. Therefore, the methodology was optimized and applied to study cellular properties and GPCR signaling in LCLs. A prototypical GPCR present on LCLs, the cannabinoid receptor 2 (CB_2R), was selected for proof-or-principle. Effects of several compound types were studied and proved comparable between LCLs of two unrelated individuals with the same genotype, providing the first evidence that the technology and model system were well suited to evaluate genetic influences on GPCR-mediated drug responses.

Chapter 4 presents the case of another GPCR, the adenosine A_{2A} receptor ($A_{2A}R$). The $A_{2A}R$ is a potential drug target for a variety of respiratory and inflammatory conditions, including Parkinson's disease, as well as the receptor for caffeine. After identifying which adenosine receptor subtypes were present on LCLs, the cellular effects of various types of compounds targeting the $A_{2A}R$ were compared between LCLs derived from a family of four individuals, consisting of parents and their identical twin children. In the presence of a specific type of genetic variation, an intron Single nucleotide polymorphism (SNP) that is potentially linked to caffeine-induced sleep disorders, different cellular effects were found for a specific type of compound, a partial agonist, but not for other compounds such as full agonists or antagonists. Although this does not provide causal evidence that response differences are directly related to this genetic variation, it does show that the chosen methodology is capable of picking up individual differences in GPCR signaling.

After this demonstration, genetic differences in other GPCRs were studied. The CB_2R is a GPCR investigated intensively as therapeutic target due to its important role in the immune system. In chapter 5, responses to agonists, partial agonists and antagonists of various chemical classes were characterized in LCLs from individuals with varying CB_2R genotypes. One of the interesting findings was that endogenous cannabinoids such as 2-AG induced cellular effects vastly different from all synthetic cannabinoids, especially in their time-profile. More importantly, it was also found that compounds with different chemical scaffolds showed different sensitivity to a highly common amino-acid altering polymorphism in the CB_2R, the Q63R variant. In a similar manner it may be possible to identify compounds prone to personal differences, so for precision medicine, or more suited as drugs for the general population early on in drug development.

Genetic differences may however not only influence drug effects, but can alter a person's susceptibility to disease or alter disease progression. Chapter 6 presents the case of the Glucose-Dependent Insulinotropic Polypeptide Receptor (GIPR), in which an amino-acid altering SNP that has often been associated with diseases changed the cellular effects of the endogenous ligand. The GIPR plays an important role in whole-body metabolism, and its amino-acid altering SNP E354Q has been associated with several diseases including diabetes. When studying this receptor in a panel of LCLs of individuals with different genotypes for E354Q, responses to the endogenous agonist GIP showed enhanced potency in Q354 homozygous individuals. This study hereby provides more insight into how GPCR polymorphisms could change physiology in the human individual.

In summary, a novel cellular approach for studying genetic effects on GPCRs has been explored and detailed throughout this thesis. Several GPCRs and different types of genetic

variations were investigated, and the findings highlight that various kinds of genetic differences in GPCRs, can profoundly influence drug response. These include differing effects depending on compound type or chemical scaffold, as well as on endogenous signaling. The overall conclusion from the results described in this thesis and forthcoming opportunities for drug discovery and treatment are discussed in detail in chapter 7. In concert, the findings in this thesis may contribute to the progress of applying precision medicine concepts to the GPCR class of drug targets and hence the development of clinically more effective and more tailored drugs.

Samenvatting

Historisch gezien richt zich medische behandeling op het voorschrijven van één geneesmiddel om alle patiënten met een specifieke ziekte of aandoening te behandelen, ook bekend als 'one-size-fits-all'. Het wordt echter steeds duidelijker dat verschillen tussen personen, zoals in levensstijl of genen, zowel het verloop van een ziekte als het effect van een geneesmiddel kunnen veranderen. Om medische behandeling en medicijnontwikkeling hierop aan te kunnen passen, een concept bekend als 'precision medicine', is het essentieel om te identificeren hoe en welke genetische verschillen, d.w.z. polymorfismen, de geneesmiddelrespons beïnvloeden. Dit proefschrift richt zich op het bestuderen van genetische verschillen in een bepaalde klasse van doelwitten voor geneesmiddelen, de G-eiwit gekoppelde receptoren (GPCRs), door gebruik te maken van een combinatie van een persoonlijk cellulair model en een recent ontwikkelde label-vrije meettechnologie.

In hoofdstuk 1 worden de hoofonderwerpen en concepten rondom precision medicine, GPCRs en genetische verschillen, die in dit proefschrift aan bod komen, geïntroduceerd. Hoofdstuk 2 gaat verder met de discussie over het concept om persoonlijke cellulaire modellen te gebruiken en belicht de voordelen die de label-vrije meettechnologie biedt om deze te onderzoeken. Om de geneesmiddelwerking en ziekteprocessen in het menselijke individu beter te kunnen begrijpen, zijn meer fysiologische representatieve model systemen nodig. Hiervoor bieden cellulaire modellen afkomstig van patiënten specifieke voordelen. Traditionele GPCR bepalingsmethoden zijn vaak gebaseerd op labels, wat nadelen met zich meebrengt als het doel is om de fysiologische situatie zo goed mogelijk te benaderen. Recent ontwikkelde label-vrije cellulaire bepalingsmethoden maken het bestuderen van complexe biologische processen in hun natuurlijke omgeving mogelijk. Voorbeelden en voordelen van de combinatie van deze twee worden in hoofdstuk 2 besproken.

Hoofdstuk 3 beschrijft de optimalisatie en toepassing van een dergelijke, op weerstand gebaseerde label-vrije technologie, de xCELLigence, voor een bepaald type persoonlijke cellijnen, de lymfoblastoïde cellijnen (LCLs) van individuen van het Nederlandse Tweelingen Register (NTR), voor directe meeting van de cellulaire effecten van GPCR stimulatie. Over het algemeen wordt deze label-vrije technologie alleen toepasbaar op hechtende cellen geacht, terwijl LCLs suspensie cellen zijn. Daarom werd de methodologie geoptimaliseerd en toegepast om zowel de cellulaire eigenschappen en GPCR activatie in LCLs te kunnen

bestuderen. Een GPCR die in LCLs aanwezig is, de Cannabinoïde receptor 2 (CB_2R), werd geselecteerd als voorbeeld ter demonstratie. De effecten van verschillende typen chemische verbindingen werden bestudeerd en bleken vergelijkbaar tussen LCLs van twee niet verwante individuen met hetzelfde genotype, wat het proof-of-principle leverde dat deze technologie en het cellulaire model systeem goed geschikt waren om genetische invloeden op GPCR-gemedieerde geneesmiddelrespons te onderzoeken.

Hoofdstuk 4 laat het voorbeeld van een andere GPCR, de Adenosine A_{2A} receptor ($A_{2A}R$) zien. De $A_{2A}R$ is een mogelijk aangrijpingspunt voor geneesmiddelen voor een breed aantal van ademhalings- en ontstekingsaandoeningen, waaronder de ziekte van Parkinson, en is ook de receptor voor cafeïne. Na het bepalen van welke subtypes van adenosinereceptoren aanwezig waren in LCLs, werden de cellulaire effecten van verschillende typen chemische verbindingen die op de $A_{2A}R$ aangrijpen vergeleken tussen de LCLs van een familie van vier, bestaande uit ouders en hun eeneiige tweelingkinderen. Bij aanwezigheid van een bepaalde genetische variant, een Single Nucleotide Polymorphism (SNP) in een intron die eerder in verband is gebracht met cafeïne-gerelateerde slaapstoornissen, werden afwijkende cellulaire effecten gezien voor een bepaald type verbinding, namelijk een partiële agonist, maar niet bij andere typen verbindingen zoals volle agonisten of antagonisten. Hoewel dit geen direct causaal verband aantoont tussen de verschillen in respons en de genetische variatie, laat het wel zien dat de gekozen methode geschikt is om individuele verschillen in GPCR effecten te detecteren.

Na deze demonstratie weden genetische verschillen in andere GPCRs bestudeerd. De CB_2R is een GPCR die intensief onderzocht wordt als mogelijk therapeutisch doelwit vanwege zijn belangrijke rol in het immuunsysteem. In hoofdstuk 5 werd de respons op agonisten, partiële agonisten en antagonisten van verschillende chemische klassen in LCLs van meerdere individuen met verschillend CB_2R genotype gekarakteriseerd. Één van de interessante bevindingen was dat endogene cannabinoïdes zoals 2-AG duidelijk andere cellulaire effecten induceerden dan alle synthetische cannabinoïdes, vooral in hun tijdsprofiel. Nog belangrijker is dat ook werd gevonden dat verbindingen van verschillende chemische signatuur verschillend reageerden op een veel voorkomende aminozuur-veranderende polymorfisme in de CB_2R, de Q63R variant.

Genetische verschillen kunnen echter niet alleen de effecten van geneesmiddelen beïnvloeden, maar ook de vatbaarheid van een persoon voor een ziekte of het verloop van een ziekte veranderen. In hoofdstuk 6 wordt het geval van de Glucose-afhankelijke Insulinotrope Polypeptide receptor (GIPR) gepresenteerd, waarin een aminozuur-veranderende SNP, die al vaak met ziektes geassocieerd werd, de cellulaire effecten van het

endogene ligand veranderde. De GIPR speelt een belangrijke rol in het metabolisme in het hele lichaam, en deze aminozuur-veranderende SNP, E354Q, wordt onder andere met diabetes geassocieerd. Tijdens het bestuderen van deze receptor in een panel van meerdere individuen met verschillende genotype van E354Q, werd een verhoogde potentie van de endogene agonist GIP op Q354 homozygote individuen aangetoond. Dit onderzoek verschaft hiermee meer inzicht in hoe polymorfismen in GPCRs de fysiologie in een menselijk individu kunnen veranderen.

Samengevat wordt in dit proefschrift een nieuwe cellulaire aanpak voor het bestuderen van genetische effecten op GPCRs onderzocht en beschreven. Meerdere GPCRs en diverse soorten genetische verschillen werden bestudeerd, en de bevindingen tonen aan dat verschillende soorten van genetische variatie in GPCRs, bijvoorbeeld veel voorkomend of juist zelden, verscheidende effecten kunnen hebben. Deze verschillende effecten kunnen afhankelijk zijn van het type ligand of de chemische signatuur van een verbinding, en van invloed zijn op de endogene signaalverwerking. De algemene conclusie uit de resultaten van dit proefschrift en de daaruit ontstaande mogelijkheden voor geneesmiddelonderzoek en behandeling wordt uitgebreid in hoofdstuk 7 besproken en van commentaar voorzien. Samen kunnen de bevindingen in dit proefschrift bijdragen tot vooruitgang in de mogelijkheden om ‘precision medicine’ op de GPCR-klasse der geneesmiddeldoelwitten toe te passen en zo ook tot de ontwikkeling van effectievere, op de persoon toegesneden geneesmiddelen.

List of publications

Hillger JM, Lieuw W, Heitman LH, IJzerman AP. *Label-free technology and patient cells: from early drug development to precision medicine*. Drug Discov Today, 2017 Aug 1. pii: S1359-6446(17)30153-8.

Hillger JM, le Roy B, Wang Z, Krieger-Mulder T, Boomsma DI, Slagboom PE, Danen EHJ, IJzerman AP, Heitman LH. *Phenotypic screening of cannabinoid receptor 2 ligands shows different sensitivity to genotype*. Biochemical Pharmacology, 2017. **130**: p.60-70.

Hillger JM, Diehl C, Van Spronsen E, Boomsma DI, Slagboom PE, Heitman LH, IJzerman AP. *Getting personal: Endogenous adenosine receptor signaling in Lymphoblastoid Cell Lines.* Biochemical Pharmacology, 2016. **115**: p.114-22.

Hillger JM, Schoop J, Boomsma DI, Slagboom PE, IJzerman AP, Heitman LH. *Label-free detection of GPCR-mediated drug responses in personal cell lines.* Biosensors and Bioelectronics, 2015. **74**: p. 233–242.

Tollstoy Tegler L, Corin K, Hillger JM, Wassie B, Yu Y, Zhang S. *Cell-free expression, purification, and ligand-binding analysis of Drosophila melanogaster olfactory receptors DmOR67a, DmOR85b and DmORCO*. Scientific Reports, 2015. **5**: 7867.

Guo D, Hillger JM, IJzerman AP, Heitman LH. *Drug-target residence time – a case for G protein-coupled receptors*. Medicinal Research Reviews, 2014. **34**(4): p. 856-92.

Vilums M, Zweemer AJM, Yu Z, de Vries H, Hillger JM, Gross R, Clemens J, Barmare F, Krenitsky P, Brussee H, Stamos D, Saunders J, Heitman LH, IJzerman AP. *Structure-Kinetics Relationships – an overlooked parameter in hit-to-lead optimization: a case of cyclopentylamines as CCR2 antagonists.* Journal of Medicinal Chemistry, 2013. **56**(19): p. 7706-14.

Curriculum Vitae

Julia Maria Hillger was born in Hamburg, Germany, the 17th of May 1988. After graduating from high school at the German International School in The Hague, the Netherlands, she started studying Bio-Pharmaceutical Sciences at Leiden University in 2006. During her studies she performed two internships at the Medicinal Chemistry division of the Leiden Academic Centre for Drug Research, under the supervision of Prof. Ad IJzerman, Dr. Johannes Brussee and Dr. Laura Heitman. Her work on the synthesis and design of small molecule antagonists of the CCR2 Chemokine receptor was awarded the Suzanne Hovinga award for best thesis of Bio-Pharmaceutical and Biomedical Sciences at Leiden University in 2011 and the 2nd prize for the KNCV Golden Master Award 2011 by the Royal Netherlands Chemical Society for best master research thesis.

Subsequently she performed a third internship at the Massachusetts Institute of Technology, Cambridge, USA, at the Center of Biomedical Engineering under the supervision of Dr. Shuguang Zhang. Here she studied how to turn GPCRs water-soluble by using a cell-free production methodology, focusing on the chemokine receptors CX3CR1 and CCR5.

In 2012 she obtained her MSc. degree *cum laude*. For her overall study results she was awarded the KNMP student prize 2012, an annual award by the Royal Dutch Pharmacists Association for pharmacy students acknowledging their study results.

In the same year she started her PhD study at the Medicinal Chemistry division at Leiden University, under the supervision of Prof. Ad IJzerman and Dr. Laura Heitman. This research was focused on label-free technology and genetic influences in GPCRs, and involved collaboration with Prof. Dorret Boomsma, from the Department of Biological Psychology of the Vrije Universiteit Amsterdam, and Prof. Eline Slagboom from the Section of Molecular Epidemiology, Department of Medical Statistics and Bioinformatics of the Leiden University Medical Center. Throughout her PhD studies she presented work described in this thesis at various national and international conferences. In 2012, she was awarded the 1st poster prize at the LACDR Spring Symposium as well as the 1st poster prize at the FIGON Dutch Medicine Days 2015. Julia is currently working as a Technical Support Specialist at Cell Signaling Technology Europe in Leiden, the Netherlands.

Acknowledgements

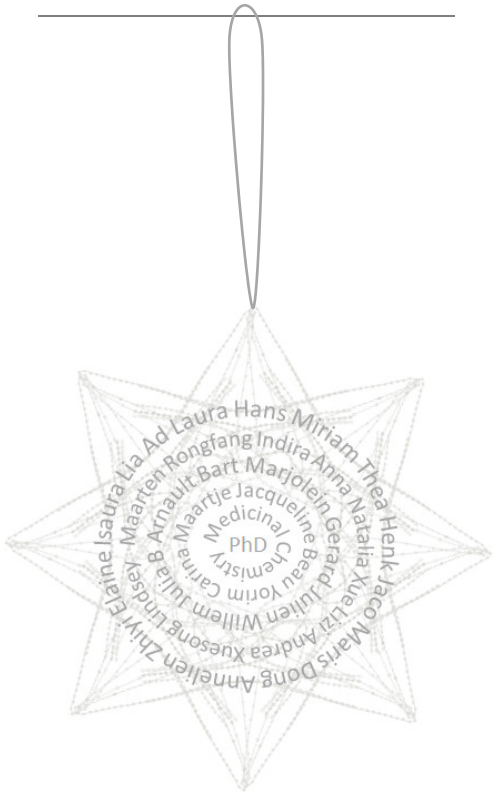

This thesis has been a work of the past four years, throughout which I have had the pleasure to learn from, teach and work with many different people. I'm certain that without their contribution and support, this thesis would have looked quite differently. I should like to thank everyone I have collaborated with for their support and input that enabled this thesis to reach its current state.

In particular I would like to thank Ad and Laura, for their never-ending patience, for teaching me and supporting me throughout not just these four years, but ever since I set foot in Medicinal Chemistry so many years ago as a Bachelor student. I have had many supervisors throughout my time at MedChem, starting with Rob and Maris as a student, and as a PhD candidate Laura, Ad and briefly Miriam. You have all taught me many different things and made me feel right at home from the very beginning. Thank you for that, your constructive criticism, practical input, guiding hand and insightful advice.

I would also like to thank all of my colleagues and students I met throughout that time. To my colleagues I would like to give thanks for all the fun times and laughter, but also for being a listening ear when sharing some of the same experiences. To my many office mates, Indira, Miriam, Zhiyi, Maarten, Andrea, Anna and Xuesong. To my students, for all of their contributions and things they taught me as well. Especially my master students Carina, Yorim, Jacqueline, Beau and Maartje, who were involved in parts of this thesis. I very much enjoyed the experiences with you and I'm happy to say that some of you have even become friends. To Rongfang, who has shared much advice about becoming a mum during your PhD. To Thea and Henk, for always being ready to save the day with their very practical advice and many years of hands-on experience. And to my paranymphs Anna and Natalia, for their support during my defense.

Finally, to my friends and family, who have both grown in number throughout my four years as a PhD student. To my parents and grandparents, for first inspiring me to do science. To my cat Psoe, always ready with cuddles and comfort. But especially to my husband Olaf, for all his support and understanding, and to our son Logan, for his decided lack of understanding and all the fun distractions. I'm happy to have shared this part of my life with you and am looking forward to many more to come.